APPLICATIONS OF IRREVERSIBLE THERMODYNAMICS: BULK AND INTERFACIAL ELECTRONIC, IONIC, MAGNETIC AND THERMAL TRANSPORT

A Dissertation

by

MATTHEW RYAN SEARS

Submitted to the Office of Graduate Studies of
Texas A&M University
in partial fulfillment of the requirements for the degree of

DOCTOR OF PHILOSOPHY

August 2011

Major Subject: Physics

APPLICATIONS OF IRREVERSIBLE THERMODYNAMICS: BULK AND INTERFACIAL ELECTRONIC, IONIC, MAGNETIC AND THERMAL TRANSPORT

A Dissertation

by

MATTHEW RYAN SEARS

Submitted to the Office of Graduate Studies of
Texas A&M University
in partial fulfillment of the requirements for the degree of

DOCTOR OF PHILOSOPHY

Approved by:

Chair of Committee,	Wayne Saslow
Committee Members,	Glenn Agnolet
	Helmut Katzgraber
	Abraham Clearfield
Head of Department,	Edward Fry

August 2011

Major Subject: Physics

ABSTRACT

Applications of Irreversible Thermodynamics:
Bulk and Interfacial Electronic, Ionic, Magnetic and Thermal Transport.

(August 2011)

Matthew Ryan Sears, B.S., University of Rochester

Chair of Advisory Committee: Dr. Wayne M. Saslow

Irreversible thermodynamics is a widely-applicable toolset that extends thermodynamics to describe systems undergoing irreversible processes. It is particularly useful for describing macroscopic flow of system components, whether conserved (e.g., particle number) or non-conserved (e.g., spin). We give a general introduction to this toolset and calculate the entropy production due to bulk and interfacial flow. We compare the entropy production and heating rate of bulk and interfacial transport, as well as interfacial charge and spin transport. We then demonstrate the power and applicability of this toolset by applying it to three systems.

We first consider metal oxide growth, and discuss inconsistency in previous theory by Mott. We show, however, that Mott's solution is the lowest order of a consistent asymptotic solution, with the ion and electron concentrations and fluxes going as power series in $t^{-k/2}$, where $k = 1, 2, \ldots$. We find that this gives corrections to the "parabolic growth law" that has oxide thickness going as $t^{1/2}$; the lowest order correction is logarithmic in t.

We then consider the effect on spin of electric currents crossing an interface between a ferromagnet (FM) and non-magnetic material (NM). Previous theories for electrical potential and spin accumulation neglect chemical or magnetic contributions to the energy. We apply irreversible thermodynamics to show that both contributions are pivotal in predicting the spin accumulation, particularly in the NM. We also show

that charge screening, not considered in previous theories, causes spin accumulation in the FM, which may be important in ferromagnetic semiconductors.

Finally, we apply irreversible thermodynamics to thermal equilibration in a thin-film FM on a substrate. Recent experiments suggest that applying a thermal gradient across the length of the system causes a spin current along the thickness; this spin current is present much farther from the heat sources than expected. We find that, although the interaction between the separate thermal equilibration processes increases the largest equilibration length, thermal equilibration does not predict a length as large as the experimentally measured length; it does predict, however, a thermal gradient along the thickness that has the shape of the measured spin current.

To my loving parents, Jim & Carol

ACKNOWLEDGMENTS

I thank all those who, through great or tough love, made this work possible.

I thank A for her support, kindness, and flexibility. Many a strong individual has crumbled under less stress, and she has borne it with a quiet grace. The value of her steadfast composure can not be measured.

I would be remiss if I did not acknowledge Hawkeye for his much-needed companionship throughout the research and writing phases of this work. Although perhaps lacking in input, he provided two terrific ears in his role as a sounding board.

I thank the Department of Energy for partial financial support.

I thank all of my committee members, Drs. Abraham Clearfield, Glenn Agnolet, Helmut Katzgraber, and Wayne Saslow, for their patience and poignant questions (as well as their equally-important willingness to do the necessary paperwork). It is because of their recommendations that this work is readable.

For his support and extensive suggestions for public presentations, I thank Dr. Helmut Katzgraber. If ever I give a good talk, Dr. Katzgraber will be to blame.

Above all, I thank my chair, Dr. Saslow, for his patience, expertise, and support.

TABLE OF CONTENTS

CHAPTER Page

CHAPTER Page

LIST OF TABLES

LIST OF FIGURES

FIGURE Page

CHAPTER I

INTRODUCTION

Irreversible thermodynamics, the thermodynamic method to macroscopically describe systems undergoing irreversible processes, was formulated in the early to middle 20th century, by some accounts beginning with the seminal work by Onsager in 1931.[1] For a complete treatment of the techniques of irreversible thermodynamics, see, for example, Refs. 2, 3, or 4.

Most real-world processes involve continual irreversible flow; take, for instance, the exchange of matter within living cells, the deposition of energy from the sun to a planet's atmosphere, or the flow of current through an ordinary resistor. This small set demonstrates the broad and ubiquitous nature of such processes. Irreversible thermodynamics is a method by which one can find the fluxes and concentrations of the carriers (of heat, mass, charge, etc.) in such systems, as well as the time evolution and spatial dependence of thermodynamic quantities (such as temperature and voltage). Some phenomenological transport equations, such as Ohm's Law, existed prior to the foundation of irreversible thermodynamics, which gives the analytic framework to derive such experimentally-observed relations.

Although very general, irreversible thermodynamics only applies to systems near equilibrium; it does not treat situations like the free expansion of a gas.

Illustrated below by the example of one-dimensional heat flow, the general method of irreversible thermodynamics for stationary states is as follows:

- write down the static thermodynamic energy differential dE in terms of extensive thermodynamic quantities (e.g., entropy S) and their correlated intensive

---

The journal model is Physical Review B.

quantities (e.g., temperature T);

- write the relation between the time rates of change of each of the extensive thermodynamic quantities and the divergence of their respective fluxes, known as "continuity equations" (e.g., the current density of entropy j_i^S is related to its time rate of change $\partial_t S$ and the entropy production, or source, $\mathcal{S}_S$ by $\partial_t S + \partial_i j_i^S = \mathcal{S}_S$);

- use the energy differential to replace the time rate of change of entropy (energy) in the continuity equation for entropy (energy);

- use the other continuity equations to replace the remaining time derivatives;

- Write the equation for the rate of increase of the entropy density so that it contains a single divergence term and terms associated with the appropriate thermodynamic variables, each of which is shown to be a product of a thermodynamic gradient or "force" and its conjugate flux or for non-conserved quantities (e.g., spin), a thermodynamic sum or difference and its conjugate "source";

- employ the Second Law of Thermodynamics to set the divergence term to zero and to determine the form of all of the fluxes and sources (below we give an example where the temperature gradient is the "force" associated with the energy flux – this type of relation is called a "flux-force" relation);

- and substitute these flux-force relations into the continuity equations to obtain a set of coupled partial differential equations.

Solving the resulting set of equations with the appropriate boundary conditions then gives the intensive thermodynamic properties and the thermodynamic fluxes in the subsystems.

Throughout this work, rather than extensive thermodynamic quantities (e.g., entropy S) we employ thermodynamic densities (e.g., entropy density $s = S/V$, where V is the volume). Since the volume is taken to be constant for the systems studied by this work, this does not affect our results. To apply this technique to systems in which the volume is not static, one must integrate the relevant equations over V.

To illustrate the method outlined above, consider the example of ordinary one-dimensional thermal flow. With energy density ε, entropy density s, and temperature T, static thermodynamics gives

$$d\varepsilon = T ds. \tag{1.1}$$

Continuity of energy and entropy give

$$\dot{\varepsilon} + \partial_x j^{\varepsilon}_x = 0, \tag{1.2}$$

$$\dot{s} + \partial_x j^{s}_x = \mathcal{S}_s \geq 0. \tag{1.3}$$

Here, j^{ε} is the energy flux, j^s is the entropy flux, and $\mathcal{S}_s$ is the entropy production (per unit volume). Energy conservation and the Second Law of Thermodynamics have been employed by respectively setting the right-hand-side (RHS) of Eq. (1.2) to be zero and the RHS of Eq. (1.3) to be non-negative. Substitution for $\dot{s}$ from Eq. (1.1) into Eq. (1.3) gives

$$\frac{\dot{\varepsilon}}{T} + \partial_x j^{s}_x = \mathcal{S}_s \geq 0. \tag{1.4}$$

Substitution for $\dot{\varepsilon}$ from Eq. (1.2) then relates the divergence of all the fluxes to the entropy production, which must be non-negative:

$$-\frac{\partial_x j^{\varepsilon}_x}{T} + \partial_x j^{s}_x = \mathcal{S}_s \geq 0. \tag{1.5}$$

In the spirit of irreversible thermodynamics, the left-hand-side (LHS) of Eq. (1.5) is then rewritten to contain only a single divergence term:

$$\partial_x \left(j_x^s - \frac{j_x^\varepsilon}{T} \right) - \frac{j_x^\varepsilon}{T^2} \partial_x T = \mathcal{S}_s \geq 0. \tag{1.6}$$

Because the divergence term cannot be guaranteed to be everywhere non-negative, its argument must be zero, i.e.,

$$j_x^s - \frac{j_x^\varepsilon}{T} = 0. \tag{1.7}$$

One may alternatively argue that Eq. (1.1) guarantees the above relation. For the gradient term $-j_x^\varepsilon \partial_x T$ to be non-negative regardless of the sign of $\partial_x T$, we must have

$$j_x^\varepsilon = -\kappa \partial_x T, \tag{1.8}$$

where κ is a positive constant. This is the usual force-flux relation for heat flow, and κ is the thermal conductivity. We note that Eq. (1.8) is a statistical rather than mechanical law, whereas, for example, gravitational forces are mechanical in nature.

Combination of energy continuity Eq. (1.2) and the force-flux relation Eq. (1.8) gives the steady-state temperature and energy (heat) flux. In steady state, the time derivative $\dot{\varepsilon}$ is neglected, so that substitution of Eq. (1.8) into Eq. (1.2) gives

$$\partial_x^2 T = 0. \tag{1.9}$$

As expected, for a single one-dimensional system, the temperature is linear in x and the heat flux is constant. Application of appropriate boundary conditions gives the full solution for the temperature and heat flux. For the simple example of an electrically insulating rod whose ends at $x = -d/2$ and $x = d/2$ are maintained at

respective temperatures T_L and T_R,

$$T = \frac{T_L + T_R}{2} + \left(\frac{T_R - T_L}{d} \right) x. \tag{1.10}$$

Application of this technique may be more complicated, particularly for complex systems. There may be multiple subsystems, and fluxes of many different quantities, which in principle *each* depend on the gradients of *all* of the varying intrinsic thermodynamic parameters. Further, consideration of multiple spatial dimensions can make analytic solution difficult. Although such complexities increase the difficulty of solving for the transport in a given system, they also increase the richness of the physics involved. A number of approaches and applications close to the spirit of this work are available,[5–12] including works by the present author.[13,14]

Additional complications occur in systems where fluxes cross one or more interfaces, as in most modern devices. (In reality, every real-world electronic system involves electric flow across interfaces, e.g., any soldered joint.) The potentially nontrivial contributions of interfaces to transport therefore bear study. The effect of boundaries on flow was first studied in the context of heat flow between a superfluid and an ordinary solid by Kapitza (see Ref. 15). More relevant to modern devices, the first analytic theory for interfacial transport including spin using irreversible thermodynamics was done by Johnson and Silsbee.[16] Although this work is very general, it does not consider spin flip due to the interface, nor does it find the entropy production or heating rate. It also considers only the case of metals.

This dissertation addresses such concerns. For the general case, it finds the rate of heating and entropy production due to transport in bulk and across interfaces, and finds the conditions for interfacial heating to dominate bulk heating. In addition to metals, it includes semiconductors and insulators, and discusses the parallels between flow in semiconductors and in spintronics devices. The wide applicability of irre-

versible thermodynamics to modern devices is demonstrated by consideration of three particular systems: a long-considered system involving particle flow via electronic and ionic transport; a more recently observed system involving bulk and interfacial magnetic flow via spin-up and spin-down electron transport; and a very recently observed system involving bulk and interfacial thermal flow via phonon (lattice vibration) and magnon (spin wave) transport.

CHAPTER II

RATE OF HEATING AND ENTROPY PRODUCTION DUE TO BULK AND INTERFACIAL TRANSPORT

Interfaces have a marked effect on flow. It is known that apparent voltage and temperature discontinuities, determined by extrapolation from the bulk, appear at interfaces in the presence of heat or electric current. For small currents, these discontinuities are proportional to the heat or electric current. For heat current, the coefficient of proportionality is known as the thermal boundary resistance, and was first studied at low temperatures by Kapitza for the solid–liquid ^{4}He interface.[15,17–19] For electric current, the coefficient of proportionality is known as the surface resistance, or specific resistance.[20] In principle, there can also be off-diagonal terms, e.g., corresponding to a discontinuity in the temperature causing an electric current.[16] There also are spin-dependent conduction effects across surfaces, as studied, for example, in Refs. 16, 21, and 22.

Johnson and Silsbee[16] studied the surface and bulk transport coefficients including spin-dependent conduction and off-diagonal terms, but without considering details of the non-conservation of the spin current due to spin-flip processes, and did not study the rate of heating or entropy production near the surface. This chapter considers these non-conservation phenomena. It also includes the chemical potential μ of the charge-carriers. For metals, μ is nearly independent of carrier density and can be neglected (compared to electrical potential energy), but the same is not necessarily true for semiconductors or insulators, where small changes in carrier density can have a large effect on μ.

This chapter determines the conditions under which bulk heating dominates surface heating, and vice-versa. It also discusses the distinction between heating and

entropy production; the former implies the latter, but the converse is not true. (We note that the only commonly-known case where entropy production does not imply heating is that of thermal conduction.) It does not consider length scales so small that ordinary heat conduction (e.g., the Fourier law) is not expected to hold, due either to classical or quantum size effects.[23]

This dissertation does not consider systems for which the interface is a distinct thermodynamic system. For a system that is out of thermodynamic equilibrium a surface temperature may not be a well-defined quantity. (See Refs. 24 and 25 for molecular dynamics simulations of heat flow across an interface, which show a sharp temperature jump at the atomic level.) Moreover, thermometers that measure different properties, but are calibrated in the bulk, need not read equivalent temperatures near the surface. This is because near surfaces the thermal distribution function is not defined solely in terms of thermodynamic properties, but also in terms of surface solutions of the transport equation.[26,27]

Section A of this chapter calculates bulk and interfacial fluxes, heating rates, and entropy production in systems in which a single carrier is transported. It also discusses the distinction between heating and entropy production, giving some examples where the latter increases while the former remains constant. It further estimates the conditions under which entropy production from interfacial flow dominates that from bulk flow. Section B calculates fluxes, the rate of heating, and entropy production a two-carrier system, specifically considering up- and down-spin electrons; its results qualitatively apply to semiconductors where electrons and holes are the carriers. It also estimates when heating from interfacial spin currents is of comparable magnitude to heating from interfacial electric currents.

This chapter (and much of this dissertation) is related to recent work on "spin caloritronics," whereby heat currents can cause spin currents and spin currents can

cause heat currents.[28–30] (More precisely, gradients of temperature cause both heat and spin currents, as do gradients of spin-dependent potential.) The former, known as the spin-Seebeck effect, has recently been measured[31–33] using the inverse spin Hall effect, and in one case[33] the measurements (of an electrical voltage) display a profile that is associated with spatially exponential decay away from the heat input and output leads. Chapter V gives those details.

A. Single Carrier Systems

1. Rate of Entropy Production

For a single carrier conductor, we assume that the bulk energy density ε, bulk number density n, and bulk entropy density s are related by

$$d\varepsilon = Tds + \tilde{\mu}dn. \tag{2.1}$$

The electrochemical potential

$$\tilde{\mu} = \mu - e\phi, \tag{2.2}$$

where μ is the chemical potential. The continuity relations for the conserved number and energy densities are

$$\frac{\partial n}{\partial t} + \partial_i j_i^n = 0, \tag{2.3}$$

$$\frac{\partial \varepsilon}{\partial t} + \partial_i j_i^{\varepsilon} = 0. \tag{2.4}$$

The equation for the non-conserved entropy density is

$$\frac{\partial s}{\partial t} + \partial_i j_i^s \equiv \mathcal{S}_s \geq 0. \tag{2.5}$$

Alternatively one can use the dissipation function

$$R = T\mathcal{S}_s \tag{2.6}$$

as the primary quantity. R has the units of a rate of heating, but is only a rate of heating when energy is transformed into heat, not when it already is in the form of heat.

In considering heat transfer between systems at different temperatures, and in the absence of temperature jump effects, one must work with TR rather than the dissipation function R for the net entropy to increase. See Sec. 4.2.1 of Ref. 34.

Combining the above Eqs. (2.1)-(2.5) yields

$$\begin{aligned} 0 \leq T\mathcal{S}_s &= -\partial_i j_i^{\varepsilon} + \tilde{\mu}\partial_i j^n + T\partial_i j^s \\ &= \partial_i \left(-j_i^{\varepsilon} + \tilde{\mu} j_i^n + T j_i^s\right) - j_i^s \partial_i T - j_i^n \partial_i \tilde{\mu}. \end{aligned} \tag{2.7}$$

Following the approach of irreversible thermodynamics, this has been written as a single divergence term and the sum of products of unknown fluxes with gradients of the thermodynamic intensive quantities. Since the divergence term may be either positive or negative, it must always be zero to ensure that entropy never decreases, i.e., $\mathcal{S}_s \geq 0$. Thus

$$j_i^{\varepsilon} = \tilde{\mu} j_i^n + T j_i^s, \tag{2.8}$$

and

$$0 \leq T\mathcal{S}_s = -j_i^s \partial_i T - j_i^n \partial_i \tilde{\mu}. \tag{2.9}$$

As in the example in Chapter I, if there is no number current j_i^n, then the energy current j_i^{ϵ} consists only of a heat current $j_i^Q \equiv T j_i^s$. In that case the energy is only in the form of heat, and there is no additional heat production, although there is entropy production.

2. Bulk Fluxes and Rate of Entropy Production

In bulk, by the non-negativity of Eq. (2.9), the linearized (that is, neglecting second and higher order derivatives) flux densities take the form

$$j_i^s = -\frac{\kappa}{T}\partial_i T - L_{sn}\partial_i\tilde{\mu}, \tag{2.10}$$

$$j_i^n = -L_{ns}\partial_i T - \frac{\sigma}{e^2}\partial_i\tilde{\mu}, \tag{2.11}$$

where κ is the (positive) thermal conductivity, σ is the (positive) electrical conductivity, e is electric charge, and $L_{sn} = L_{ns}$ by the Onsager principle. Irreversible thermodynamics cannot provide values for any of these material-dependent coefficients, but Kubo theory can give these coefficients in terms of equilibrium correlation functions.[11,12,35] Moreover, although they are treated in this chapter, cross-terms are typically neglected in normal mode calculations for real world systems (including the calculations in Chaps. IV and V).

By Eqs. (2.9)-(2.11), the rate of entropy production in the bulk (per unit volume) is given by

$$\mathcal{S}_s = \frac{\kappa}{T^2}\left(\partial_i T\right)^2 + \frac{\sigma}{e^2 T}\left(\partial_i\tilde{\mu}\right)^2 + 2\frac{L_{sn}}{T}\left(\partial_i\tilde{\mu}\right)\left(\partial_i T\right). \tag{2.12}$$

By $\mathcal{S}_s \geq 0$ we have $\kappa \geq 0$, $\sigma \geq 0$, and $L_{sn}^2 \leq (\sigma\kappa)/(e^2 T)$. As noted in the introduction, pure thermal conduction already involves heat flow, so there is no production of heat in that case.

On the other hand, the entropy production due to current flow does cause heating, at the rate per volume of

$$R \equiv -j_i^n\partial_i\tilde{\mu} = \frac{\sigma}{e^2}\left(\partial_i\tilde{\mu}\right)^2 + L_{sn}(\partial_i\tilde{\mu})(\partial_i T). \tag{2.13}$$

Only the first term is Joule heating. The second term is like Thomson heating, in that it can have either sign. (Because Thomson heating, as discussed in Ref. 36, involves

the artificial maintenance of the same temperature distribution both with and without current flow, we hesitate to call this cross-term Thomson heating, although the latter involves both a temperature gradient and a voltage gradient.) For a large $\partial_i T$, this term can even dominate, but the net entropy production $\mathcal{S}_s$ remains non-negative.

3. Distinguishing Heating from Entropy Production

When calculating the rate of heating, this elimination, by hand, of the part of $T\mathcal{S}_s$ associated with heat flow is related to a similar effect discussed in Ref. 37 of damping of a sound wave. In that case the mechanical energy $E_{\rm mech}$ of the sound wave (which, implicitly, has zero entropy) dissipates into heat, which increases the entropy S of the background system by $\dot{E}_{\rm mech} = -T\dot{S}$. $\dot{E}_{\rm mech}$ is determined by a volume integration over the equivalent of R, evaluated for the sound wave, and is proportional to the square of the sound wave amplitude (including temperature oscillations in the sound wave). This results in hot spots (as, for a standing wave, is perhaps familiar from a microwave oven) that separately diffuse. However, this energy is already heat energy. Once deposited as heat, its diffusion causes a further increase in entropy, but no additional energy goes into the system.

Another example where entropy increase and heating are distinct is a gas of interacting atoms that has a multi-nanometer range for repulsion. Let all the atoms initially be placed within an interaction volume of one another. When they become thermally disordered, the increase in entropy can be treated as in the present work, but only the interaction energy converts into heat.

In spin-Seebeck experiments,[31–33] the applied thermal gradient causes heat flow between various subsystems, which in turn induces a spin current.[38] Although it increases the entropy of the system, the heat flow is not associated with heating; however, spin and electrical currents both increase the entropy of the system and

cause heating. Spin currents are addressed in Section B. The spin-Seebeck effect is discussed in detail in Chapter V.

4. Surface Fluxes and Rate of Entropy Production

At low temperatures, or when the material properties change significantly on crossing the interface (int), the changes in T and μ at the interface can be very large, and Eq. (2.12) integrated over the surface region (assuming that T and $\tilde{\mu}$ are well-defined in this region) can be smaller than the surface entropy production rate $\mathcal{S}_{\rm int}$. We now consider $\mathcal{S}_{\rm int}$. This involves considerations of the characteristic mean-free-path $\ell_{\rm mfp}$ and the distance a over which the thermodynamic quantities adjust to the surface.

The total rate (per unit area) of entropy production at the interface, $\mathcal{S}_{\rm int}$, is obtained by integrating the volume rate of entropy production over the surface region. By Eq. (2.9), taking flow only in the x-direction,

$$\mathcal{S}_{\rm int} = \int_{\rm int} dx \mathcal{S}_s = -\int_{\rm int} dx \frac{(j_x^s \partial_x T + j_x^n \partial_x \tilde{\mu})}{T}. \tag{2.14}$$

In steady-state, the energy and number flux densities given in Eqs. (2.8) and (2.11) are uniform across this region. If T and μ are also nearly uniform, by Eq. (2.8) the entropy flux density will also be nearly uniform, so

$$\begin{aligned} \mathcal{S}_{\rm int} &\approx -\frac{j_x^s}{T}\int_{\rm int} dx \partial_x T - \frac{j_x^n}{T}\int_{\rm int} dx \partial_x \tilde{\mu} \\ &\approx -\frac{j_x^s}{T}\left(\Delta T\right)_{\rm int} - \frac{j_x^n}{T}\left(\Delta\tilde{\mu}\right)_{\rm int}. \end{aligned} \tag{2.15}$$

Here $(\Delta T)_{\rm int}$ and $(\Delta\tilde{\mu})_{\rm int}$ are the differences of temperature and electrochemical potential across the interface region. On setting $\tilde{\mu} = \mu - e\phi \approx -e\phi$ (not appropriate for insulators or semiconductors), Eq. (2.15) agrees with Eq. (12) of Ref. 16.

We now apply the same type of irreversible thermodynamics approach to the

surface region as to the bulk in Section 2. In bulk the fluxes are proportional to the gradients of the intensive thermodynamic quantities. At a surface, the fluxes are taken to be proportional to the differences across the interface of the intensive thermodynamic quantities. Thus

$$j^s = -\frac{h_K}{T}\,(\Delta T)_{\rm int} - L'_{sn}\,(\Delta\tilde{\mu})_{\rm int}\,, \tag{2.16}$$

$$j^n = -L'_{ns}\,(\Delta T)_{\rm int} - \frac{\bar{g}}{e^2}\,(\Delta\tilde{\mu})_{\rm int}\,. \tag{2.17}$$

Here, h_K is the thermal boundary resistance, and is of the order of the difference in the products of the specific heat times a characteristic sound velocity on each side, and $\bar{g}$ is a surface conductance, with units $1/\Omega$-m^2. (We reserve g for the g-factor of the charge carriers; for metals $g \approx -2$.) By the Onsager principle (assumed to apply at surfaces as well as in bulk), $L'_{sn} = L'_{ns}$. Thus, the total rate of entropy across the surface region is

$$\mathcal{S}_{\rm int} \approx \frac{h_K}{T^2}\,(\Delta T)^2_{\rm int} + \frac{\bar{g}}{e^2 T}\,(\Delta\tilde{\mu})^2_{\rm int} + 2\frac{L'_{sn}}{T}\,(\Delta\tilde{\mu})_{\rm int}\,(\Delta T)_{\rm int}\,. \tag{2.18}$$

The condition $\mathcal{S}_{\rm int} \geq 0$ implies that $h_K \geq 0$, $\bar{g} \geq 0$, and $L'^2_{sn} \leq (\bar{g}h_K)/(e^2T)$.

5. Estimates

We consider a metal-metal interface, for which $\tilde{\mu} \approx -e\phi$. For characteristic values of current density[39] ($J \approx 10^{12}$ A/m^2) and surface conductance[20] ($\bar{g} \approx 10^{15}$ $1/\Omega$-m^2), a characteristic potential difference across the interface is $(\Delta\phi)_{\rm int} \approx 10^{-3}$ V. Then, when $(\Delta T)_{\rm int} = 0$ the appropriate part of $T\mathcal{S}_{\rm int}$ gives a rate of heating per unit area of

$$\mathcal{R}_{\rm int} = T\mathcal{S}_{\rm int} = \frac{\bar{g}}{e^2}(\Delta\tilde{\mu})^2_{\rm int} \approx \bar{g}(\Delta\phi)^2_{\rm int} \approx 10^9 \frac{\rm W}{\rm m^2}. \tag{2.19}$$

We may also apply this to a multilayer system where interference effects between

the layers, and where mean-free paths connecting them, can be neglected.[22] At a separation s of 100 nm between layers, the net effect of the interfaces corresponds to a bulk conductance of $\bar{g}s \approx 10^8$ 1/Ω-m and the rate of heating per unit volume (from the values above) is approximately 10^{16} W/m^3.

As already discussed, there is entropy production because of heat flow, but there is no heating rate associated with heat flux, because the energy is already in the form of heat. For an interface across which there is only a temperature jump, the rate of entropy production is given by

$$\mathcal{S}_{\rm int} \approx \frac{h_K}{T^2} \left(\Delta T\right)^2_{\rm int} . \tag{2.20}$$

Nevertheless, there is an *apparent* heating rate, whose value we now determine. Typical values for thermal boundary resistance[19] ($R_K = h_K^{-1} \approx 2{\times}10^{-3}$K-m^2/W at $T = 1$K for Rh:Fe on Al_2O_3) and energy flux ($J^\varepsilon \approx 10^{-7}$W/m^2) give a value for the temperature difference across the interface of $(\Delta T)_{\rm int} \approx 2 \times 10^{-2}$K, so $(\Delta T)_{\rm int}/T \approx 0.02$. Then

$$T\mathcal{S}_{\rm int} = \frac{h_K}{T}(\Delta T)^2_{\rm int} \approx 0.2\frac{\rm W}{\rm m^2}. \tag{2.21}$$

This apparent heating rate is about ten orders of magnitude smaller than for the example of a true surface heating rate due to the electrochemical potential gradient, given above in Eq. (2.19). Thus, if thermal flow were erroneously included in calculations of heating in a real world system, the error would likely be negligible.

6. Entropy Production Rates: Bulk *vs* Surface

We now consider the conditions under which the interface entropy production rate $\mathcal{S}_{\rm int}$ can dominate over the near-surface space-integral $\mathcal{S}_{\rm bulk}$ of the bulk entropy production rate $\mathcal{S}_s$. For simplicity we consider only carrier flow in the x-direction,

with no cross-terms, so $L_{sn} \approx 0$.

Three characteristic lengths are associated in this problem: one associated with transport (a mean-free path $\ell_{\rm mfp}$), a characteristic sample size (d), and a distance over which there is an interface adjustment (a).

Equating the bulk and surface carrier currents μj^n and using $\partial_x \tilde{\mu} \sim (\Delta\tilde{\mu})_{\rm bulk}/d$ gives

$$(\Delta\tilde{\mu})_{\rm int} \approx \frac{\sigma}{hd} (\Delta\tilde{\mu})_{\rm bulk} \,. \tag{2.22}$$

With this result, Eq. (2.13), and Eq. (2.18), for $(\Delta T)_{\rm int} = 0$ the integrated bulk rate of entropy production near the surface (per unit area) is on the order of

$$\mathcal{S}_{\rm bulk} \sim a\sigma \frac{(\Delta\tilde{\mu})^2_{\rm bulk}}{d^2} \sim a\frac{\bar{g}^2}{\sigma}(\Delta\tilde{\mu})^2_{\rm int} \sim \frac{a\bar{g}}{\sigma}\mathcal{S}_{\rm int}. \tag{2.23}$$

Thus, when $a\bar{g}/\sigma \gg 1$ (good electrical matching between the two materials), the contributions from the bulk electrochemical potential gradients dominate those near the surface. On the other hand, when $a\bar{g}/\sigma \ll 1$ (poor electrical matching between the two materials), the contribution from the surface jump in electrochemical potential dominates.

B. Two-Carrier Systems – Spin

For itinerant magnets the theory should include two carriers. A specific case would be the interface between a metal and a magnetic material, where spin-up and spin-down electrons have different electrochemical potentials on each side of the interface. (The same approach can be applied to interfaces involving electrons and holes, rather than up-spin and down-spin electrons. Just as the spin current is not conserved, because up-spins and down-spins can flip, so too the difference between the electric currents due to electrons and holes is not conserved, due to electron-hole

recombination.) For simplicity we consider that the magnetization direction $\hat{M}$ is fixed, and takes the same value in both materials. Because of spin-flip processes even a nonmagnetic material can develop a magnetization (this effect, known as spin accumulation, is discussed in more detail in Chap. IV). With a somewhat different notation, and including terms associated with $\partial_i \hat{M}$, for the bulk many of these results (but not surface heating) have been derived previously.[40] Transport of spin across surfaces was considered by a number of authors, but they did not consider heating rates.[16,21,22]

Before presenting the thermodynamics a few definitions are needed. First, the theory employs the "magnetization potential" $-\vec{H}^*$. $\vec{H}^*$ is the difference between the external fields (magnetic, anisotropy, dipole) and the internal field due to exchange. In equilibrium $\vec{H}^* = \vec{0}$. For a more detailed discussion of $\vec{H}^*$, see Ref. 40. The *chemical* potentials are denoted by $\mu_\uparrow$ and $\mu_\downarrow$, and are determined, for example, from energy band theory. The *electrochemical* potentials are denoted by $\tilde{\mu}_\uparrow$ and $\tilde{\mu}_\downarrow$, and satisfy $\tilde{\mu}_{(\uparrow,\downarrow)} = \mu_{(\uparrow,\downarrow)} - e\phi$. Finally, the *magnetoelectrochemical* potentials are denoted by $\bar{\mu}_\uparrow$ and $\bar{\mu}_\downarrow$, and satisfy

$$\bar{\mu}_{(\uparrow,\downarrow)} = \mu_{(\uparrow,\downarrow)} - e\phi \pm (\gamma\hbar/2)\vec{H}^* \cdot \hat{M}, \tag{2.24}$$

where γ is the gyromagnetic ratio, which satisfies

$$\gamma = |g|\mu_B/\hbar. \tag{2.25}$$

Here g is the electron spin g-factor and μ_B is the Bohr magneton. In some cases it is more convenient to write in terms of μ_B rather than γ. In equilibrium $\bar{\mu}_\uparrow = \bar{\mu}_\downarrow$.

We note that there is some ambiguity in the definition of the external fields and the internal fields, but there is no ambiguity in the definition of $\vec{H}^*$. For example, the lattice anisotropy and the dipole fields depends on the magnetization, and for that

reason can be considered to be internal or external. The uniform exchange field is certainly internal, but the non-uniform exchange field might be considered internal or external. Only the applied magnetic field and the internal exchange field should be uniquely considered external and internal.

1. Rate of Entropy Production

With these definitions, the bulk energy density ε, bulk electron number densities for up spins $n_\uparrow$ and down spins $n_\downarrow$, and bulk entropy density s are related by

$$d\varepsilon = Tds + \bar{\mu}_\uparrow dn_\uparrow + \bar{\mu}_\downarrow dn_\downarrow. \tag{2.26}$$

The continuity relations for energy density and entropy density, Eqs. (2.4) and (2.5) respectively, still apply. Continuity relations for the (non-conserved) number flux densities are

$$\frac{\partial n_\uparrow}{\partial t} + \partial_i j_{\uparrow i} = S_\uparrow, \tag{2.27}$$

$$\frac{\partial n_\downarrow}{\partial t} + \partial_i j_{\downarrow i} = S_\downarrow = -S_\uparrow, \tag{2.28}$$

where $S_\uparrow$ is the (density) rate at which spin-down electrons flip to spin-up electrons. These forms ensure that the total number current,

$$J_i^n \equiv (j_{\uparrow i} + j_{\downarrow i}), \tag{2.29}$$

is conserved, since summation of Eqs. (2.27) and (2.28) gives

$$\frac{\partial \left(n_\uparrow + n_\downarrow\right)}{\partial t} + \partial_i J_i^n = 0. \tag{2.30}$$

However, the dimensionless spin current,

$$J_i^\sigma \equiv j_{\uparrow i} - j_{\downarrow i}, \tag{2.31}$$

is not conserved:

$$\frac{\partial\left(n_{\uparrow}-n_{\downarrow}\right)}{\partial t}+\partial_i J_i^{\sigma}=2S_{\uparrow}. \tag{2.32}$$

By Eqs. (2.4), (2.5), (2.27) and (2.28), we have

$$\begin{aligned} 0\leq T\mathcal{S}_s =&\partial_i\left(-j_i^{\varepsilon}+Tj_i^s+\bar{\mu}_{\uparrow}j_{\uparrow i}+\bar{\mu}_{\downarrow}j_{\downarrow i}\right)\\ &-j_i^s\partial_i T-j_{\uparrow i}\partial_i\bar{\mu}_{\uparrow}-j_{\downarrow i}\partial_i\bar{\mu}_{\downarrow}-\left(\bar{\mu}_{\uparrow}-\bar{\mu}_{\downarrow}\right)S_{\uparrow}. \end{aligned} \tag{2.33}$$

As before, for the entropy to never decrease, the divergence must be zero, so we take

$$j_i^{\varepsilon}=Tj_i^s+\bar{\mu}_{\uparrow}j_{\uparrow i}+\bar{\mu}_{\downarrow}j_{\downarrow i}. \tag{2.34}$$

Then,

$$T\mathcal{S}_s=-j^s\partial_i T-j_{\uparrow}\partial_i\bar{\mu}_{\uparrow}-j_{\downarrow}\partial_i\bar{\mu}_{\downarrow}-\left(\bar{\mu}_{\uparrow}-\bar{\mu}_{\downarrow}\right)S_{\uparrow}. \tag{2.35}$$

Not only does each flux (carrier current and the heat current) contribute to the rate of heating, but there is also a contribution from the source term for spin-flip. Each flux appears with its conjugate "force" or thermodynamic gradient, whereas the source term appears with a difference in thermodynamic potentials. (Reference 41 finds a similar heating rate for semiconductors, where the source term associated with electron and hole recombination appears with the sum of electron and hole potentials.) For conserved spin current (i.e., $S_{\uparrow}=0$), Eq. (2.35) agrees with Eq. (53) of Ref. 16.

2. Bulk Fluxes and Rate of Entropy Production

In the bulk, from Eq. (2.35), we take the linearized flux densities to be

$$j_i^s=-\frac{\kappa}{T}\partial_i T-L_{s\uparrow}\partial_i\bar{\mu}_{\uparrow}-L_{s\downarrow}\partial_i\bar{\mu}_{\downarrow}, \tag{2.36}$$

$$j_{\uparrow i}=-L_{\uparrow s}\partial_i T-\frac{\sigma_{\uparrow}}{e^2}\partial_i\bar{\mu}_{\uparrow}-L_{\uparrow\downarrow}\partial_i\bar{\mu}_{\downarrow}, \tag{2.37}$$

$$j_{\downarrow i}=-L_{\downarrow s}\partial_i T-L_{\downarrow\uparrow}\partial_i\bar{\mu}_{\uparrow}-\frac{\sigma_{\downarrow}}{e^2}\partial_i\bar{\mu}_{\downarrow}, \tag{2.38}$$

where $\sigma_\uparrow$ and $\sigma_\downarrow$ are the respective electrochemical conductivities of up spins and down spins. By the Onsager principle, $L_{\uparrow\downarrow} = L_{\downarrow\uparrow}$, $L_{\uparrow s} = L_{s\uparrow}$, and $L_{s\downarrow} = L_{\downarrow s}$. Further, to ensure the non-negativity of Eq. (2.35) even in the absence of gradients of intensive variables, $S_\uparrow$ is driven by the difference in electrochemical potentials

$$S_\uparrow = -\alpha \left(\bar{\mu}_\uparrow - \bar{\mu}_\downarrow \right), \tag{2.39}$$

where α is positive, and proportional to a characteristic spin-flip rate. (A similar relation holds in semiconductors, where, rather than up- and down-spin scattering, there is electron and hole recombination.[41])

We now expand the electromagnetochemical potentials as

$$\bar{\mu}_\uparrow = \bar{\mu}_\uparrow^{(0)} + \frac{\partial \bar{\mu}_\uparrow}{\partial n_\uparrow} \delta n_\uparrow, \quad \bar{\mu}_\downarrow = \bar{\mu}_\downarrow^{(0)} + \frac{\partial \bar{\mu}_\downarrow}{\partial n_\downarrow} \delta n_\downarrow. \tag{2.40}$$

Using $\bar{\mu}_\uparrow^{(0)} = \bar{\mu}_\downarrow^{(0)}$ we then have

$$S_\uparrow = -\alpha \left(\frac{1}{\bar{N}_\uparrow} \delta n_\uparrow - \frac{1}{\bar{N}_\downarrow} \delta n_\downarrow \right), \tag{2.41}$$

where $\bar{N}_\uparrow \equiv (\partial n_\uparrow / \partial \bar{\mu}_\uparrow)$ and $\bar{N}_\downarrow \equiv (\partial n_\downarrow / \partial \bar{\mu}_\downarrow)$ are the densities of states.

We now relate this to T_1 relaxation of the magnetization M of a uniform system, where

$$M = -\frac{|g|\mu_B}{2} (n_\uparrow - n_\downarrow). \tag{2.42}$$

Recall that g is the charge carrier g-factor. Particle conservation gives $\delta n_\downarrow = -\delta n_\uparrow$, so $\delta M = -|g|\mu_B \delta n_\uparrow$ and $S_\uparrow = -\alpha(\bar{N}_\uparrow^{-1} + \bar{N}_\downarrow^{-1}) \delta n_\uparrow$. Then Eq. (2.32), with $\partial_i J_i^\sigma$ neglected, yields

$$\frac{\partial M}{\partial t} = -|g|\mu_B \frac{\partial}{\partial t} (\delta n_\uparrow) = -\frac{M}{T_1}, \tag{2.43}$$

where $T_1^{-1} = \alpha(\bar{N}_\uparrow^{-1} + \bar{N}_\downarrow^{-1})$.

The dissipation function $R = T\mathcal{S}_s$ is given for the bulk by

$$\begin{aligned} T\mathcal{S}_s =& \frac{\kappa}{T}\left(\partial_i T\right)^2 + \frac{\sigma_\uparrow}{e^2}\left(\partial_i \bar{\mu}_\uparrow\right)^2 + \frac{\sigma_\downarrow}{e^2}\left(\partial_i \bar{\mu}_\downarrow\right)^2 + 2L_{s\uparrow}\left(\partial_i \bar{\mu}_\uparrow\right)\left(\partial_i T\right) \\ &+ 2L_{s\downarrow}\left(\partial_i \bar{\mu}_\downarrow\right)\left(\partial_i T\right) + 2L_{\uparrow\downarrow}\left(\partial_i \bar{\mu}_\uparrow\right)\left(\partial_i \bar{\mu}_\downarrow\right) + \alpha\left(\bar{\mu}_\uparrow - \bar{\mu}_\downarrow\right)^2. \end{aligned} \tag{2.44}$$

This is sufficiently complex that each term deserves comment. The term in $(\partial_i T)^2$ is from heat current, the terms in $(\partial_i \bar{\mu}_\uparrow)^2$ and $(\partial_i \bar{\mu}_\downarrow)^2$ are from Joule losses of the individual carriers,[42] the next three are cross-terms, and the last term gives the dissipation due to spin-flip processes. $\mathcal{S}_s \geq 0$ forces various conditions on both the diagonal and the cross-terms, of which the latter usually are small. The diagonal terms satisfy $\kappa \geq 0$, $\sigma_\uparrow \geq 0$, $\sigma_\downarrow \geq 0$, and $\alpha \geq 0$. Equation (2.44) indicates that it is not the current or spin current (both of them thermodynamic fluxes) that determines the rate of entropy production and heating, but rather the gradients of the magnetoelectrochemical potentials (both of them thermodynamic forces).

3. Surface Rate of Entropy Production

Consider flow along x, so that we may drop the directional indices on the fluxes. Then, rewriting Eq. (2.35) with Eqs. (2.29) and (2.31) gives

$$T\mathcal{S}_s = -j^s \partial_x T - \frac{1}{2}J^n \partial_x\left(\bar{\mu}_\uparrow + \bar{\mu}_\downarrow\right) - \frac{1}{2}J^\sigma \partial_x\left(\bar{\mu}_\uparrow - \bar{\mu}_\downarrow\right) - \left(\bar{\mu}_\uparrow - \bar{\mu}_\downarrow\right) S_\uparrow. \tag{2.45}$$

In steady-state J^n is constant across the interface region, but J^σ is not. Moreover, j^s is not obviously a near-conserved quantity, unlike for a single carrier. However, since j^ε is conserved, we use Eq. (2.34) to write

$$j^s = \frac{1}{T}j^\varepsilon - \frac{1}{2}J^n\left(\frac{\bar{\mu}_\uparrow}{T} + \frac{\bar{\mu}_\downarrow}{T}\right) - \frac{1}{2}J^\sigma\left(\frac{\bar{\mu}_\uparrow}{T} - \frac{\bar{\mu}_\downarrow}{T}\right). \tag{2.46}$$

With both J^σ and the difference in electromagnetochemical potentials considered to be first order in small deviations from equilibrium, the last term is second order. Thus j^s is a nearly-conserved quantity.

Integrating the volume rate of heating given in Eq. (2.45) over the interface region yields

$$\begin{aligned} T\mathcal{S}_{\text{int}} = &- j^s \left(\Delta T\right)_{\text{int}} - \frac{1}{2} J^n \left[\left(\Delta\bar{\mu}_\uparrow\right)_{\text{int}} + \left(\Delta\bar{\mu}_\downarrow\right)_{\text{int}}\right] \\ &- \frac{1}{2}\int_{\text{int}} dx J^\sigma \partial_x \left(\bar{\mu}_\uparrow - \bar{\mu}_\downarrow\right) - \int_{\text{int}} dx \left(\bar{\mu}_\uparrow - \bar{\mu}_\downarrow\right) S_\uparrow. \end{aligned} \tag{2.47}$$

Integrating the third term by parts and using Eq. (2.32) with the time-derivative set to zero (steady-state, so that $\partial_x J^\sigma = 2S_\uparrow$) gives

$$-\frac{1}{2}\int_{\text{int}} dx J^\sigma \partial_x \left(\bar{\mu}_\uparrow - \bar{\mu}_\downarrow\right) = \int_{\text{int}} dx \left(\bar{\mu}_\uparrow - \bar{\mu}_\downarrow\right) S_\uparrow - \frac{1}{2}\Delta\big(\left(\bar{\mu}_\uparrow - \bar{\mu}_\downarrow\right) J^\sigma\big)_{\text{int}}. \tag{2.48}$$

The first term on the RHS of Eq. (2.48) cancels the last term on the RHS of Eq. (2.47), and the second term is evaluated on each side of the interface. Then Eq. (2.47) becomes

$$T\mathcal{S}_{\text{int}} = -j^s \left(\Delta T\right)_{\text{int}} - \frac{1}{2} J^n \left[\left(\Delta\bar{\mu}_\uparrow\right)_{\text{int}} + \left(\Delta\bar{\mu}_\downarrow\right)_{\text{int}}\right] - \frac{1}{2}\Delta\big(\left(\bar{\mu}_\uparrow - \bar{\mu}_\downarrow\right) J^\sigma\big)_{\text{int}}. \tag{2.49}$$

The last term, which is a new result, appears to be well-defined, but because J^σ is not conserved, it is not clear how to interpret this unambiguously. Nevertheless, if the spin diffusion length, over which up and down spins flip, is sufficiently long relative to the surface region, so that one measures J^σ within a spin diffusion length of the interface, then this term should be well-defined. In what follows we will assume this to be the case.

4. Surface Fluxes and Rate of Entropy Production

The entropy and the spin up and spin down number fluxes can be linearized in differences in the appropriate intensive thermodynamic quantities across the interface, so

$$j^s = -\frac{h_K}{T}\left(\Delta T\right)_{\rm int} - L'_{s\uparrow}\left(\Delta\bar{\mu}_\uparrow\right)_{\rm int} - L'_{s\downarrow}\left(\Delta\bar{\mu}_\downarrow\right)_{\rm int}, \tag{2.50}$$

$$j_\uparrow = -L'_{\uparrow s}\left(\Delta T\right)_{\rm int} - \frac{g_\uparrow}{e^2}\left(\Delta\bar{\mu}_\uparrow\right)_{\rm int} - L'_{\uparrow\downarrow}\left(\Delta\bar{\mu}_\downarrow\right)_{\rm int}, \tag{2.51}$$

$$j_\downarrow = -L'_{\downarrow s}\left(\Delta T\right)_{\rm int} - L'_{\downarrow\uparrow}\left(\Delta\bar{\mu}_\uparrow\right)_{\rm int} - \frac{g_\downarrow}{e^2}\left(\Delta\bar{\mu}_\downarrow\right)_{\rm int}. \tag{2.52}$$

Here $g_\uparrow$ and $g_\downarrow$ are surface conductances of spin up and spin down particles, and by the Onsager principle $L'_{\uparrow\downarrow} = L'_{\downarrow\uparrow}$, $L'_{\uparrow s} = L'_{s\uparrow}$, and $L'_{s\downarrow} = L'_{\downarrow s}$. For a calculation of a spin-dependent interfacial surface resistance, see Ref. 43.

By the definitions given by Eqs. (2.29) and (2.31), the total number current and spin current can be written from Eqs. (2.51)-(2.52) as

$$J^n = -\left(L'_{\uparrow s} + L'_{\downarrow s}\right)\left(\Delta T\right)_{\rm int} - \left(\frac{g_\uparrow}{e^2} + L'_{\downarrow\uparrow}\right)\left(\Delta\bar{\mu}_\uparrow\right)_{\rm int} - \left(\frac{g_\downarrow}{e^2} + L'_{\uparrow\downarrow}\right)\left(\Delta\bar{\mu}_\downarrow\right)_{\rm int}, \tag{2.53}$$

$$J^\sigma = -\left(L'_{\uparrow s} - L'_{\downarrow s}\right)\left(\Delta T\right)_{\rm int} - \left(\frac{g_\uparrow}{e^2} - L'_{\downarrow\uparrow}\right)\left(\Delta\bar{\mu}_\uparrow\right)_{\rm int} + \left(\frac{g_\downarrow}{e^2} - L'_{\uparrow\downarrow}\right)\left(\Delta\bar{\mu}_\downarrow\right)_{\rm int}. \tag{2.54}$$

Substitution for j^s and J^n from Eqs. (2.50) and (2.53) into Eq. (2.49) yields

$$\begin{aligned} T\mathcal{S}_{\rm int} = &-\frac{1}{2}\Delta\left(\left(\bar{\mu}_\uparrow - \bar{\mu}_\downarrow\right)J^\sigma\right)_{\rm int} + \frac{h_K}{T}\left(\Delta T\right)^2_{\rm int} + \frac{1}{2}\left(\frac{g_\uparrow}{e^2} + L'_{\downarrow\uparrow}\right)\left(\Delta\bar{\mu}_\uparrow\right)^2_{\rm int} \\ &+ \frac{1}{2}\left(\frac{g_\downarrow}{e^2} + L'_{\downarrow\uparrow}\right)\left(\Delta\bar{\mu}_\downarrow\right)^2_{\rm int} + \frac{1}{2}\left(3L'_{s\uparrow} + L'_{\downarrow s}\right)\left(\Delta\bar{\mu}_\uparrow\right)_{\rm int}\left(\Delta T\right)_{\rm int} \\ &+ \frac{1}{2}\left(3L'_{s\downarrow} + L'_{\uparrow s}\right)\left(\Delta\bar{\mu}_\downarrow\right)_{\rm int}\left(\Delta T\right)_{\rm int} + \frac{1}{2}\left(\frac{g_\uparrow + g_\downarrow}{e^2} + 2L'_{\downarrow\uparrow}\right)\left(\Delta\bar{\mu}_\uparrow\right)_{\rm int}\left(\Delta\bar{\mu}_\downarrow\right)_{\rm int}. \end{aligned} \tag{2.55}$$

If the spin current J^σ is approximately uniform near the surface, then use of

Eq. (2.54) simplifies Eq. (2.55) to

$$\begin{aligned} T\mathcal{S}_{\rm int} =& \frac{h_K}{T}\left(\Delta T\right)_{\rm int}^2 + \frac{g_\uparrow}{e^2}\left(\Delta\bar{\mu}_\uparrow\right)_{\rm int}^2 + \frac{g_\downarrow}{e^2}\left(\Delta\bar{\mu}_\downarrow\right)_{\rm int}^2 + 2L'_{s\uparrow}\left(\Delta\bar{\mu}_\uparrow\right)_{\rm int}\left(\Delta T\right)_{\rm int} \\ & + 2L'_{s\downarrow}\left(\Delta\bar{\mu}_\downarrow\right)_{\rm int}\left(\Delta T\right)_{\rm int} + 2L'_{\downarrow\uparrow}\left(\Delta\bar{\mu}_\uparrow\right)_{\rm int}\left(\Delta\bar{\mu}_\downarrow\right)_{\rm int}. \end{aligned} \tag{2.56}$$

as in Ref. 16, which gives an approximation for each of the coefficients.

5. Comparison of Electric and Spin Current Heating

Equation (2.56) permits a comparison of surface heating due to electric current (equivalently, due to a voltage jump across the surface region) with heating due to spin current (equivalently, due to the difference in $\vec{H}^* \cdot \hat{M}$ across the surface region). We consider a metal-metal interface where temperature is uniform, spin is conserved across the interface, and $g_\uparrow \approx g_\downarrow \approx \bar{g}/2$.

For the purposes of estimation, we neglect the chemical potentials $\mu_\uparrow$ and $\mu_\downarrow$, appropriate for metals. The limitations of this approximation are discussed above. Then Eq. (2.24) gives

$$\left(\Delta\bar{\mu}_{\uparrow,\downarrow}\right)_{\rm int}^2 \approx -e^2(\Delta\phi)_{\rm int}^2 + \frac{\gamma^2\hbar^2}{4}(\Delta H_\parallel^*)_{\rm int}^2 \mp \gamma\hbar e(\Delta\phi)_{\rm int}(\Delta H_\parallel^*)_{\rm int}. \tag{2.57}$$

Here we define

$$H_\parallel^* \equiv \vec{H}^* \cdot \hat{M}. \tag{2.58}$$

To find the heating due to $(\Delta\phi)_{\rm int}$ and $(\Delta H_\parallel^*)_{\rm int}$, we substitute Eq. (2.57) into the second and third terms of Eq. (2.56).

Suppose (as above) that the surface region is characterized by surface conductivity $\bar{g} = 10^{15}$ $1/\Omega$-m^2, and voltage difference $(\Delta\phi)_{\rm int} = 10^{-3}$ V. Neglecting cross-terms,

the rate of heating, per unit area, due *only* to the voltage difference is given by

$$\mathcal{R}_{\rm int}^{elec} = T\mathcal{S}_{\rm int}^{elec} \approx \bar{g}\left[(\Delta\phi)_{\rm int}\right]^2 \approx 10^9 \ \frac{\rm W}{\rm m^2}. \tag{2.59}$$

(Cancellation of the term proportional to $(\Delta\phi)_{\rm int}(\Delta H_{\parallel}^{*})_{\rm int}$ is only approximate.)

On the other hand, neglecting cross-terms, the rate of heating due *only* to spin current is given by

$$\mathcal{R}_{\rm int}^{spin} = T\mathcal{S}_{\rm int}^{spin} \approx \frac{\bar{g}}{e^2}\left[\frac{\gamma\hbar}{2}(\Delta H_{\parallel}^{*})_{\rm int}\right]^2 = \frac{\bar{g}}{4e^2}\left[|g|\mu_B(\Delta H_{\parallel}^{*})_{\rm int}\right]^2, \tag{2.60}$$

where the relation given by Eq. (2.25) has been used. For $|g| \approx 2$ and $\mu_B \approx 5.8 * 10^{-5}$ eV/T,

$$\mathcal{R}_{\rm int}^{spin} \approx 3.4 * 10^6 \left[(\Delta H_{\parallel}^{*})_{\rm int}\right]^2 \frac{\rm W}{\rm T^2{-}m^2}. \tag{2.61}$$

Thus, a $(\Delta H_{\parallel}^{*})_{\rm int} \approx 20$ T gives about the same heating as a voltage difference of $(\Delta\phi)_{\rm int} = 10^{-3}$ V.

CHAPTER III

METAL OXIDE GROWTH*

Most metals (M) develop a surface oxide layer (MO) on exposure to an oxygen atmosphere (O), as depicted in Fig. 1. This metal oxide layer develops as metal ions come in contact with oxide ions, presumably at the M/MO or the MO/O interface. Once any oxide is present, further oxide growth is determined by the physical and chemical properties of the oxide, through which ions (and electrons) must travel. The ions transported through the oxide may be either oxygen ions or metal ions, the latter being more likely as metal ions are generally more mobile, having lost electrons. In some cases, oxygen ions rather than metal ions are transported, e.g., the oxidation of copper.[44] The results of this chapter apply to either case, on application of simple mathematical transformations (such as sign reversal of the electric charge, $e \to -e$); this is discussed further below. Effects due to lattice mismatch between the oxide layer and the metal, such as the cracking or flaking of the oxide in the case of iron, are not considered here.

Some metals develop oxides with a self-limited thickness, e.g., aluminum. At room temperature, their respective oxides essentially stop growing at thicknesses on the order of 10 Å. Presumably, such oxides do not allow direct ionic conduction, so that growth is limited by an ionic tunneling length. Other metal oxides permit ionic flow, and may grow to macroscopic thicknesses. Metals which develop such freely-growing oxides include iron and zinc. These oxides are scientifically and industrially useful. The rate of metal oxide growth is therefore of interest in device manufacturing.

---

*Reprinted with permission from "Consistent Asymptotic Expansion of Mott's Solution for Oxide Growth" by M. R. Sears and W. M. Saslow, 2010. *Solid State Ionics*, 181, 1074, Copyright 2010 by Elsevier.

(For some metal oxide device applications, alternative growth methods are used, such as pulsed laser deposition; see, for instance, Ref. 45. However, for applications that require a metal/metal oxide interface, native growth of metal oxide in an oxygen environment is a technically simple and financially viable method.) As the size of devices decreases, precise determination of the oxide growth rate is required.

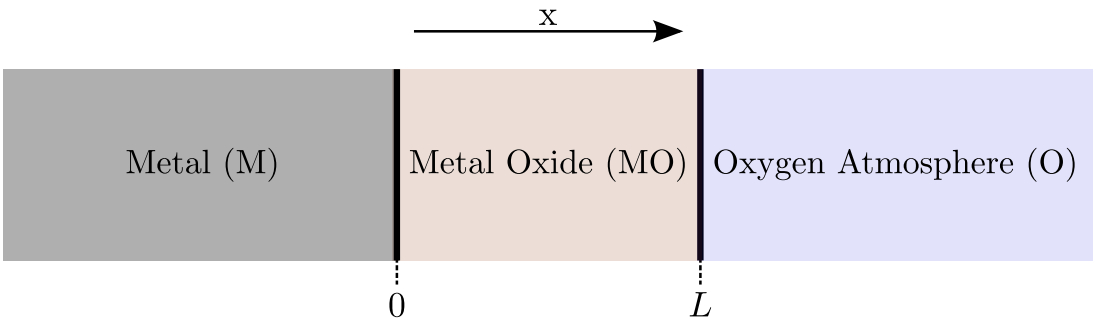

Fig. 1. Growth of metal oxide (MO) on metal (M) in an oxygen atmosphere (O). The thickness L, of interest for device fabrication, is dependent on the chemical reactions at the M/MO and MO/O surfaces. Because the amount of metal is reduced as it is ionized and converted into metal oxide, a moving coordinate system is employed where the M/MO interface defines $x = 0$ and the MO/O interface is at $x = L(t)$.

The growth rate was theoretically described in a series of works by N.F. Mott.[44,46–48] Mott considered the implications of experimental results,[49] in particular the parabolic relation

$$L^2 = 2At, \tag{3.1}$$

where L is the thickness of the oxide, t is time, and A is a constant. The rate of

growth is thus

$$\frac{dL}{dt} = \sqrt{\frac{A}{2}} t^{-1/2}. \tag{3.2}$$

For specificity, the metal fills $x < 0$, that metal oxide fills $0 < x < L$, and the oxygen gas fills $L < x$ (see Fig. 1). This means that a moving coordinate system is employed where $x = 0$ represents the M/MO interface, and $x = L(t)$ represents the MO/O interface.

Before proceeding, we note that although experimental results for metal oxide growth rate imply a parabolic rate, precise measurement is difficult. Even recent results that show parabolic growth do not have the precision to determine other contributions to growth rate at low t. See, for example, Ref. 50.

A field and fluxes that vary as $t^{-1/2}$ are expected on the basis of a gradient of concentration, with the values of the carrier concentrations pinned by the two surfaces and the length L determining the gradient.[49] That is, $dL/dt \sim 1/L$ gives a parabolic law. Wagner obtained a parabolic growth law using an oversimplified theory involving only the Nernst-Planck equation, which is equivalent to a bulk irreversible thermodynamics flux-force equation, and some additional assumptions.[51] Mott obtained a parabolic growth law using a more complete argument[46] that invokes the Nernst-Planck equations, Gauss's Law, and (implicitly) the continuity equations.

For electron and ion number currents (j_a, j_b) and ion valence $Z = 1$, Mott assumed that the total current $J = e(j_b - j_a)$ in the oxide is zero, so

$$j_a = j_b. \tag{3.3}$$

Since oxide grows when metal ions reach the MO/O interface, the growth rate is

$$\frac{dL}{dt} = j_b \Omega, \tag{3.4}$$

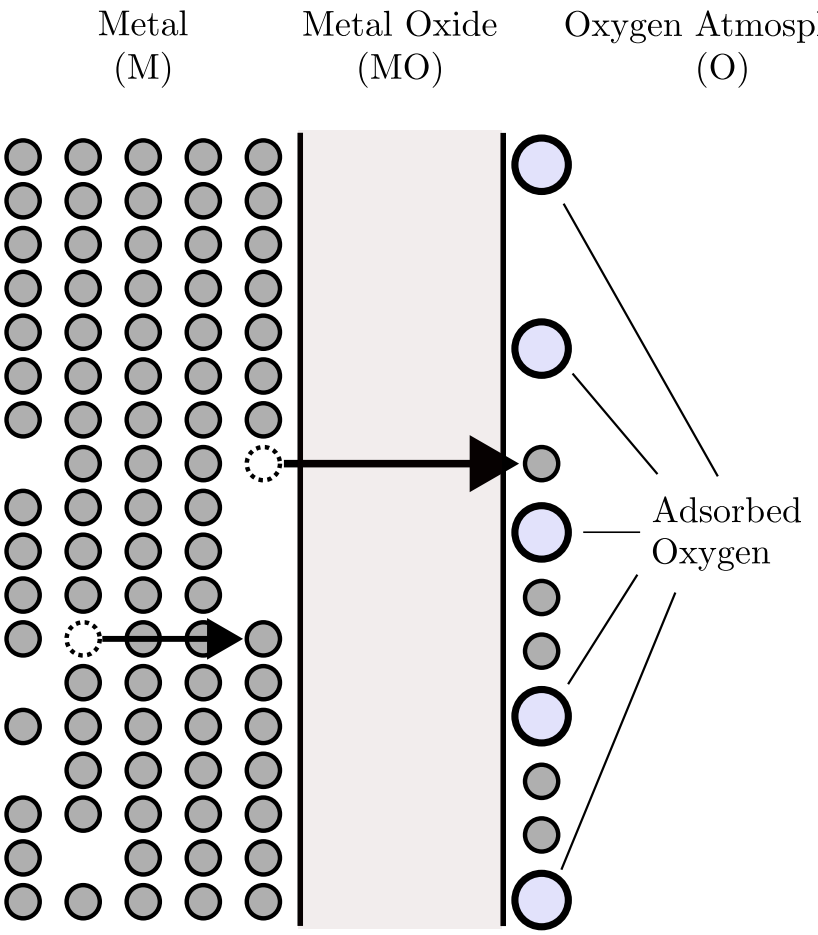

Fig. 2. The first of two methods by which oxide grows at the M/MO interface (see also Fig. 3). Here, metal ions leave the bulk of the metal near the M/MO interface, are transported across the oxide, and are taken up into new oxide at the MO/O interface. The sites near the M/MO interface in the metal that are vacated by the transported ions are then filled by ions from deeper in the bulk metal.

where Ω is the volume per metal ion in the newly formed oxide. Figures 2 and 3 model two processes by which oxides grow and adjust by ion deposition at the MO/O interface. Comparison of Eq. (3.4) with Eq. (3.2) shows that

$$j_b \sim t^{-1/2} \tag{3.5}$$

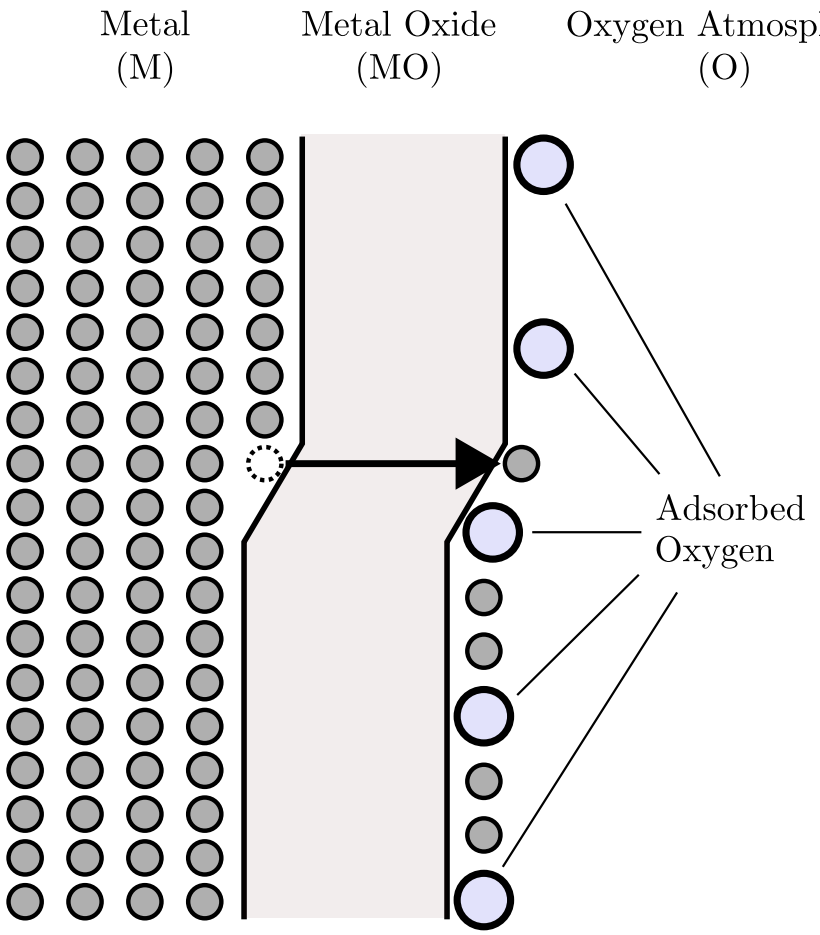

Fig. 3. The second of two methods by which oxide grows at the M/MO interface (see also Fig. 2). Here, as in Fig. 2, metal ions leave the bulk of the metal near the M/MO interface, are transported across the oxide, and are taken up into new oxide at the MO/O interface. Rather than bulk metal ions adjusting, however, after some time the entire oxide adjusts inward toward the metal, now occupying the vacancies left by ions that have been transported across the oxide.

for the asymptotic behavior of the ion fluxes. By the Nernst-Planck equations, the electric field E and the ion density gradients $(\partial_x n_a, \partial_x n_b)$ also have the same behavior. Moreover, the quantities $(j_a, j_b, E, \partial_x n_a, \partial_x n_b)$ are all uniform throughout the oxide.

The surface charge Σ predicted by Mott's theory can be calculated. We assume that the metal and the gas are neutral, so by Gauss's Law the surface charges $(\Sigma(0), \Sigma(L))$ and the electric fields $(E(0), E(L))$ are related by

$$E(0) = \frac{\Sigma(0)}{\epsilon}, \qquad E(L) = -\frac{\Sigma(L)}{\epsilon}. \tag{3.6}$$

Moreover, by continuity the assumption that there is charge and current only within the oxide leads to the conditions

$$J(0) = \frac{d\Sigma(0)}{dt}, \qquad J(L) = -\frac{d\Sigma(L)}{dt}. \tag{3.7}$$

This model immediately poses the questions of whether Mott's solution is self-consistent, and whether it is the beginning of an asymptotic series in powers of $t^{-1/2}$. To answer self-consistency, note that the uniform but decreasing-with-time $E \sim t^{-1/2}$ leads to no bulk charge and to interfaces with equal and opposite charge, so they behave like a capacitor. Since E decreases with time, so must the charge on the capacitor. However, the model assumes zero current. Hence Mott's solution is not self-consistent.

Nevertheless we show, in response to the question about a consistent power series solution, that each of the continuous variables can be expanded in an asymptotic series in $t^{-k/2}$, where Mott's solution corresponds to $k = 1$, and that non-zero current J appears at order $k = 3$. We also show that all of the continuous variables can depend upon position. This means that the bulk can develop a local and total charge density, with the surfaces not having equal and opposite charges, so that the capacitor model holds only to lowest order. It has previously been shown that steady non-equilibrium current flow can cause local charge densities in the bulk.[52,53]

The fact that an expansion can be made of j_b in powers of $t^{-1/2}$ leads to

$$\frac{dL}{dt} = \sqrt{\frac{A}{2}} t^{-1/2} + Bt^{-1} + \ldots, \tag{3.8}$$

so that

$$L = \sqrt{2A} t^{1/2} + B \ln t + \ldots \tag{3.9}$$

to higher accuracy than given by the pure parabolic law. This prediction can be subjected to experimental study. In practice, we must assume that

$$L = \sqrt{2A} t^{1/2} + B \ln t + C + \ldots \tag{3.10}$$

because $\ln t$ is of order unity. This gives corrections that might be important for thin layers of oxides.

Section A of this chapter discusses transport in two-component ionic systems, including the equations of motion, as well as the surface chemical reactions that drive ionic transport and oxide growth. It also introduces the expansion notation used in this chapter. Section B finds the relations between the expansion coefficients, and discusses the method of solution at any order, which requires solution of all previous orders. Section C gives the explicit solution for the lowest (first) order expansion coefficients, and Sec. D summarizes the results for the second order expansion coefficients. Section E discusses the oxide growth rate predicted by the current theory, including the first correction to the parabolic growth law that, as mentioned above, goes as $\ln(t)$. Appendices A and B give the explicit solution for the respective second and third order expansion coefficients. (Most of the work in this chapter and its associated appendices has previously been published.[54])

A. On Two-Component Ionic Transport

Let the subscripts a and b denote electrons and metal ions respectively. Let n_0 and n_0/Z be the uniform equilibrium concentration of electrons and metal ions respectively, n_a and n_b be their additional concentrations, ν_a and ν_b be their mobilities, D_a and D_b be their diffusion coefficients, $q_a = -e$ and $q_b = Ze$ be their charges, E be the electric field, k_B be the Boltzmann constant, T be the temperature, and x be the position.

Note that we use the Einstein Relations to rewrite the mobilities, which can have either sign, in terms of diffusion constants, which are always positive. Since we always consider Z positive, if we want to consider oxygen ions and holes as the carriers, then only the sign of the electric charge e must be changed. For M^{3+} and O^{2-}, we let $e \to 2e$ and $Z = 3/2$. Therefore our results are quite general.

1. Equations for Two-Component Transport

The Einstein Relations are given by

$$\frac{\nu_a}{D_a} = \frac{q_a}{k_B T}, \quad \frac{\nu_b}{D_b} = \frac{q_b}{k_B T}, \tag{3.11}$$

where all quantities are defined experimentally. For electrons and metal ions, $-Zq_a = q_b$, so

$$\nu_b D_a = -Z\nu_a D_b, \quad -\frac{\nu_a}{D_a} = \frac{\nu_b}{ZD_b} = \frac{1}{V_T}, \tag{3.12}$$

where

$$V_T = \frac{k_B T}{e} \tag{3.13}$$

denotes a thermal voltage.

The one-dimensional Nernst-Planck equations for the number flux densities as-

sociated with metal ions and electrons are

$$j_a = \nu_a(n_0 + n_a)E - D_a\partial_x n_a, \tag{3.14}$$

$$j_b = \nu_b\left(\frac{n_0}{Z} + n_b\right)E - D_b\partial_x n_b, \tag{3.15}$$

where the electric field $E = -\nabla\phi$, and n_a and n_b are deviations from the respective equilibrium densities n_0 and n_0/Z. These are the flux-force relations analogous to Eqs. (2.37) and (2.38) where cross-terms have been neglected, and the system is taken to be non-magnetic so that $\bar{\mu} = \tilde{\mu}$. Rewriting mobilities in terms of diffusion constants using Eq. (3.11),

$$j_a = -\frac{D_a}{V_T}(n_0 + n_a)E - D_a\partial_x n_a, \tag{3.16}$$

$$j_b = \frac{D_b}{V_T}(n_0 + Zn_b)E - D_b\partial_x n_b, \tag{3.17}$$

We also use the number continuity equations,

$$\partial_t n_a + \partial_x j_a = 0, \quad \partial_t n_b + \partial_x j_b = 0, \tag{3.18}$$

and Gauss's Law,

$$\partial_x E = \frac{e}{\epsilon}(Zn_b - n_a), \tag{3.19}$$

where e is electron charge in Coulombs, and ϵ is the permittivity of the oxide.

With the charge density and current density defined by

$$\rho = -e(n_a - Zn_b), \qquad J = -e(j_a - Zj_b), \tag{3.20}$$

use of the number continuity equations yields the charge continuity equation

$$\partial_t\rho + \partial_x J = 0. \tag{3.21}$$

2. Expansion Notation

We seek a series solution in powers of $t^{-1/2}$ for the electron and ion concentrations (densities) and fluxes, as well as for the electric field. They must satisfy the Nernst-Planck equations, the continuity equations, and Gauss's Law. Following Mott (who, in turn, was following experiment), we take the lowest order fluxes and field to vary as $t^{-1/2}$. Examining the structure of the Nernst-Planck equation for electrons given in Eq. (3.16), and inserting terms of order $t^{-1/2}$, the nonlinear term $n_a E$ will contain terms of order t^{-1}. Iteration yields that the series must be in powers of $t^{-k/2}$ for integer k.

The assumption of no net bulk charge is consistent at lowest order, but it is not true in general. We assume only that electron transport is dominated by thermal emission rather than tunneling, and that metal ions are soluble in the oxide, but not oxygen ions. (The theory however can be generalized to oxygen-soluble oxides with the appropriate transformations of e and Z.) We also assume that any defects in the oxide are "frozen," so that no metal ions or electrons have their origin in the oxide itself, and no new oxide is formed within the layer.

We thus make an expansion of the form

$$j_a = \sum_{k=1} J_{ak} t^{-k/2}, \qquad j_b = \sum_{k=1} J_{bk} t^{-k/2}, \tag{3.22}$$

$$n_a = \sum_{k=1} N_{ak} t^{-k/2}, \qquad n_b = \sum_{k=1} N_{bk} t^{-k/2}, \tag{3.23}$$

$$\Sigma^{(0)} = \sum_{k=1} \Sigma_k^{(0)} t^{-k/2}, \qquad \Sigma^{(L)} = \sum_{k=1} \Sigma_k^{(L)} t^{-k/2}, \tag{3.24}$$

$$E = \sum_{k=1} E_k t^{-k/2}, \tag{3.25}$$

$$J = \sum_{k=1} J_k t^{-k/2}, \qquad \rho = \sum_{k=1} \rho_k t^{-k/2}. \tag{3.26}$$

Here J_{ak}, J_{bk}, N_{ak}, N_{bk}, E_k, ρ_k, and J_k are functions of the position along the direction of growth, x. From the above definitions, the dimensionality of J_{ak} and J_{bk} is concentration times velocity times $t^{k/2}$, the dimensionality of N_{ak} and N_{bk} is concentration times $t^{k/2}$, the dimensionality of the surface charge density coefficients $\Sigma_k^{(0)}$ and $\Sigma_k^{(L)}$ is charge per area times $t^{k/2}$, the dimensionality of E_k is electric field times $t^{k/2}$, the dimensionality of ρ_k is charge density times $t^{k/2}$, and the dimensionality of J_k is current density times $t^{k/2}$.

3. On Specifying Chemical Reaction Rates at Surfaces

In the presence of a true chemical reaction at a surface there is a single reaction rate, typically specified by a Butler-Volmer relation[55–57] between the fluxes of all of the relevant components. In the present case the fluxes of the carriers are independent of one another, so that there are two statements about carrier fluxes at each surface, for a total of four conditions. Near equilibrium (as we have here, in the asymptotic regime), neglecting cross-terms, each flux j will be proportional to its corresponding $\Delta\tilde{\mu}$ across the interface (either M/MO or MO/O), as in Eq. (2.17):

$$j_{a,b} = \frac{\bar{g}_{a,b}}{q_{a,b}^2}(\Delta\tilde{\mu}_{a,b})_{\text{int}} \tag{3.27}$$

at each surface, so there are four $\bar{g}$'s. (The equation becomes nonlinear far from equilibrium.) Thus j_a and j_b are proportional to a non-equilibrium quantity, which we take to be a field E_1, as in Ref. 48. All of the unknown integration constants will be linear or higher in E_1.

This chapter does not carry this procedure any further by considering the chemical reactions at the surface in detail. It is sufficient for the purposes of this dissertation to know that this can be done, and that in the present problem there are four constants associated with boundary conditions at the two surfaces for the two carriers.

In principle, all of the quantities appearing in the solutions to the transport equations are determined by these surface reaction rates. For a true chemical reaction, which we expect to be described by a Butler-Volmer equation, the fluxes at each surface, because they are related, will be described by only a single independent coefficient $\bar{g}$. Note also that the Butler-Volmer equation is non-linear, so that the boundary conditions can be nonlinear. Because we do not consider the boundary conditions in detail, we neglect this possibility.

B. Relations between Expansion Coefficients for Any t-dependence

1. Continuity Relations and Charge Conservation

The continuity relations given in Eq. (3.18) yield

$$\sum_{k=1}(\partial_x J_{ak})t^{-k/2} + \sum_{m=1} N_{am}\left(-\frac{m}{2}\right)t^{-(m+2)/2} = 0, \tag{3.28}$$

for subscript a, and a similar relation holds for b. With $m = (k-2)$, so that $\sum_{m=1} \to \sum_{k=3}$, comparison of like powers of t yields, for $k = 1$ and $k = 2$,

$$\partial_x J_{ak} = 0, \quad \partial_x J_{bk} = 0, \qquad\qquad (k = 1, 2), \tag{3.29}$$

and, for $k \geq 3$,

$$\begin{aligned} \partial_x J_{ak} &= \left(\frac{k-2}{2}\right) N_{a(k-2)}, \\ \partial_x J_{bk} &= \left(\frac{k-2}{2}\right) N_{b(k-2)}, \qquad\qquad (k \geq 3). \end{aligned} \tag{3.30}$$

By definition we have

$$\rho_k = e\left(ZN_{bk} - N_{ak}\right), \qquad J_k = e\left(ZJ_{bk} - J_{ak}\right), \tag{3.31}$$

and charge conservation for each k is

$$\partial_t \rho_k + \partial_x J_k = 0. \tag{3.32}$$

Charge conservation at each surface ($x = 0$ and $x = L$) yields

$$\frac{d\Sigma^{(0)}}{dt} = -J|_{x=0} = -e(Zj_b - j_a)|_{x=0}, \tag{3.33}$$

$$\frac{d\Sigma^{(L)}}{dt} = J|_{x=L} = e(Zj_b - j_a)|_{x=L}, \tag{3.34}$$

so that

$$\sum_{k=1} \left(-\frac{k}{2}\right) \Sigma_k^{(0)} t^{-(k+2)/2} = -e \sum_{k=1} \left(ZJ_{bk} - J_{ak}\right)|_{(x=0)} t^{-k/2}, \tag{3.35}$$

$$\sum_{k=1} \left(-\frac{k}{2}\right) \Sigma_k^{(L)} t^{-(k+2)/2} = e \sum_{k=1} \left(ZJ_{bk} - J_{ak}\right)|_{(x=L)} t^{-k/2}. \tag{3.36}$$

Comparing powers of t gives, for $k = 1$ and $k = 2$,

$$\begin{aligned} ZJ_{bk}|_{(x=0)} &= J_{ak}|_{(x=0)}, \\ ZJ_{bk}|_{(x=L)} &= J_{ak}|_{(x=L)}, \qquad\qquad (k = 1, 2), \end{aligned} \tag{3.37}$$

and, for $k \geq 3$,

$$\begin{aligned} -\left(\frac{k-2}{2}\right) \Sigma_{(k-2)}^{(0)} &= -e\left(ZJ_{bk} - J_{ak}\right)|_{(x=0)}, \\ -\left(\frac{k-2}{2}\right) \Sigma_{(k-2)}^{(L)} &= e\left(ZJ_{bk} - J_{ak}\right)|_{(x=L)}, \qquad\qquad (k \geq 3). \end{aligned} \tag{3.38}$$

Charge conservation over both surface and bulk yields

$$\sum_{k=1} \left(\Sigma_k^{(0)} + \Sigma_k^{(L)}\right) t^{-k/2} = e \int_0^L \sum_{k=1} (N_{ak} - ZN_{bk}) t^{-k/2} dx, \tag{3.39}$$

so that, for each k,

$$\Sigma_k^{(0)} + \Sigma_k^{(L)} = e \int_0^L (N_{ak} - ZN_{bk}) dx. \tag{3.40}$$

2. Gauss's Law

Gauss's Law, as given in Eq. (3.19), reads

$$\sum_{k=1}(\partial_x E_k)t^{-k/2} = \frac{1}{\epsilon}\left(\sum_{k=1}\rho_k t^{-k/2}\right), \tag{3.41}$$

so, for each k,

$$\partial_x E_k = \frac{1}{\epsilon}\rho_k. \tag{3.42}$$

Gauss's Law at the surfaces, Eq. (3.6), gives, for each k,

$$E_k(0) = \frac{\Sigma_k^{(0)}}{\epsilon}, \quad E_k(L) = -\frac{\Sigma_k^{(L)}}{\epsilon}. \tag{3.43}$$

3. Nernst-Planck (Flux-Force) Equations

The Nernst-Planck equation for species a, Eq. (3.16), can be written as

$$\sum_{k=1} J_{ak}t^{-k/2} = -\frac{D_a}{V_T}n_0\sum_{k=1}E_k t^{-k/2} - \frac{D_a}{V_T}\sum_{m,k=1}N_{ak}E_m t^{-(m+k)/2} - D_a\sum_{k=1}(\partial_x N_a)t^{-k/2}, \tag{3.44}$$

or,

$$\sum_{k=1}\left(J_{ak} + \frac{D_a}{V_T}n_0 E_k + D_a\partial_x N_{ak}\right)t^{-k/2} = -\frac{D_a}{V_T}\sum_{m,k=1}N_{ak}E_m t^{-(m+k)/2}, \tag{3.45}$$

with a similar form for species b,

$$\sum_{k=1}\left(J_{bk} - \frac{D_b}{V_T}n_0 E_k + D_b\partial_x N_{bk}\right)t^{-k/2} = \frac{ZD_b}{V_T}\sum_{m,k=1}N_{bk}E_m t^{-(m+k)/2}. \tag{3.46}$$

By matching coefficients of powers of t, equations are obtained for any k.

4. Solving the Transport Equations

There are five first-order differential equations for five continuous variables, so there are five integration constants at each order. For $k \geq 3$ the current density J_k at $x = L$ is known from the $k-2$ (which must be previously determined) value of surface charge density $\Sigma_{k-2}^{(L)}$. Therefore only four integration constants need be determined. These can be thought of as fixed by the "reaction rates" of each charge carrier at each of the interfaces discussed above, which will not be specified. A sequential solution starting with $k = 1$ is thus necessary for solution at arbitrary k due to the dependence of each solution on lower-order solutions.

The cases $k = 1$ and $k = 2$ are somewhat simpler than $k \geq 3$. Nevertheless, for each k the solution method is the same: (i) from the continuity equations find the ion fluxes J_{ak} and J_{bk}; (ii) from all of the five equations find an equation for ρ_k and solve it; (iii) use this ρ_k in Gauss's Law to find E_k; and (iv) find N_{ak} and N_{bk} by substitution of J_{ak}, J_{bk} and E_k into the Nernst-Planck equations.

C. Transport in Metal Oxide for $t^{-1/2}$-dependence

For $k = 1$, the calculations are simple, but illustrate what happens in higher orders. The continuity relations given in Eq. (3.29) give J_{a1} and J_{b1} to be uniform, and charge conservation at each surface, Eq. (3.37), gives

$$J_{a1} = Z J_{b1}. \tag{3.47}$$

The Nernst-Planck Eqs. (3.45) and (3.46) yield

$$J_{a1} + \frac{D_a}{V_T} n_0 E_1 + D_a \partial_x N_{a1} = 0, \tag{3.48}$$

$$J_{b1} - \frac{D_b}{V_T} n_0 E_1 + D_b \partial_x N_{b1} = 0, \tag{3.49}$$

where E_1 is taken to be a uniform, experimentally determined value.

From the uniformity of E_1,

$$\partial_x E_1 = 0, \tag{3.50}$$

so that Gauss's Law yields

$$\rho_1 = 0, \quad N_{a1} = Z N_{b1}. \tag{3.51}$$

Substitution of fluxes from Eq. (3.47) and concentrations from Eq. (3.51) into the Nernst-Planck equations gives

$$J_{a1} + \frac{D_a}{V_T} n_0 E_1 + D_a \partial_x N_{a1} = 0, \tag{3.52}$$

$$\frac{J_{a1}}{Z} - \frac{D_b}{V_T} n_0 E_1 + D_b \partial_x N_{b1} = 0. \tag{3.53}$$

Thus, with Eq. (3.51), we have

$$J_{a1} = Z J_{b1} = -(1+Z) \frac{D_a D_b}{D_b - D_a} \frac{n_0 E_1}{V_T}, \tag{3.54}$$

$$N_{a1} = Z N_{b1} = \frac{R_D n_0 E_1}{V_T} x + M_1. \tag{3.55}$$

Here, the dimensionless ratio between diffusion constants

$$R_D \equiv \left(\frac{D_a + Z D_b}{D_b - D_a} \right), \tag{3.56}$$

and M_1 is a constant of integration, with units of concentration times $\mathrm{s}^{1/2}$, determined by the surface reaction rates, and therefore linear in E_1. (Recall that J_{a1} and N_{a1} are first order coefficients, which must be multiplied by $t^{1/2}$ to find the respective flux and number densities j_a and n_a.) Although constants of integration associated with reaction rates were discussed earlier, they are now considered more explicitly.

Figure 4 illustrates the effect of an "improper" value of M_1. As M_1 increases,

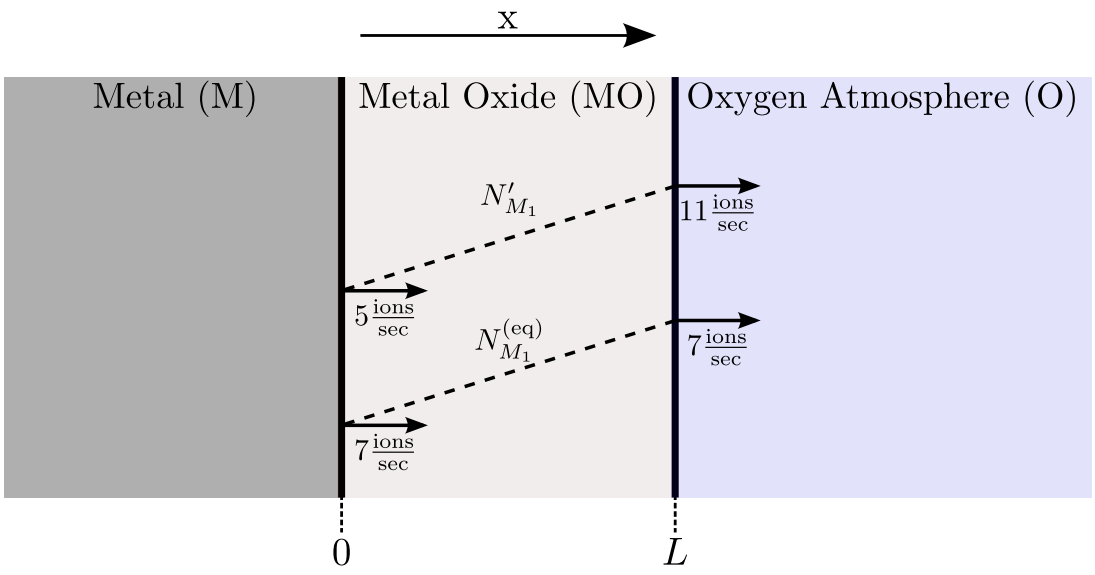

Fig. 4. A model that illustrates the effect of the constant concentration M_1 of metal ions. The dotted lines represent the linear concentration of ions in the metal oxide, as in equation (3.55). Here N'_{M_1} has too high a value of M_1 to maintain steady-state flow; this high concentration of ions in the oxide suppresses ion injection at the M/MO surface and enhances ion expulsion at the MO/O surface. Only the particular value of M_1 in $N^{(eq)}_{M_1}$ permits an equal rate of ions to enter and leave the oxide, here taken to be 7 ions per second. The ion flux rates of 5 and 11 ions per second are fabricated here for example.

the increasing concentration of metal ions near the metal/oxide surface opposes new ions from entering, just as the high concentration of metal ions near the oxide/gas interface encourages more ions to be deposited on the oxide/gas surface. For M_1 too large, the number of metal ions in the bulk would be insufficient to maintain the high rate of ions exiting the oxide, and would drop to some equilibrium value. Thus, M_1 is determined by constraining the oxide to have no net ion-loading or ion-unloading in the bulk at order $k = 1$. Note that E_1, which is proportional to the parabolic growth rate coefficient A of Eq. (3.1), is also related to the surface reaction rates. As

discussed above, net surface reaction rates generally involve a Butler-Volmer equation, but not far from equilibrium (as in the Mott solution) they can be linearized in the differences of various electrochemical potentials. This ensures that there is no net surface reaction rate in the limit of equilibrium.

From Gauss's Law at the surfaces. Eq. (3.43),

$$E_1(0) = \frac{\Sigma_1^{(0)}}{\epsilon}, \quad E_1(L) = -\frac{\Sigma_1^{(L)}}{\epsilon}. \tag{3.57}$$

Since E_1 is uniform,

$$\Sigma_1^{(0)} = -\Sigma_1^{(L)} = \epsilon E_1. \tag{3.58}$$

For $|\nu_a| \gg |\nu_b|$ (or equivalently in this case, $D_a \gg D_b$), Mott and Cabrera[48] find for monovalent ions that

$$J_{a1} = -2D_b \frac{\partial N_{a1}}{\partial x}. \tag{3.59}$$

The above results are consistent with this.

D. Transport in Metal Oxide for t^{-1}-dependence

The $k = 2$ results, that is, the t^{-1}-dependent quantities, are the lowest order for which the results are completely new. The mathematical details are given in Appendix A, and the results are summarized here. Recall that all coefficients at this order must be multiplied by t to find the physical variables j, n, and E. With the constant M_{21}, in units s/m^2, determined by surface reaction rates, the second order flux density coefficients are

$$J_{a2} = ZJ_{b2} = -(1+Z)\left(\frac{D_a D_b}{ZD_b + D_a}\right) M_{21}, \tag{3.60}$$

and there is no net charge flux,

$$J_2 = ZeJ_{b2} - eJ_{a2} = 0. \tag{3.61}$$

With the constants M_{20}, $P_{a2}^{(+)}$ and $P_{a2}^{(-)}$, each in units of s/m, given by surface reaction rates (and thus linear in E_1), the $k = 2$ coefficients of the concentrations of electrons and ions are given by

$$N_{a2} = M_{20} + M_{21}x + P_{a2}^{(+)}e^{x/l_s} + P_{a2}^{(-)}e^{-x/l_s}, \tag{3.62}$$

$$N_{b2} = \frac{M_{20}}{Z} - \frac{1}{Z}\frac{R_D\epsilon E_1^2}{V_T e} + \frac{M_{21}}{Z}x - P_{a2}^{(+)}e^{x/l_s} - P_{a2}^{(-)}e^{-x/l_s}. \tag{3.63}$$

Here, l_s is the screening length,

$$l_s = \sqrt{\frac{V_T\epsilon}{(1+Z)n_0 e}} = \sqrt{\frac{k_B T\epsilon}{(1+Z)n_0 e^2}}. \tag{3.64}$$

There is a net charge in the bulk, given by $\rho_2 t^{-1}$, where

$$\rho_2 = P_2^{(+)}e^{x/l_s} + P_2^{(-)}e^{-x/l_s} - \frac{R_D\epsilon E_1^2}{V_T}, \tag{3.65}$$

and

$$P_2^{(+)} = -(1+Z)eP_{a2}^{(+)}, \quad P_2^{(-)} = -(1+Z)eP_{a2}^{(-)}. \tag{3.66}$$

Note that ρ_2 has, in addition to surface charge within a screening length of the two surfaces, a uniform charge density with sign determined by $e/(D_a - D_b)$ and independent of the sign of E_1 (or, equivalently, the direction of current flow). Since $D_a \gg D_b$ here, the term is positive. If, rather than electrons and metal ions, holes and oxygen ions are the carriers, then the sign of ρ_2 goes as $-e/(D_a - D_b)$; however, for that case $D_b \gg D_a$, so it is again positive. As for the ionic system (battery) considered by Ref. 52, this uniform charge density leads to a quadratic voltage profile within the bulk, beyond a screening length of either surface.

The second order coefficient of the electric field is

$$E_2 = \frac{l_s}{\epsilon}\left(P_2^{(+)}e^{x/l_s} - P_2^{(-)}e^{-x/l_s}\right) - \frac{R_D E_1^2}{V_T}x + \frac{V_T M_{21}}{n_0 R_D} - \frac{M_1 E_1}{n_0}. \tag{3.67}$$

The surface charge coefficients are given by

$$\Sigma_2^{(0)} = l_s\left(P_2^{(+)} - P_2^{(-)}\right) + \frac{\epsilon V_T M_{21}}{n_0 R_D} - \frac{\epsilon M_1 E_1}{n_0}, \tag{3.68}$$

$$\Sigma_2^{(L)} = -l_s\left(P_2^{(+)}e^{L/l_s} - P_2^{(-)}e^{-L/l_s}\right) + \frac{\epsilon R_D E_1^2}{V_T}L - \frac{\epsilon V_T M_{21}}{n_0 R_D} + \frac{\epsilon M_1 E_1}{n_0}. \tag{3.69}$$

The solution satisfies

$$\Sigma_2^{(0)} + \Sigma_2^{(L)} + \int_0^L \rho_2 dx = 0, \tag{3.70}$$

so there is no net charge in the system.

E. Growth Rate of Metal Oxide Films

The t^{-1} solution (and the $t^{-3/2}$ solution, found in Appendix B) gives new results for the thickness and growth rate of metal oxide. As mentioned above, the oxide layer grows as metal ions reach the MO/O surface and are taken into lattice positions to form new oxide. Thus, the rate of growth of the oxide depends on the rate j_b at which metal ions arrive at the surface, according to Eq. (3.4), that is, $dL/dt = \Omega j_b$. The metal ion number flux (using Eqs. (3.54), (3.60), and (B.4)) is given by

$$\begin{aligned} j_b = &-\left(\frac{1+Z}{Z}\right)\frac{D_a D_b}{D_b - D_a}\frac{n_0 E_1}{V_T}t^{-1/2} - \left(\frac{1+Z}{Z}\right)\left(\frac{D_a D_b}{Z D_b + D_a}\right)M_{21}t^{-1} \\ &+ \left(\frac{R_D n_0 E_1}{4V_T Z}x^2 + \frac{M_1}{2Z}x + \frac{K_3}{Z} + \frac{\epsilon E_1}{2Ze}\right)t^{-3/2} + \ldots, \end{aligned} \tag{3.71}$$

where K_3 is a constant of integration determined by interfacial reaction rates (and thus linear in E_1). Examination of the first term in Eq. (3.71) shows that, if $D_b < D_a$ (as for ions relative to electrons), then the microscopics must give $E_1 > 0$ for a

positive growth rate. Substitution of Eq. (3.71) into Eq. (3.4) gives the oxide growth rate dL/dt. Then, keeping only terms of second order, integration with respect to t gives

$$L = \sqrt{2A}t^{1/2} + B\ln t + \ldots, \tag{3.72}$$

where

$$A = 2\left(\frac{1+Z^2}{Z}\right)^2\left(\frac{D_aD_b}{D_b-D_a}\right)^2\frac{n_0^2E_1^2\Omega^2}{V_T^2}, \tag{3.73}$$

$$B = \frac{D_aD_b}{D_a+Z^2D_b}\left[(1-Z)\frac{M_1E_1}{V_T} - \frac{1+Z^2}{Z}M_{21}\right]\Omega. \tag{3.74}$$

A sampling of the current literature[50,58–62] suggests more precise data is necessary to confirm the logarithmic form of the correction term.

The Appendices present the $k = 2$ and $k = 3$ solutions in detail, and show that the method can be used for any k to find the fluxes, concentrations, surface charges and electric field. As a consequence one can have confidence that the Mott solution gives the leading term in the complete solution of the complete set of transport equations. The most easily verifiable prediction from the viewpoint of experiment is the prediction that the first correction to the linear growth law is logarithmic. Thus, by the methods detailed in this chapter, the approach taken by Mott for parabolic growth of oxide films can be turned into a consistent asymptotic expansion, and the explicit form of the lowest three orders is given. Up to four integration constants appear at each order, related to the surface reaction rates. At higher order the bulk film is found to be non-uniformly charged, with a corresponding nonzero current density (see Eq. (B.5)).

CHAPTER IV

INTERFACES, MULTILAYERS, AND SPIN VALVES: SPIN INJECTION AND ACCUMULATION BY ELECTRIC CURRENT

Although electronic and ionic flow has been studied since the early 19th Century, spin flow has become important only much more recently. In particular, spin transport across interfaces between metals and ferromagnets has been an important topic since the discovery of giant magnetoresistance (GMR).[63,64] About a decade after its discovery, it became the principle behind the predominant method of reading stored data, as it is to this day. The magnetic read-head of a hard drive contains a multilayer consisting of a thin non-magnetic layer sandwiched between two ferromagnetic layers (see Fig. 5). Resistance to electrical current is strongly dependent on whether the magnetizations of the ferromagnetic layers are aligned parallel or antiparallel. As mentioned earlier, theory for spin current and electrical potential at a metal/ferromagnet interface is given by Johnson and Silsbee;[16] an appendix of that work is devoted to electrical currents crossing such interfaces, and it considers the effect on spin fluxes and on electrical voltage. Detailed theories for electrical currents passing through metal/ferromagnet multilayers (that is, series of interfaces) is given by Valet and Fert[22] (including solutions for the electric field and spin fluxes) and Hershfield and Zhao.[65] However, each of these three works neglects some part of the internal potential (discussed below), and none of them considers semiconductors.

This chapter revisits the problem of spin transport across the interface between a non-magnetic material and a ferromagnet, and calculates the electric field, electric potential, spin fluxes, and spin accumulation due to interfaces and multilayers of ferromagnets and non-magnetic materials. It shows that inclusion of both internal magnetic field (neglected by Ref. 65) and chemical potential (neglected by Refs. 16

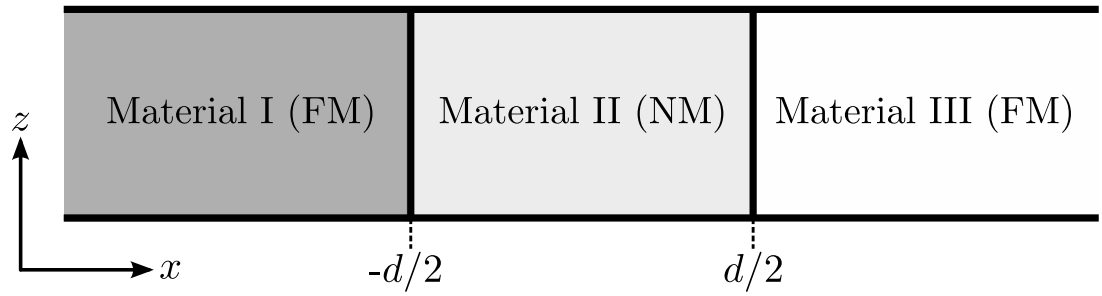

Fig. 5. A ferromagnetic multilayer, with a non-magnet sandwiched between two ferromagnets. In principle, this is how the materials that comprise a hard disk read head are arranged. In that case, material I is always magnetized in the same direction, say z. The hard disk "platter" then spins near material III, (to the far right of the figure, not pictured) and depending on the local magnetization of the disk, the magnetization of material III is along either z or -z. Electrical resistance to current along x, which depends on the relative magnetization alignment of materials I and III, is then measured, thereby determining the local magnetization of the hard disk. For read heads, material II is typically copper, while materials I and III are typically cobalt and/or permalloy.

and 22) are necessary for prediction of spin accumulation near the interface; the effect on spin accumulation of neglecting either contribution is shown to be about a factor of ten for copper. Further, it includes the surface screening mode, neglected by previous works, which for semiconductors plays an essential role in determining the spin current crossing the interface and the spin accumulation near the interface.

In this chapter, we use the phrase "isolated interface" to refer to an interface that is effectively an infinite distance from any other interface, and the term "multilayer" to refer to a system with two or more interfaces, where the spacing between interfaces is on the order of a surface mode decay length (found below).

Section A of this chapter briefly discusses the equations that govern spin-dependent transport in solids, discussed in detail in Chap. II. Section B finds the deviations from

equilibrium associated with normal modes, including two surface modes associated with spin-diffusion and charge screening, and one bulk mode associated with applied electric current. Section C discusses the bulk and boundary conditions at an isolated interface, and shows the electric field, voltage, charge, and spin accumulation near an interface between cobalt and copper. It also discusses the effects of the approximations of previous theories, many of which can be significant. Section D discusses the bulk and boundary conditions in a two-interface multilayer. Appendices C and D respectively calculate the explicit form of the bulk and boundary conditions for isolated interfaces and multilayers, and write them in terms of dimensionless variables.

A. Transport Equations

Within each material, Eqs. (2.27) and (2.28) give the respective continuity of up and down spins. We consider the total electric current density J to be known, and continuous across the interface; for an isolated interface between materials I and II, we have $J = j^{(\mathrm{I})}_{\uparrow_x} + j^{(\mathrm{I})}_{\downarrow_x} = j^{(\mathrm{II})}_{\uparrow_x} + j^{(\mathrm{II})}_{\downarrow_x}$.

The magnetoelectrochemical potential $\bar{\mu}$ is defined in Eq. (2.24). In principle, $\mu_\uparrow$, $\mu_\uparrow$, ϕ, and H^* (defined by Eq. (2.58)) are different in each material (although ϕ must be continuous across the interface). In the bulk of each material, the spin fluxes are given in terms of thermodynamic gradients by Eqs. (2.37) and (2.38). We here neglect off-diagonal terms, so that

$$j_{\uparrow_i} = -\frac{\sigma_\uparrow}{e^2}\partial_i \bar{\mu}_\uparrow, \qquad j_{\downarrow_i} = -\frac{\sigma_\downarrow}{e^2}\partial_i \bar{\mu}_\downarrow. \tag{4.1}$$

We are interested in steady-state solutions, so that $\partial_t n_\uparrow = 0 = \partial_t n_\downarrow$ in the continuity Eqs. (2.27) and (2.28). Taking the gradient of Eq. (4.1) and employing Eqs. (2.27),

(2.28), and (2.39) gives

$$-\frac{\sigma_\uparrow}{e^2}\partial_i^2\bar{\mu}_\uparrow = -\alpha\left(\bar{\mu}_\uparrow - \bar{\mu}_\downarrow\right), \tag{4.2}$$

$$-\frac{\sigma_\downarrow}{e^2}\partial_i^2\bar{\mu}_\downarrow = \alpha\left(\bar{\mu}_\uparrow - \bar{\mu}_\downarrow\right). \tag{4.3}$$

Finally, Gauss's law for spin-up and spin-down electrons gives

$$\partial_i^2\phi = \frac{e}{\varepsilon_0\varepsilon}\left(n_\uparrow + n_\downarrow\right). \tag{4.4}$$

B. Normal Modes

In the following, for brevity we write solutions to be of the form e^{-x}, although for the material on the left side of the interface one should use e^x (because it must decay as $x \to -\infty$).

1. Spin Mode (S)

One solution to Eqs. (4.2)-(4.4) is characterized by a nonzero spin current $J_\sigma \equiv J_\uparrow - J_\downarrow \neq 0$ (shown below). We therefore designate it the "spin mode," and use the subscript S to denote its properties.

Define

$$\ell_{\uparrow_S}^2 \equiv \frac{\sigma_\uparrow}{\alpha e^2}, \qquad \ell_{\downarrow_S}^2 \equiv \frac{\sigma_\downarrow}{\alpha e^2}, \tag{4.5}$$

where ℓ has units of length. Equations (4.2)-(4.3) then give, with δ denoting deviations from equilibrium,

$$\partial_i^2\delta\bar{\mu}_{\uparrow_S} = \frac{1}{\ell_{\uparrow_S}^2}\left(\delta\bar{\mu}_{\uparrow_S} - \delta\bar{\mu}_{\downarrow_S}\right), \tag{4.6}$$

$$\partial_i^2\delta\bar{\mu}_{\downarrow_S} = -\frac{1}{\ell_{\downarrow_S}^2}\left(\delta\bar{\mu}_{\uparrow_S} - \delta\bar{\mu}_{\downarrow_S}\right). \tag{4.7}$$

Subtracting Eq. (4.7) from Eq. (4.6) gives

$$\partial_i^2 \left(\delta\bar{\mu}_{\uparrow_S} - \delta\bar{\mu}_{\downarrow_S}\right) = \frac{1}{\ell_{\rm sf}^2}\left(\delta\bar{\mu}_{\uparrow_S} - \delta\bar{\mu}_{\downarrow_S}\right), \tag{4.8}$$

where

$$\frac{1}{\ell_{\rm sf}^2} \equiv \frac{1}{\ell_{\uparrow_S}^2} + \frac{1}{\ell_{\downarrow_S}^2}. \tag{4.9}$$

On neglecting $H_{\|}^*$ and making the identification $\alpha \to (N_\uparrow/\tau_{\uparrow\downarrow}) = (N_\downarrow/\tau_{\downarrow\uparrow})$, Eq. (4.9) agrees with Ref. 65. We use Eqs. (4.5) and (4.9) to find α, $\ell_{\uparrow_S}$ and $\ell_{\downarrow_S}$ in terms of $\ell_{\rm sf}$, $\sigma_\uparrow$, and $\sigma_\downarrow$, since they are, in principle, measurable:

$$\alpha = \frac{\sigma_\uparrow\sigma_\downarrow}{e^2\left(\sigma_\uparrow + \sigma_\downarrow\right)\ell_{\rm sf}^2}, \tag{4.10}$$

$$\ell_{\uparrow_S} = \ell_{\rm sf}\sqrt{\frac{\sigma_\uparrow + \sigma_\downarrow}{\sigma_\downarrow}}, \quad \ell_{\downarrow_S} = \ell_{\rm sf}\sqrt{\frac{\sigma_\uparrow + \sigma_\downarrow}{\sigma_\uparrow}}. \tag{4.11}$$

Equation (4.8) gives

$$\delta\bar{\mu}_{\uparrow_S} - \delta\bar{\mu}_{\downarrow_S} = eV_S e^{-x/\ell_{\rm sf}}, \tag{4.12}$$

where V_S is unknown (with units of potential). Since Eq. (4.12) shows the difference in up- and down-spin magnetoelectrochemical potentials to decay over the length $\ell_{\rm sf}$ from an interface, this length is the distance over which an appreciable spin accumulation may be induced by an interface, and is called the "spin-diffusion" or "spin-flip" length. This length may be measurable by employing the Magneto-Optical Kerr Effect[66,67] or the Inverse Spin Hall Effect,[68] or may be derived using GMR measurements and theory.[69]

It is shown below that

$$\xi V_S = \delta\phi_S(0), \tag{4.13}$$

where $\delta\phi_S(0)$ is the deviation in electric potential at the interface due to the spin mode, and ξ is a dimensionless quantity given by

$$\xi = \left[\frac{N_\chi \left(N_\uparrow - N_\downarrow \right) + R_\sigma N_\beta^2}{N_S N_\alpha - 2N_\beta^2} \right]. \tag{4.14}$$

Here, we define

$$N_\uparrow \equiv \frac{\partial n_\uparrow}{\partial \mu_\uparrow}, \qquad N_\downarrow \equiv \frac{\partial n_\downarrow}{\partial \mu_\downarrow}, \qquad N_\chi \equiv \frac{\chi}{g\mu_B^2 \mu_0}, \tag{4.15}$$

$$N_S \equiv \frac{\varepsilon_0 \varepsilon}{e^2 \ell_{\mathrm{sf}}^2}, \quad N_\alpha \equiv N_\uparrow + N_\downarrow + 2N_\chi, \tag{4.16}$$

$$N_\beta^2 \equiv 2N_\uparrow N_\downarrow + N_\chi \left(N_\uparrow + N_\downarrow \right), \tag{4.17}$$

$$R_\sigma \equiv \frac{\ell_{\mathrm{sf}}^2}{\ell_{\uparrow_S}^2} - \frac{\ell_{\mathrm{sf}}^2}{\ell_{\downarrow_S}^2} = \frac{\sigma_\downarrow - \sigma_\uparrow}{\sigma_\uparrow + \sigma_\downarrow}, \tag{4.18}$$

where χ is the magnetic susceptibility for an isotropic material (defined by $\chi_{ij} = \chi\delta_{ij}$). Each N has units of a density of states, and R_σ is a dimensionless ratio ($R_\sigma = 0$ for $\sigma_\uparrow = \sigma_\downarrow$, i.e., a non-magnetic material). Thus, for a non-magnetic material (NM) we have $\xi^{(\mathrm{NM})} = 0$, since $N_\uparrow^{(\mathrm{NM})} = N_\downarrow^{(\mathrm{NM})}$ and $R_\sigma^{(\mathrm{NM})} = 0$.

Substitution of Eq. (4.12) into Eqs. (4.6) and (4.7) yields

$$\delta\bar{\mu}_{\uparrow_S} = \frac{\ell_{\mathrm{sf}}^2}{\ell_{\uparrow_S}^2} e V_S e^{-x/\ell_{\mathrm{sf}}} = \frac{\sigma_\downarrow}{\sigma_\uparrow + \sigma_\downarrow} e V_S e^{-x/\ell_{\mathrm{sf}}}, \tag{4.19}$$

$$\delta\bar{\mu}_{\downarrow_S} = -\frac{\ell_{\mathrm{sf}}^2}{\ell_{\downarrow_S}^2} e V_S e^{-x/\ell_{\mathrm{sf}}} = -\frac{\sigma_\uparrow}{\sigma_\uparrow + \sigma_\downarrow} e V_S e^{-x/\ell_{\mathrm{sf}}}. \tag{4.20}$$

Equations (4.19) and (4.20) give $\delta\bar{\mu}_{\uparrow_S} = -(\ell_{\downarrow_S}^2/\ell_{\uparrow_S}^2)\delta\bar{\mu}_{\downarrow_S} = -(\sigma_\downarrow/\sigma_\uparrow)\delta\bar{\mu}_{\downarrow_S}$, which agrees with Ref. 65. Thus, the total electric current associated with the spin mode is zero:

$$-e\delta J_S = -e\left(\delta j_{\uparrow_S} + \delta j_{\downarrow_S} \right) = \frac{\sigma_\uparrow}{e}\partial_i \delta\bar{\mu}_{\uparrow_S} + \frac{\sigma_\downarrow}{e}\partial_i \delta\bar{\mu}_{\downarrow_S} = 0. \tag{4.21}$$

On the other hand, the total spin current J_σ in the spin mode may be nonzero:

$$\delta J_{\sigma_S} = \delta j_{\uparrow_S} - \delta j_{\downarrow_S} = -\frac{\sigma_\uparrow}{e^2}\partial_i \delta\bar{\mu}_{\uparrow_S} + \frac{\sigma_\downarrow}{e^2}\partial_i \delta\bar{\mu}_{\downarrow_S} = -\frac{2\sigma_\uparrow}{e^2}\partial_i \delta\bar{\mu}_{\uparrow_S} = 2\alpha\ell_{\mathrm{sf}}^2 eV_S e^{-x/\ell_{\mathrm{sf}}}. \tag{4.22}$$

The deviation in the internal magnetic field $H_\parallel^*$ in the spin mode can be written in terms of the difference between $\delta n_\uparrow$ and $\delta n_\downarrow$:

$$\delta H_\parallel^* = \delta\vec{H}^* \cdot \hat{M} = \frac{\mu_0 \delta\vec{M}}{\chi} \cdot \hat{M} = \frac{\mu_0\mu_B}{\chi}(\delta n_\uparrow - \delta n_\downarrow), \tag{4.23}$$

where where μ_0 is the permeability of free space (necessary because we use the SI unit of Tesla for $H_\parallel^*$ and $\vec{H}^*$) with units of $\mathrm{T^2\text{-}m^3\text{-}J^{-1}}$ and $\hat{M}$ defines the direction of up-spins. Then linearizing Eq. (2.24) gives

$$\delta\bar{\mu}_{(\uparrow,\downarrow)} = \frac{\delta n_{(\uparrow,\downarrow)}}{N_{(\uparrow,\downarrow)}} - e\delta\phi \pm \frac{(\delta n_\uparrow - \delta n_\downarrow)}{2N_\chi}. \tag{4.24}$$

Equations (4.12) and (4.24) give the difference of the spin potentials to be

$$\delta\bar{\mu}_{\uparrow_S} - \delta\bar{\mu}_{\downarrow_S} = \left(\frac{N_\uparrow + N_\chi}{N_\chi N_\uparrow}\right)\delta n_{\uparrow_S} - \left(\frac{N_\downarrow + N_\chi}{N_\chi N_\downarrow}\right)\delta n_{\downarrow_S} = eV_S e^{-x/\ell_{\mathrm{sf}}}, \tag{4.25}$$

and Eqs. (4.19), (4.20), and (4.24) give the sum of the spin potentials to be

$$\delta\bar{\mu}_{\uparrow_S} + \delta\bar{\mu}_{\downarrow_S} = \frac{\delta n_{\uparrow_S}}{N_\uparrow} + \frac{\delta n_{\downarrow_S}}{N_\downarrow} - 2e\delta\phi_S = R_\sigma eV_S e^{-x/\ell_{\mathrm{sf}}}. \tag{4.26}$$

Equations (4.25)-(4.26) and Gauss's law,

$$\partial_i^2 \delta\phi_S = \frac{e}{\varepsilon_0\varepsilon}\left(\delta n_{\uparrow_S} + \delta n_{\downarrow_S}\right), \tag{4.27}$$

relate $\delta n_{\uparrow_S}$, $\delta n_{\downarrow_S}$, and $\delta\phi_S$.

a. Spin Diffusion Mode in a Non-Magnetic Material (NM)

We now solve for the simpler case of a non-magnetic material (NM). Equation (4.26) may be solved for $\delta n_{\uparrow_S} + \delta n_{\downarrow_S}$, which may then be substituted into Eq. (4.27). For the non-magnetic case the solution is $\delta\phi_S^{(\mathrm{NM})} = 0$, so that the total charge in the spin mode is $-e(\delta n_{\uparrow_S}^{(\mathrm{NM})} + \delta n_{\downarrow_S}^{(\mathrm{NM})}) = 0$; that is, the spin mode does not lead to a nonzero potential or charge distribution in a non-magnetic material.

It does, however, lead to a nonzero *spin accumulation*, defined by

$$\Delta_{\uparrow\downarrow} n \equiv \delta n_\uparrow - \delta n_\downarrow. \tag{4.28}$$

Solving Eq. (4.25) under the NM condition that $\delta n_{\uparrow_S}^{(\mathrm{NM})} = -\delta n_{\downarrow_S}^{(\mathrm{NM})}$ and $N_\uparrow = N_\downarrow$ gives

$$\delta n_{\uparrow_S}^{(\mathrm{NM})} = -\delta n_{\downarrow_S}^{(\mathrm{NM})} = \frac{N_\uparrow N_\chi e V_S}{2\,(N_\uparrow + N_\chi)} e^{-x/\ell_{\mathrm{sf}}}. \tag{4.29}$$

The spin accumulation is therefore given by

$$\Delta_{\uparrow\downarrow} n_S^{(\mathrm{NM})} = \delta n_{\uparrow_S}^{(\mathrm{NM})} - \delta n_{\downarrow_S}^{(\mathrm{NM})} = \frac{N_\uparrow N_\chi e V_S}{(N_\uparrow + N_\chi)} e^{-x/\ell_{\mathrm{sf}}}. \tag{4.30}$$

Johnson and Silsbee[16] (JS) and Valet and Fert22 (VF) neglect $\delta\mu_{\uparrow,\downarrow}$, and Hershfield and Zhao (HZ) neglect $\delta H_\parallel^*$, which by Eq. (4.24) are equivalent to respectively taking $N_{\uparrow,\downarrow} \to \infty$ and $N_\chi \to \infty$. So, with $\zeta_{(\mathrm{ref})}$ defined by

$$\Delta_{\uparrow\downarrow} n_{S_{(\mathrm{ref})}}^{(\mathrm{NM})} = \zeta_{(\mathrm{ref})} \Delta_{\uparrow\downarrow} n_S^{(\mathrm{NM})}, \tag{4.31}$$

so that comparison to Eq. (4.30) gives $\zeta_{(\mathrm{present})} = 1$ for the present theory, then we find

$$\zeta_{(\mathrm{HZ})} = 1 + \frac{N_\uparrow}{N_\chi}, \quad \zeta_{(\mathrm{JS/VF})} = 1 + \frac{N_\chi}{N_\uparrow}. \tag{4.32}$$

Using Eq. (4.29) and $\delta\phi_S = 0$, Eqs. (4.24) and (4.19) give

$$\delta\bar{\mu}_{\uparrow_S}^{(\mathrm{NM})} = \frac{eV_S}{2} e^{-x/\ell_{\mathrm{sf}}} = \frac{\ell_{\mathrm{sf}}^2}{\ell_{\uparrow_S}^2} eV_S e^{-x/\ell_{\mathrm{sf}}}, \tag{4.33}$$

which is consistent for a non-magnetic material (for which $\ell_{\uparrow_S}^2 = \ell_{\downarrow_S}^2 = 2\ell_{\mathrm{sf}}^2$). Further, for $\delta n_{\uparrow_S} = -\delta n_{\downarrow_S}$ and $\delta\phi_S = 0$, Eq. (4.24) gives that $\delta\bar{\mu}_{\uparrow_S} = -\delta\bar{\mu}_{\downarrow_S}$. By Eq. (4.1), the up- and down-spin currents in a non-magnetic material are given by

$$\delta j_{\uparrow_S}^{(\mathrm{NM})} = \frac{\sigma_\uparrow V_S}{2e\ell_{\mathrm{sf}}} e^{-x/\ell_{\mathrm{sf}}}, \tag{4.34}$$

$$\delta j_{\downarrow_S}^{(\mathrm{NM})} = -\frac{\sigma_\downarrow V_S}{2e\ell_{\mathrm{sf}}} e^{-x/\ell_{\mathrm{sf}}}. \tag{4.35}$$

Since $\sigma_\uparrow = \sigma_\downarrow$, the spin current is given by

$$\delta J_{\sigma_S}^{(\mathrm{NM})} = \delta j_{\uparrow_S}^{(\mathrm{NM})} - \delta j_{\downarrow_S}^{(\mathrm{NM})} = \frac{\sigma_\uparrow V_S}{e\ell_{\mathrm{sf}}} e^{-x/\ell_{\mathrm{sf}}}. \tag{4.36}$$

b. Spin Diffusion Mode in a Ferromagnet (FM)

We now solve for the spin mode potential and spin concentrations of a ferromagnet (FM), where $N_\uparrow \neq N_\downarrow$ and $\sigma_\uparrow \neq \sigma_\downarrow$. As shown below, Eq. (4.25) relates $\delta n_{\uparrow_S}^{(\mathrm{FM})}$ to $\delta n_{\downarrow_S}^{(\mathrm{FM})}$, then Eq. (4.26) relates them to $\delta\phi_S^{(\mathrm{FM})}$. Equation (4.27) can thus be written in terms of only $\delta\phi_S^{(\mathrm{FM})}$.

Equation (4.25) gives

$$\delta n_{\downarrow_S}^{(\mathrm{FM})} = \left[\frac{N_\downarrow\left(N_\uparrow + N_\chi\right)}{N_\uparrow\left(N_\downarrow + N_\chi\right)}\right] \delta n_{\uparrow_S}^{(\mathrm{FM})} - \left(\frac{N_\chi N_\downarrow eV_S}{N_\downarrow + N_\chi}\right) e^{-x/\ell_{\mathrm{sf}}}. \tag{4.37}$$

Substituting Eq. (4.37) into Eq. (4.26) multiplied by $(N_\uparrow/N_\alpha)(N_\downarrow + N_\chi)$ and solving for $\delta n_{\uparrow_S}^{(\mathrm{FM})}$ gives

$$\delta n_{\uparrow_S}^{(\mathrm{FM})} = \frac{N_\uparrow}{N_\alpha} eV_S e^{-x/\ell_{\mathrm{sf}}} \left[N_\chi + R\left(N_\downarrow + N_\chi\right)\right] + 2e\frac{N_\uparrow}{N_\alpha}\left(N_\downarrow + N_\chi\right)\delta\phi_S^{(\mathrm{FM})}. \tag{4.38}$$

Finally, substitution of Eqs. (4.37) and (4.38) into Eq. (4.27) gives

$$\begin{aligned}\partial_x^2\delta\phi_S^{(\mathrm{FM})} =& \frac{e}{\varepsilon_0\varepsilon}\left\{1+\left[\frac{N_\downarrow\left(N_\uparrow+N_\chi\right)}{N_\uparrow\left(N_\downarrow+N_\chi\right)}\right]\right\}\delta n_{\uparrow_S}^{(\mathrm{FM})} - \frac{e}{\varepsilon_0\varepsilon}\left(\frac{N_\downarrow N_\chi eV_S}{N_\downarrow+N_\chi}\right)e^{-x/\ell_{\mathrm{sf}}} \\ =& \frac{2e^2N_\beta^2}{\varepsilon_0\varepsilon N_\alpha}\left\{\delta\phi_S^{(\mathrm{FM})}+\frac{V_S}{2}e^{-x/\ell_{\mathrm{sf}}}\left[R_\sigma+\frac{N_\chi\left(N_\uparrow-N_\downarrow\right)}{N_\beta^2}\right]\right\}, \end{aligned} \tag{4.39}$$

where we have used the identity

$$N_\beta^2 - N_\alpha N_\downarrow = \left(N_\uparrow - N_\downarrow\right)\left(N_\downarrow + N_\chi\right). \tag{4.40}$$

Using Eq. (4.16) we write Eq. (4.39) as

$$\partial_x^2\delta\phi_S^{(\mathrm{FM})} = \frac{2N_\beta^2}{N_SN_\alpha\ell_{\mathrm{sf}}^2}\left\{\delta\phi_S^{(\mathrm{FM})}+\frac{V_S}{2}\left[\frac{N_\chi}{N_\beta^2}\left(N_\uparrow-N_\downarrow\right)+R_\sigma\right]e^{-x/\ell_{\mathrm{sf}}}\right\}. \tag{4.41}$$

Equation (4.41) gives

$$\delta\phi_S^{(\mathrm{FM})} = \left[\frac{N_\chi\left(N_\uparrow-N_\downarrow\right)+R_\sigma N_\beta^2}{N_SN_\alpha-2N_\beta^2}\right]V_Se^{-x/\ell_{\mathrm{sf}}} \equiv \xi V_Se^{-x/\ell_{\mathrm{sf}}}, \tag{4.42}$$

Solving Eq. (4.42) for ξ gives Eq. (4.14).

Substituting Eq. (4.42) into Eqs. (4.38) and (4.37) on using Eq. (4.13) gives

$$\delta n_{\uparrow_S}^{(\mathrm{FM})} = N_\uparrow e\xi V_Se^{-x/\ell_{\mathrm{sf}}}\left\{\frac{-2N_\chi N_\downarrow+N_S\left[N_\chi+R_\sigma\left(N_\downarrow+N_\chi\right)\right]}{N_\chi\left(N_\uparrow-N_\downarrow\right)+R_\sigma N_\beta^2}\right\}, \tag{4.43}$$

$$\delta n_{\downarrow_S}^{(\mathrm{FM})} = N_\downarrow e\xi V_Se^{-x/\ell_{\mathrm{sf}}}\left\{\frac{2N_\chi N_\uparrow+N_S\left[-N_\chi+R_\sigma\left(N_\uparrow+N_\chi\right)\right]}{N_\chi\left(N_\uparrow-N_\downarrow\right)+R_\sigma N_\beta^2}\right\}. \tag{4.44}$$

Thus, the charge distribution in a ferromagnet associated with the spin mode is

$$\delta\rho_S^{(\mathrm{FM})} = -e\left(\delta n_{\uparrow_S}^{(\mathrm{FM})}+\delta n_{\downarrow_S}^{(\mathrm{FM})}\right) = e^2N_S\xi V_Se^{-x/\ell_{\mathrm{sf}}} = -\frac{\varepsilon_0\varepsilon}{\ell_{\mathrm{sf}}^2}\xi V_Se^{-x/\ell_{\mathrm{sf}}}. \tag{4.45}$$

This result may also be obtained by using Eq. (4.42) and Gauss's Law.

Further, Eqs. (4.43) and (4.44) give the spin accumulation to be

$$\begin{aligned}\Delta_{\uparrow\downarrow} n_S^{(\mathrm{FM})} =& \delta n_{\uparrow_S}^{(\mathrm{FM})} - \delta n_{\downarrow_S}^{(\mathrm{FM})} \\ =& e N_\chi \xi V_S e^{-x/\ell_{\mathrm{sf}}} \left\{ \frac{-4N_\uparrow N_\downarrow + N_S \left[N_\uparrow + N_\downarrow + R_\sigma \left(N_\uparrow - N_\downarrow\right)\right]}{N_\chi \left(N_\uparrow - N_\downarrow\right) + R_\sigma N_\beta^2} \right\}. \end{aligned} \tag{4.46}$$

Substitution of Eq. (4.46) into Eq. (4.23) gives the deviation in effective magnetic field

$$\begin{aligned}\delta H_{\parallel_S}^{*(\mathrm{FM})} &= \frac{\mu_0 \mu_B}{\chi} \left(\delta n_{\uparrow_S}^{(\mathrm{FM})} - \delta n_{\downarrow_S}^{(\mathrm{FM})} \right) \\ &= \frac{e \mu_0 \mu_B N_\chi \xi V_S}{\chi} e^{-x/\ell_{\mathrm{sf}}} \left\{ \frac{-4N_\uparrow N_\downarrow + N_S \left[N_\uparrow + N_\downarrow + R_\sigma \left(N_\uparrow - N_\downarrow\right)\right]}{N_\chi \left(N_\uparrow - N_\downarrow\right) + R_\sigma N_\beta^2} \right\} \\ &= \frac{e \xi V_S}{g \mu_B} e^{-x/\ell_{\mathrm{sf}}} \left\{ \frac{-4N_\uparrow N_\downarrow + N_S \left[N_\uparrow + N_\downarrow + R_\sigma \left(N_\uparrow - N_\downarrow\right)\right]}{N_\chi \left(N_\uparrow - N_\downarrow\right) + R_\sigma N_\beta^2} \right\}. \end{aligned} \tag{4.47}$$

2. Charge-Screening Mode (Q)

The second solution to Eqs. (4.2)-(4.4) has $\delta\bar{\mu}_\uparrow = 0 = \delta\bar{\mu}_\downarrow$ so that $J_\uparrow = 0 = J_\downarrow$. This mode is therefore entirely static (no spin nor charge current), corresponding to electric screening and characterized only by charge and potential gradients. We therefore follow Ref. 65 by designating it the "charge mode," and use the subscript Q to denote its properties.

By Eq. (4.24), setting $\delta\bar{\mu}_{\uparrow_Q} - \delta\bar{\mu}_{\downarrow_Q}$ to zero (because each is individually zero) gives

$$N_\downarrow \left(N_\uparrow + N_\chi\right) \delta n_{\uparrow_Q} = N_\uparrow \left(N_\downarrow + N_\chi\right) \delta n_{\downarrow_Q}, \tag{4.48}$$

and setting $\delta\bar{\mu}_{\uparrow_Q} + \delta\bar{\mu}_{\downarrow_Q}$ to zero gives

$$\delta\phi_Q = \frac{1}{2e} \left(\frac{\delta n_{\uparrow_Q}}{N_\uparrow} + \frac{\delta n_{\downarrow_Q}}{N_\downarrow} \right). \tag{4.49}$$

Substitution of Eq. (4.48) into Eq. (4.49) multiplied by $N_\uparrow(N_\downarrow + N_\chi)$ yields

$$N_\uparrow(N_\downarrow + N_\chi)\delta\phi_Q = \frac{N_\alpha}{2e}\delta n_{\uparrow_Q}, \tag{4.50}$$

where N_α is defined in Eq. (4.16). Substitution of Eqs. (4.48) and (4.50) into Gauss's Law, Eq. (4.4), multiplied by $N_\uparrow(N_\downarrow + N_\chi)$ then gives

$$\frac{N_\alpha}{2e}\partial_i^2\delta n_{\uparrow_Q} = \frac{2e^2}{\varepsilon_0\varepsilon}\left[N_\uparrow\left(N_\downarrow + N_\chi\right) + N_\downarrow\left(N_\uparrow + N_\chi\right)\right]\delta n_{\uparrow_Q}. \tag{4.51}$$

Equation (4.51) can be written

$$\partial_i^2\delta n_{\uparrow_Q} = \frac{1}{\ell_Q^2}\delta n_{\uparrow_Q}, \tag{4.52}$$

where

$$\ell_Q^2 \equiv \frac{\varepsilon_0\varepsilon}{2e^2}\frac{N_\alpha}{N_\beta^2}. \tag{4.53}$$

For $\chi \to \infty$ and $\varepsilon \to 1$, Eq. (4.53) gives $\ell_Q^2 = \varepsilon_0\varepsilon/[e^2(N_\uparrow + N_\downarrow)]$, which agrees with Ref. 65.

We now define the quantity ϕ_{0_Q} (with units of V) such that

$$\delta n_{\uparrow_Q} \equiv 2e\frac{N_\uparrow}{N_\alpha}\left(N_\downarrow + N_\chi\right)\phi_{0_Q}e^{-x/\ell_Q}, \tag{4.54}$$

which satisfies Eq. (4.52). Then Eq. (4.48) gives

$$\delta n_{\downarrow_Q} = 2e\frac{N_\downarrow}{N_\alpha}\left(N_\uparrow + N_\chi\right)\phi_{0_Q}e^{-x/\ell_Q}, \tag{4.55}$$

$$\delta\rho_Q = -e\left(\delta n_{\uparrow_Q} + \delta n_{\downarrow_Q}\right) = -2e^2\frac{N_\beta^2}{N_\alpha}\phi_{0_Q}e^{-x/\ell_Q} = -\frac{\varepsilon_0\varepsilon}{\ell_Q^2}\phi_{0_Q}e^{-x/\ell_Q}, \tag{4.56}$$

and Eq. (4.49) gives

$$\delta\phi_Q = \phi_{0_Q}e^{-x/\ell_Q}. \tag{4.57}$$

Equation (4.57) shows that $\phi_{0_Q} = \delta\phi_Q(0)$.

Use of Eqs. (4.54) and (4.55) gives

$$\Delta_{\uparrow\downarrow} n_Q = \delta n_{\uparrow_Q} - \delta n_{\downarrow_Q} = 2e\frac{N_\chi}{N_\alpha}(N_\uparrow - N_\downarrow)\phi_{0_Q} e^{-x/\ell_Q}, \tag{4.58}$$

which is nonzero in a ferromagnet, where $N_\uparrow \neq N_\downarrow$. Substitution of Eq. (4.58) into Eq. (4.23) gives

$$\delta H^*_{\|_Q} = \frac{2\mu_0\mu_B e N_\chi}{\chi N_\alpha}\left(N_\uparrow - N_\downarrow\right)\phi_{0_Q} e^{-x/\ell_Q} = \frac{2e}{g\mu_B N_\alpha}\left(N_\uparrow - N_\downarrow\right)\phi_{0_Q} e^{-x/\ell_Q}. \tag{4.59}$$

Like the spin mode, the charge mode has zero net current $\delta J^n_Q = \delta j_{\uparrow_Q} + \delta j_{\downarrow_Q}$, although unlike the spin mode the charge mode involves zero net spin current $\delta J^\sigma_Q = \delta j_{\uparrow_Q} - \delta j_{\downarrow_Q} = 0$.

3. Bulk Mode (dc)

This chapter considers a system which has, in the bulk, a uniform constant electric current. The mode associated with this current, which we designate the "dc mode" and denote by the sub/superscript *dc*, is characterized by a constant electric field (which in principle differs for each material). We define this field as

$$\delta\vec{E}_{dc} \equiv A\hat{x}, \tag{4.60}$$

where A is a constant (with units of V/m) which must be determined. Furthermore, Eq. (4.60) gives, for the potential associated with this mode,

$$\delta\phi_{dc} = -Ax + B, \tag{4.61}$$

where B is another constant (with units of V) which must be determined. By Gauss's Law there is clearly no overall (bulk or surface) charge associated with this mode, as

expected. Further, Eqs. (4.61) and (4.24) give

$$\delta\bar{\mu}_{\uparrow_{dc}} = \delta\bar{\mu}_{\downarrow_{dc}} = -e\delta\phi_{dc} = eAx - eB. \tag{4.62}$$

Equation (4.1) gives

$$j_{\uparrow_{dc}} = -\frac{\sigma_{\uparrow}A}{e}, \quad j_{\downarrow_{dc}} = -\frac{\sigma_{\downarrow}A}{e}. \tag{4.63}$$

Because $\sigma_{\uparrow}$ is not necessarily equal to $\sigma_{\downarrow}$ (e.g., as for ferromagnets), there may be a non-zero spin current associated with the *dc* mode.

4. Complete Description Near an Interface

A full description of the region near an interface involves the combination of both surface modes (S and Q) derived above, and the bulk constant current (dc) mode. For the potential, electric field, charge density near an interface located at $x = x_{\text{int}}$, from Eqs. (4.42), (4.45), (4.56), (4.57), (4.60), and (4.61) we have

$$\delta\phi = \xi V_S e^{\pm(x-x_{\text{int}})/\ell_{\text{sf}}} + \phi_{0_Q} e^{\pm(x-x_{\text{int}})/\ell_Q} - A(x - x_{\text{int}}) + B, \tag{4.64}$$

$$\delta E = \mp \frac{\xi V_S}{\ell_{\text{sf}}} e^{\pm(x-x_{\text{int}})/\ell_{\text{sf}}} \mp \frac{\phi_{0_Q}}{\ell_Q} e^{\pm(x-x_{\text{int}})/\ell_Q} + A, \tag{4.65}$$

$$\delta\rho = -\epsilon_0\epsilon \left(\frac{\xi V_S}{\ell_{\text{sf}}^2} e^{\pm(x-x_{\text{int}})/\ell_{\text{sf}}} + \frac{\phi_{0_Q}}{\ell_Q^2} e^{\pm(x-x_{\text{int}})/\ell_Q} \right). \tag{4.66}$$

The top (bottom) sign corresponds to the material on the left (right) of the interface. Recall that $\xi \to 0$ for a non-magnetic material. For the spin accumulation, Eqs. (4.30),

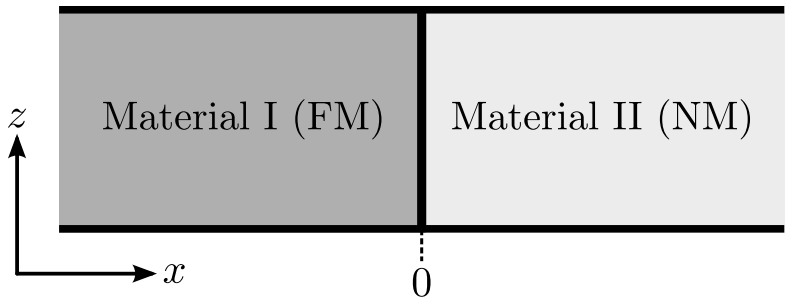

Fig. 6. An isolated interface between a ferromagnet (dark gray, at $x < 0$) and a non-magnetic material (light gray, at $x > 0$). This work considers an electric current density $J\hat{x}$, and magnetization of the FM along $\pm\hat{z}$.

(4.46), and (4.58) yield

$$\Delta_{\uparrow\downarrow} n^{(\mathrm{NM})} = \frac{N_\uparrow N_\chi e V_S}{(N_\uparrow + N_\chi)} e^{\pm(x-x_{\mathrm{int}})/\ell_{\mathrm{sf}}} + 2e\frac{N_\chi}{N_\alpha}(N_\uparrow - N_\downarrow)\phi_{0_Q} e^{\pm(x-x_{\mathrm{int}})/\ell_Q}, \tag{4.67}$$

$$\Delta_{\uparrow\downarrow} n^{(\mathrm{FM})} = eN_\chi \xi V_S e^{\pm(x-x_{\mathrm{int}})/\ell_{\mathrm{sf}}} \left\{ \frac{-4N_\uparrow N_\downarrow + N_S\left[N_\uparrow + N_\downarrow + R\left(N_\uparrow - N_\downarrow\right)\right]}{N_\chi\left(N_\uparrow - N_\downarrow\right) + RN_\beta^2} \right\}$$
$$+ 2e\frac{N_\chi}{N_\alpha}(N_\uparrow - N_\downarrow)\phi_{0_Q} e^{\pm(x-x_{\mathrm{int}})/\ell_Q}. \tag{4.68}$$

For an isolated interface at $x_{\mathrm{int}} = 0$ (see Fig. 6) between materials I (at $x < 0$) and II (at $x > 0$), in general there are eight unknowns (A, B, ϕ_{0_Q}, and V_S for each of materials I and II). There are eight corresponding conditions, here designated condition (i) through condition (viii):

(i-ii) the potential ϕ and field $\vec{E}$ must be continuous across the interface;

(iii-iv) the total electric current $-e(j_\uparrow + j_\downarrow)$ is equal to the (known) constant electric current in each material;

(v) the spin current is assumed continuous across the interface (although we take both up- and down-spin currents to be continuous, conditions (iii-iv) constrain

their sum, so that interfacial spin-current continuity is only a single condition);

(vi-vii) the up- and down-spin currents across the interface are directly proportional to the discontinuity in up- and down-spin magnetoelectrochemical potential across the interface (i.e., Eqs. (2.51)-(2.52) hold with the cross-terms neglected); and

(viii) there is an arbitrary constant voltage (which we define by setting the voltage $B^{(\mathrm{II})} \equiv 0$).

Ref. 65 similarly numbers and discusses the conditions necessary to solve for the unknowns at such a boundary. It uses the present work's conditions (iii-vii) as its conditions (1-5), although not in the same order. Furthermore, it makes use of the present work's condition (viii), though it does not number it. However, because it neglects the charge mode at the interface, it does not take potential or field to be continuous across the interface.

For a multilayer (a series of k interfaces between $k+1$ materials), condition (viii) remains a single condition because we may only define one arbitrary voltage, and there is a single condition of the type (iii-iv) for each material (for a total of $k+1$ conditions) because it applies in the bulk of each material. All five of the other conditions apply for each interface. Thus, there are $1+k+1+5k = 6k+2$ conditions.

C. Isolated Interfaces

For an isolated interface (as in Fig. 6), Appendix C uses each of the above conditions to find an explicit equation for the eight unknowns and writes the unknowns in terms of dimensionless variables. The numerical results for a cobalt/copper interface, with material parameters given by Tables I and II, are shown in the figures below in dimensionless units: Fig. 7 gives the electric potential; Fig. 8 gives the electric field; and Fig. 9 gives the spin accumulation.

Table I. Bulk and interfacial properties of cobalt and copper, and well-known constants. Here, A is the area of the interface, and R is the spin-dependent interface resistance. †Value is for the (100) orientation. ‡The susceptibility of Cobalt is field--dependent, and takes a value between 70 and 250 (see Table 2.2 of Ref. 70); we take an intermediate value.

Quantity	Value	Units	Ref
$\sigma_{\uparrow}^{\mathrm{Co}}$	2.47×10^{7}	Ω^{-1}-m^{-1}	71
$\sigma_{\downarrow}^{\mathrm{Co}}$	0.913×10^{7}	Ω^{-1}-m^{-1}	71
$\sigma_{\downarrow}^{\mathrm{Cu}}$, $\sigma_{\uparrow}^{\mathrm{Cu}}$	8.35×10^{7}	Ω^{-1}-m^{-1}	71
$\ell_{\mathrm{sf}}^{\mathrm{Co}}$	59×10^{-9}	m	71
$\ell_{\mathrm{sf}}^{\mathrm{Cu}}$	450×10^{-9}	m	71
$N_{\uparrow}^{\mathrm{Co}}$	5.10×10^{46}	J^{-1}–m^{-3}	71
$N_{\downarrow}^{\mathrm{Co}}$	19.7×10^{46}	J^{-1}–m^{-3}	71
$N_{\uparrow}^{\mathrm{Cu}}$, $N_{\downarrow}^{\mathrm{Cu}}$	3.89×10^{46}	J^{-1}–m^{-3}	71
$AR_{\uparrow}^{\mathrm{Cu/Co}}$	0.31×10^{-15}	Ω–m^2	43†
$AR_{\downarrow}^{\mathrm{Cu/Co}}$	2.31×10^{-15}	Ω–m^2	43†
χ^{Co}	≈ 100		70‡
χ^{Cu}	-0.932×10^{-5}		72
μ_B	9.27×10^{-24}	J–T^{-1}	
μ_0	$4\pi \times 10^{-7}$	N – A^{-2}	
ε_0	8.85×10^{-12}	A–s–V^{-1}–m^{-1}	
e	1.6×10^{-19}	C	
g	≈ 2		

Table II. Bulk and interfacial properties of cobalt and copper, calculated from the results of the present work (and Table I). Here α is found from Eq. (4.10).

Quantity	Value	Units
$\sigma^{\mathrm{Cu}} \equiv \sigma_{\uparrow}^{\mathrm{Cu}} + \sigma_{\downarrow}^{\mathrm{Cu}}$	16.7×10^{7}	Ω^{-1}-m^{-1}
$g_{\uparrow}$	3.23×10^{15}	Ω^{-1}-m^{-2}
$g_{\downarrow}$	0.433×10^{15}	Ω^{-1}-m^{-2}
N_{χ}^{Co}	4.63×10^{53}	J^{-1}–m^{-3}
N_{χ}^{Cu}	-4.32×10^{46}	J^{-1}–m^{-3}
N_{S}^{Co}	9.93×10^{40}	J^{-1}–m^{-3}
N_{S}^{Cu}	1.71×10^{39}	J^{-1}–m^{-3}
N_{α}^{Co}	9.26×10^{53}	J^{-1}–m^{-3}
N_{α}^{Cu}	-0.851×10^{46}	J^{-1}–m^{-3}
$N_{\beta}^{\mathrm{Co}\,2}$	1.15×10^{101}	J^{-2}–m^{-6}
$N_{\beta}^{\mathrm{Cu}\,2}$	-3.31×10^{92}	J^{-2}–m^{-6}
α^{Co}	74.8×10^{57}	J^{-1}–m^{-3}–s^{-1}
α^{Cu}	8.05×10^{57}	J^{-1}–m^{-3}–s^{-1}
$\ell_{\uparrow_S}^{\mathrm{Co}}$	114×10^{-9}	m
$\ell_{\downarrow_S}^{\mathrm{Co}}$	69.0×10^{-9}	m
$\ell_{\uparrow_S}^{\mathrm{Cu}}, \ell_{\downarrow_S}^{\mathrm{Cu}}$	636×10^{-9}	m
ℓ_{Q}^{Co}	0.0373×10^{-9}	m
ℓ_{Q}^{Cu}	0.0667×10^{-9}	m
R_{σ}^{Co}	-0.460	
R_{σ}^{Cu}	0	
ξ^{Co}	0.524	
ξ^{Cu}	0	

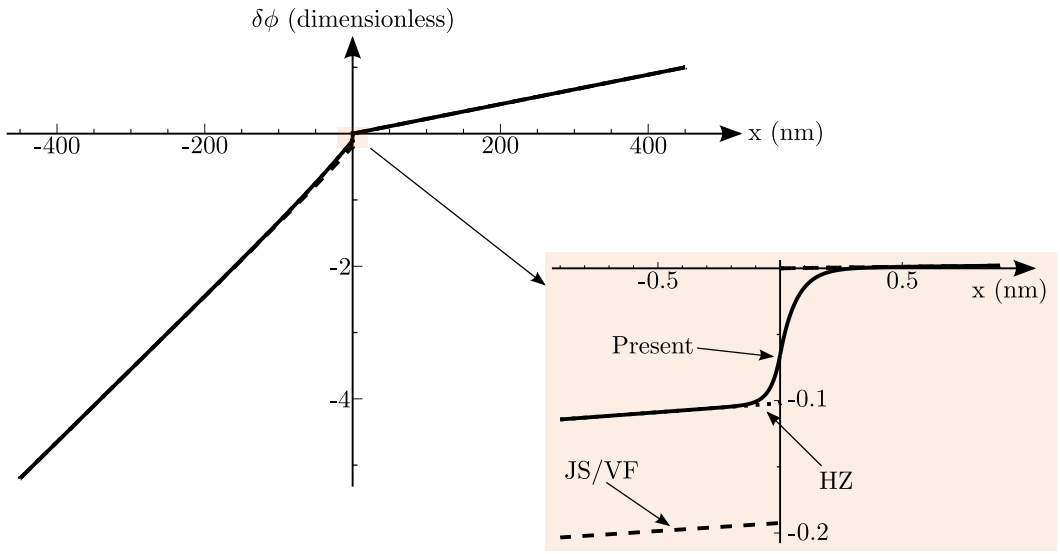

Fig. 7. The dimensionless electric potential (given by Eq. (4.64) normalized by $\tilde{V} \equiv -e\ell_{\rm sf}^{\rm Cu} J/\sigma^{\rm Cu}$) near an interface between cobalt and copper. The horizontal axis is position along x in nm. Here cobalt is at $x < 0$ and copper is at $x > 0$. The inset is a 500x magnification at the interface (thus showing the potential within about 1 nm of the interface), which shows that the electric potential is indeed continuous. The present theory is shown as a solid line, the present theory neglecting charge screening and chemical potential (as in JS) is shown as a dashed line, and the present theory neglecting charge screening and effective field $\vec{H}^*$ (as in HZ) is shown as a dotted line. The three lines are difficult to distinguish except very near the interface (see inset).

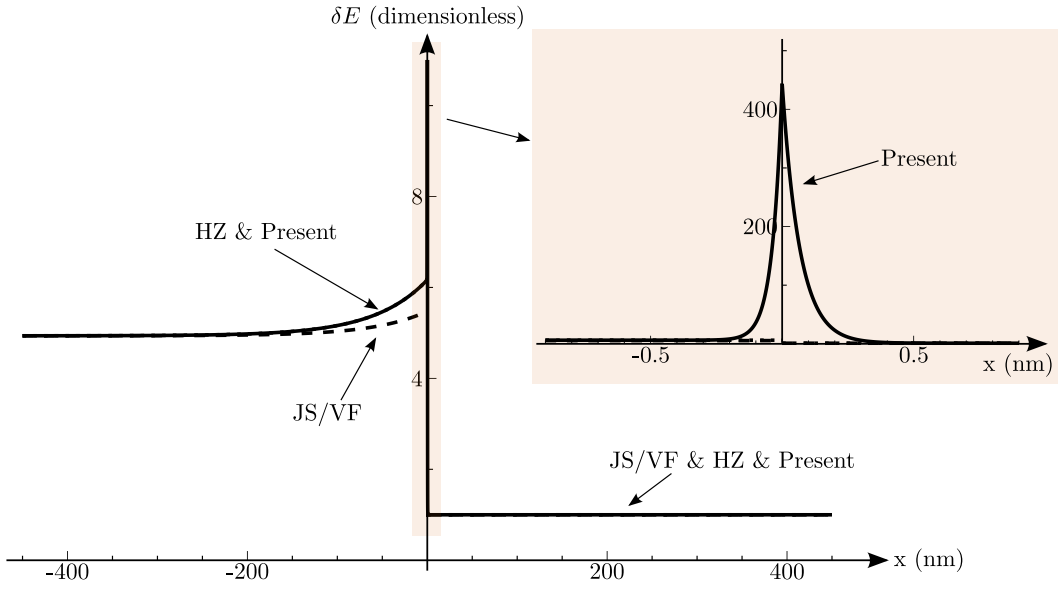

Fig. 8. The dimensionless electric field (given by Eq. (4.65) normalized by $\tilde{V}/\ell_{\rm sf}^{\rm Cu} = -eJ/\sigma^{\rm Cu}$) near an interface between cobalt and copper. The horizontal axis is position along x in nm. Here cobalt is at $x < 0$ and copper is at $x > 0$. The inset is a 500x magnification of the horizontal axis at the interface (thus showing the field within about 1 nm of the interface), which shows that the electric field is indeed continuous. The present theory is shown as a solid line, the present theory neglecting charge screening and chemical potential (as in JS) is shown as a dashed line, and the present theory neglecting charge screening and effective field $\vec{H}^*$ (as in HZ) is shown as a dotted line. The dotted line coincides closely with the present theory except within the charge screening length of the interface.

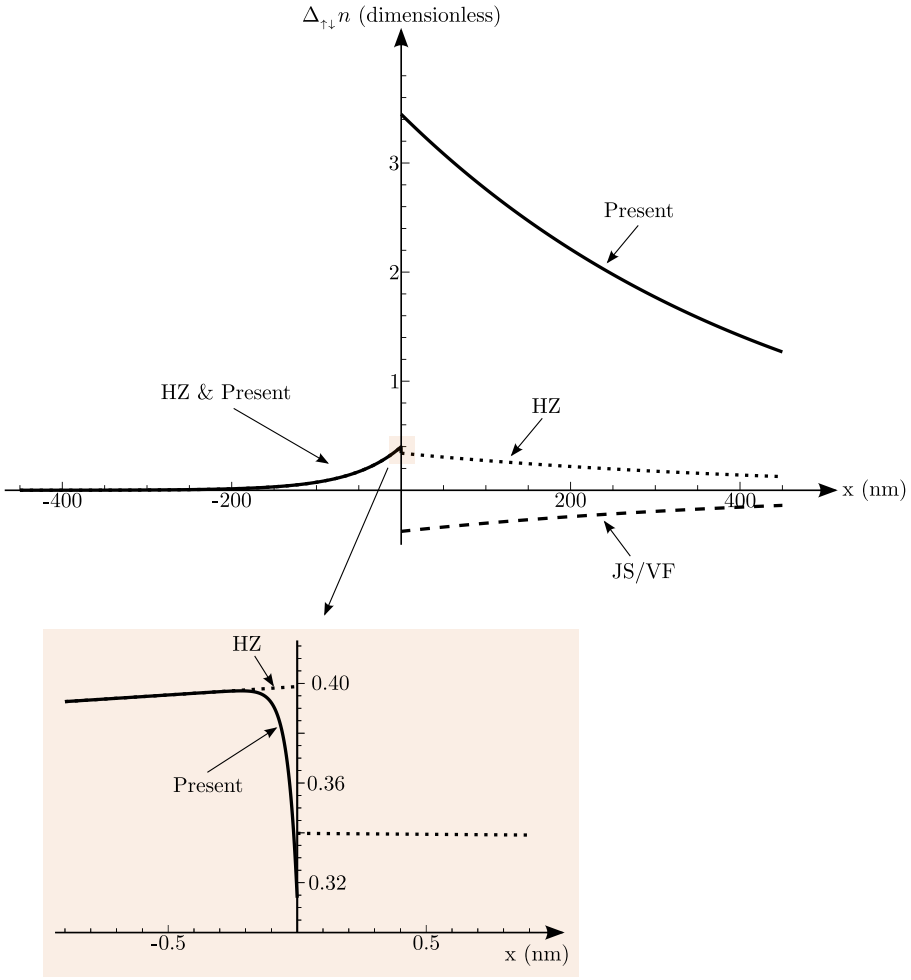

Fig. 9. The dimensionless spin accumulation (given by Eqs. (4.67) and (4.68) in arbitrary units) near an interface between cobalt and copper. The horizontal axis is position along x in nm. Here cobalt is at $x < 0$ and copper is at $x > 0$. The present theory is shown as a solid line, the present theory neglecting charge screening and chemical potential (as in JS) is shown as a dashed line, and the present theory neglecting charge screening and effective field $\vec{H}^*$ (as in HZ) is shown as a dotted line. In the FM ($x < 0$), the HZ-predicted spin accumulation closely tracks that of the present theory (deviating only within the charge-screening length of the interface, see inset), and the JS/VF-predicted spin accumulation is several orders of magnitude larger and not shown. In the NM, neither approximation predicts a spin accumulation similar to the present theory.

The insets of Figs. 7 and 8 respectively show the continuity of the electric potential and electric field at the interface.

As mentioned earlier, previous theories by Johnson and Silsbee (JS), Valet and Fert (VF) and by Hershfield and Zhao (HZ) neglect the charge mode (and therefore cannot have field and potential continuity at the interface). Additionally, JS and VF neglect the chemical potentials $\mu_\uparrow$ and $\mu_\downarrow$ and HZ neglects the internal magnetic field $H_\parallel^*$. The spin accumulation for these modes is given by the dotted (HZ) and dashed (JS/VF) lines in Fig. 9, with the relevant equations found below. The discrepancy between predicted spin accumulation, particularly in the normal metal, demonstrates that inclusion of all parts of the magnetoelectrochemical potential is essential for calculating the spin accumulation in a non-magnetic material, even to the correct order of magnitude.

1. Neglecting $H_\parallel^*$ and the Charge Mode

Neglecting the last term (proportional to $H_\parallel^*$) in Eq. (4.24), as in HZ,[65] is equivalent to taking $\chi \to \infty$ (and therefore $N_\chi \to \infty$) in the present results. We then have $N_\alpha \to 2N_\chi$, $N_\beta^2 \to N_\chi(N_\uparrow + N_\downarrow)$, and

$$\xi \to \frac{N_\uparrow - N_\downarrow + R_\sigma(N_\uparrow + N_\downarrow)}{2N_S - 2(N_\uparrow + N_\downarrow)}.$$

Therefore, $\xi^{\mathrm{Co}} \to 1.46$, as in the present theory.

The charge mode is neglected by HZ, and various properties of the spin mode are now calculated under its assumption that $H_\parallel^*$ is zero. For a non-magnetic material, $\delta\phi = 0$ and $\delta\rho = 0$ as before, and Eq. (4.29) gives

$$\delta n_{\uparrow_S}^{(\mathrm{NM})} = -\delta n_{\downarrow_S}^{(\mathrm{NM})} = \frac{eN_\uparrow V_S}{2} e^{-x/\ell_{sf}}. \tag{4.69}$$

For a ferromagnet, Eqs. (4.42)-(4.44) give the electric potential and up and down spin

concentrations in the spin mode to be

$$\delta\phi_S^{(\mathrm{FM})} = \left[\frac{N_\uparrow - N_\downarrow + R_\sigma(N_\uparrow + N_\downarrow)}{2\,(N_S - N_\uparrow - N_\downarrow)}\right] V_S e^{-x/\ell_{sf}}, \tag{4.70}$$

$$\delta n_{\uparrow_S}^{(\mathrm{FM})} = N_\uparrow e\xi V_S e^{-x/\ell_{sf}} \left\{\frac{-2N_\downarrow + N_S(1+R_\sigma)}{N_\uparrow - N_\downarrow + R_\sigma(N_\uparrow + N_\downarrow)}\right\}, \tag{4.71}$$

$$\delta n_{\downarrow_S}^{(\mathrm{FM})} = N_\downarrow e\xi V_S e^{-x/\ell_{sf}} \left\{\frac{2N_\uparrow + N_S(-1+R_\sigma)}{N_\uparrow - N_\downarrow + R_\sigma(N_\uparrow + N_\downarrow)}\right\}. \tag{4.72}$$

For the spin accumulation, Eqs. (4.69) and (4.71)-(4.72) give

$$\Delta_{\uparrow\downarrow} n^{(\mathrm{NM})} = eN_\uparrow V_S e^{-x/\ell_{sf}}, \tag{4.73}$$

$$\Delta_{\uparrow\downarrow} n^{(\mathrm{FM})} = e\xi V_S e^{x/\ell_{sf}} \left\{\frac{-4N_\uparrow N_\downarrow + N_S\left[N_\uparrow + N_\downarrow + R_\sigma\left(N_\uparrow - N_\downarrow\right)\right]}{N_\uparrow - N_\downarrow + R_\sigma(N_\uparrow + N_\downarrow)}\right\}. \tag{4.74}$$

As shown earlier in Eq. (4.32), in the non-magnet, when the charge mode and $\delta H_\parallel^*$ are neglected, the spin accumulation is underestimated by the multiplicative factor $\zeta_{(\mathrm{HZ})} = (1 + N_\uparrow/N_\chi)$, which is about 0.0986 for Cu. (Cu is a diamagnet, for which $N_\chi < 0$; in a paramagnet, for which $N_\chi > 0$, the underestimation of spin accumulation in this approximation is less striking, although it remains significant.) For the ferromagnet, the contribution to spin accumulation from the charge mode is neglected, and the spin accumulation from the spin mode agrees with the present theory to within the precision of the present calculations. Hence, the approximation taken by HZ is appropriate for ferromagnets but not for nonmagnetic materials.

Normalized Eqs. (4.73) and (4.74) are shown by the dotted lines in Fig. 9.

2. Neglecting $\mu_\uparrow$, $\mu_\downarrow$ and the Charge Mode

JS[16] and VF[22] neglect the chemical potentials $\mu_\uparrow$ and $\mu_\downarrow$ in Eq. (4.24), which is equivalent to taking $\mu_\uparrow \to 0$ and $\mu_\downarrow \to 0$ and $N_{\uparrow,\downarrow} \to \infty$ in the present theory.

The charge mode is neglected by JS/VF, and various properties of the spin mode

are now calculated under its assumption that $\mu_\uparrow$ and $\mu_\downarrow$ are zero. From Eq. (4.26) we have

$$\delta\phi_S = -\frac{R_\sigma}{2} V_S e^{-x/\ell_{sf}}, \tag{4.75}$$

so that $\xi \to -R/2$. Then, from Eqs. (4.25) and (4.27) we find

$$\delta n_{\uparrow_S} = \left[N_\chi - \left(\frac{R_\sigma}{2} \right) N_S \right] \frac{eV_S}{2} e^{-x/\ell_{sf}}, \tag{4.76}$$

$$\delta n_{\downarrow_S} = -\left[N_\chi + \left(\frac{R_\sigma}{2} \right) N_S \right] \frac{eV_S}{2} e^{-x/\ell_{sf}}. \tag{4.77}$$

The spin accumulation is thus

$$\Delta_{\uparrow\downarrow} n = N_\chi e V_S e^{-x/\ell_{sf}}. \tag{4.78}$$

As shown earlier in Eq. (4.32), in the non-magnet, when the charge mode and chemical potentials are neglected, the spin accumulation is underestimated by the multiplicative factor $\zeta_{(\mathrm{JS/VF})} = (1 + N_\chi/N_\uparrow)$, which is about -0.109 for Cu. Thus, this approximation is inappropriate for determining the spin accumulation in non-magnetic materials, particularly those that are diamagnetic.

Normalized Eq. (4.78) is shown by the dashed line in Fig. 9.

D. Multilayers

As discussed above, for a multilayer with k interfaces there are $6k + 2$ boundary conditions. For a multilayer of three materials with two interfaces (e.g., the read head of a hard drive), there are therefore 14 boundary conditions, here designated conditions (i) through condition (xiv):

(i-iv) the potential ϕ and field $\vec{E}$ must be continuous across both interfaces;

(v-vii) the total electric current $-e(j_\uparrow + j_\downarrow)$ is equal to the (known) constant electric

current within each of the three materials;

(viii-ix) the spin current is continuous across each interface (again, conditions (v-vii) constrain the sum of the spin currents, so that interfacial spin-current continuity is only a single condition at each interface);

(x-xiii) the up- and down-spin currents across each interface are directly proportional to the discontinuity in up- and down-spin magnetoelectrochemical potential across the interface (i.e., Eqs. (2.51)-(2.52) hold with the cross-terms neglected); and

(xiv) there is an arbitrary constant voltage (which we define by setting the voltage $B^{(\mathrm{II})} \equiv 0$).

Appendix D explicitly finds these fourteen conditions and writes them in terms of dimensionless variables.

CHAPTER V

TEMPERATURE AND THERMAL FLUX IN A THIN-FILM FERROMAGNET ON AN INSULATING SUBSTRATE: THE SPIN-SEEBECK EFFECT

As discussed in Chapter IV, passing electrical current through multilayers (by applying a voltage gradient $\nabla\phi$) can generate a spin current and cause an accumulation of spins. As discussed in Chapter II, however, gradients of other intrinsic thermodynamic properties can also generate spin currents. For instance, a thermal gradient ∇T can produce a spin current. This magnetic analog of the Seebeck effect, whereby electric currents are generated by ∇T, is known as the spin-Seebeck effect. This is an off-diagonal Onsager coefficient, and is not studied here; rather, we consider the temperature and heat flux.

The spin-Seebeck effect has recently been observed[31–33] in a ferromagnet film of thickness $d_F \sim 10$ nm and length $L \sim 10$ mm grown on an insulating substrate. When subjected to a temperature gradient (see Fig. 10a), a nonzero voltage difference ΔV_y across the width of the sample is observed; this signal is attributed to a spin flux along z. It is observed to decay over a very large length (much greater than a spin-diffusion length) from the heaters. Because the only applied gradient is of temperature, and fluxes are driven by gradients of intensive parameters (e.g., voltage or temperature), the temperatures in the ferromagnetic sample (F) and the substrate (s), and their associated gradients, are of interest.

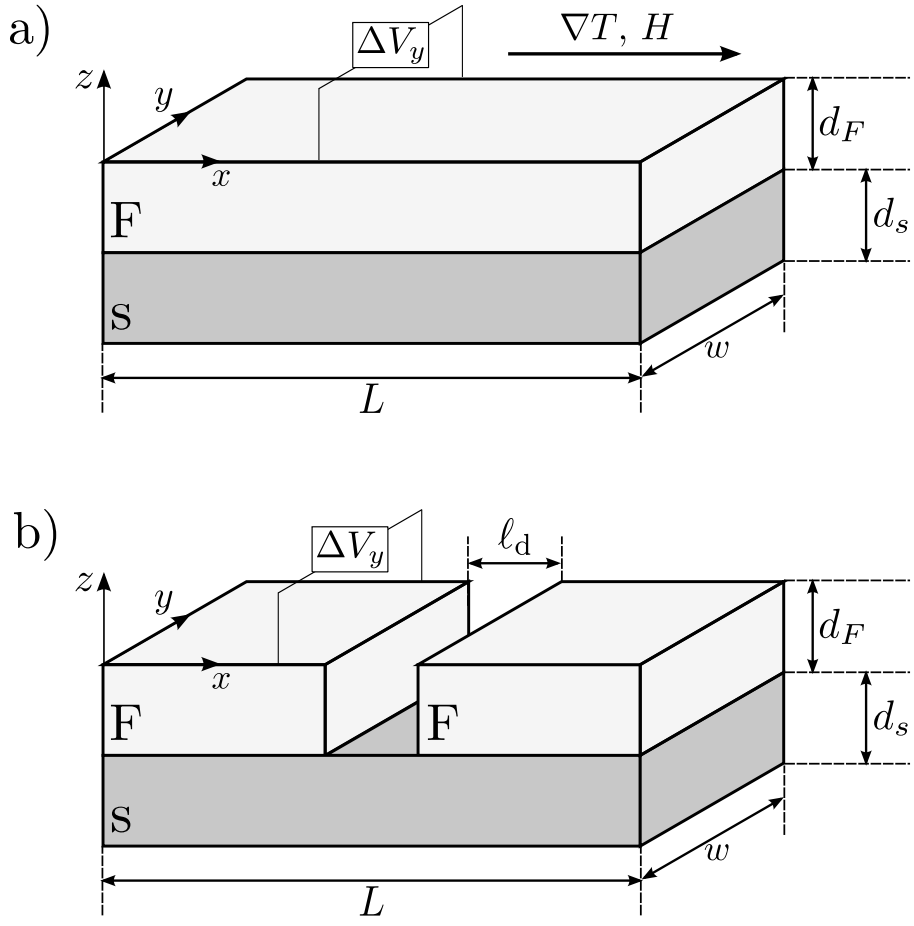

Fig. 10. The substrate (s, dark gray) and ferromagnetic sample (F, light gray) of the spin-Seebeck experiment. Here, (a) shows the typical experimental system, and (b) shows the system with a disconnection (scratch) in the sample of length ℓ_d. An external magnetic field is applied along x. The temperature at the far edges along x is maintained by a heater and a heat sink. A voltage difference ΔV_y across the sample in the y-direction is measured as a function of x by point electrodes[33] or by Pt wires (not shown) deposited on the sample.[31–33] For a scratch length $\ell_d = 350$ μm, Ref. 33 measures a similar signal ΔV_y as for the unscratched sample (a). The figure is not to scale. The heater and heat sink, which are placed at each edge of the substrate along x, are not pictured.

Reference 33 observes the measured voltage ΔV_y along y to have a $\sinh(x)$-like form along the sample, suggesting that it is a surface effect related to the leads that provide heat input and output. It has been suggested[38] that this surface effect is governed by magnon-phonon thermal equilibration[73] within the sample. However, Ref. 38 argues that for permalloy ($Ni_{81}Fe_{19}$) this equilibration should yield a maximum characteristic length of only $\lambda_{mp} = 0.3$ mm, whereas experiment shows the spin-Seebeck effect to have a characteristic length at least an order of magnitude larger.[31]

Further, the effect is unchanged for a large discontinuity[33] (approximately 350 μm) along x (see Fig. 10b); both with and without the discontinuity, a single $\sinh(x)$ is measured across the entire length L of the system. It is thus likely that the substrate, which is the only physical connection between the discontinuous regions of the sample, plays an important role. To this effect, Ref. 33 states that a possible explanation of the persistance of the signal regardless of disconnection is "thermal coupling through the substrate in which heat is carried by phonons."

The applications in Chapters II, III and IV deal with fluxes and concentrations of (conserved) particles and (non-conserved) spins. This chapter instead deals with (non-conserved) excitations, magnons (spin waves) and phonons (lattice vibrations), which are responsible for thermal conduction. We use irreversible thermodynamics to justify and extend the 1D, two-subsystem approach of Ref. 73 to the system of Fig. 10, a 2D system (with perfect symmetry in the y-direction) that contains three subsystems: sample phonons, sample magnons, and substrate phonons.

This chapter considers thermal equilibration both between magnons and phonons in the sample, as well as between the sample and the substrate (although for the most part it neglects direct equilibration between substrate phonons and sample magnons, discussed further below). For a non-magnetic sample, the characteristic length of the

sample-substrate thermal equilibration is shown below to be

$$\lambda_{ps} \sim \sqrt{\frac{\kappa d}{h_K}}. \tag{5.1}$$

Here, κ is a thermal conductivity, d is a length related to the thicknesses of the sample and substrate, and recall that h_K is the thermal boundary (Kapitza) conductance.

In addition to the geometrical length, there are three different lengths associated with Fig. 10: the magnon-phonon equilibration length λ_{mp}; the sample-substrate phonon equilibration length λ_{ps}; and an infinite length λ_∞ that leads to the usual linear thermal profile (see the example in Chapter I). Recall that Ref. 33 observes a $\sinh(x/\lambda)$ profile of the effect. If $\lambda \ll L$, then $\sinh(x/\lambda)$ will decay too close to the boundaries to be experimentally observed. Conversely, if $\lambda \gg L$, then $\sinh(x/\lambda)$ will appear to be linear in x, which may explain the linear signal observed by Refs. 31 and 32. It is therefore likely that the longer of λ_{ps} and λ_{mp} is the length observed.

When both magnon-phonon equilibration (internal to the ferromagnetic sample) and sample-substrate equilibration are present, the coupling between these two modes further separates their characteristic lengths. That is, the longer of λ_{ps} and λ_{mp} increases, and the shorter decreases. With κ_m, κ_p, and κ_s denoting the respective thermal conductivities of sample magnons, of sample phonons, and of substrate phonons, the coupling is given by a dimensionless coupling constant that is the product of R_{mp} and R_{ps}, which are shown below to be

$$R_{mp} \equiv \left(\frac{\kappa_m}{\kappa_m + \kappa_p}\right), \quad R_{ps} \equiv \left(\frac{d_s \kappa_s}{d_F \kappa_p + d_s \kappa_s}\right), \tag{5.2}$$

The thicknesses d_s and d_F are shown in Fig. 10. Thus, the sample-substrate coupling strength (and the increase of the longer equilibration length) is enhanced via R_{mp} if the magnons account for an appreciable amount of the thermal conductivity of the ferromagnet, and is enhanced via R_{ps} if the substrate is much thicker or has a much

larger heat capacity than the ferromagnetic sample.

As mentioned above, this chapter focuses solely on thermal equilibration and heat fluxes, and neglects off-diagonal Onsager coefficients, e.g., the spin currents induced by the thermal gradients. In principle, the modes found in Chap. IV are present in the spin-Seebeck system. It is possible that, in particular, the spin-diffusion mode couples with the thermal equilibration modes found in this chapter, and modifies the mode lengths accordingly. Because we show that thermal equilibration mode mixing does not yield a decay length long enough to explain the spin-Seebeck experiments, this possibility warrants further detailed study. We do not discuss it further.

Section A of this chapter employs irreversible thermodynamics to find the energy transferred between two systems at different temperatures, specifically considering systems that share a surface (e.g., the sample and substrate) and systems that share a volume (e.g., magnons and phonons in the ferromagnet). For heat flow approximated to be only along x, Section B finds the characteristic lengths of the thermal equilibration modes, as well as the spatial profiles of the phonon and magnon temperatures and heat fluxes. For heat flow along both x and z, Sec. C finds the shape of the spatial profile of temperatures and heat fluxes, and numerically solves for the characteristic lengths and z-dependence of the phonon and magnon heat flux magnitudes for an example system. Section D discusses the lengths associated with thermal equilibration, and why the present theory likely does not explain the anomalously large length measured by spin-Seebeck experiments. For heat flux along both x and z, Appendix E discusses and explicitly finds the bulk and boundary conditions, and App. F shows the algorithm used to solve the boundary conditions for the characteristic lengths, the results of which are discussed in Sec. C.

It has recently been proposed[74,75] that electron-phonon drag and magnon-phonon drag processes are important in explaining the results of the spin-Seebeck experiments.

(The kinetic theory of electron-phonon drag is found, for example, in Ref. 76.) This dissertation does not consider such effects.

A. Thermodynamics

We present here a derivation of a result central to Ref. 73, which is the basis of Ref. 38.

1. General Equilibration of Two Systems

We consider *any* two subsystems between which heat and entropy (but not matter, quasi-momentum, or momentum) flow. (This section essentially extends the example in Chapter I to two subsystems.) We later specifically consider energy equilibration between the phonon-magnon subsystems in a ferromagnet (as in Refs. 38 and 73), as well as energy equilibration between the respective phonon subsystems of a ferromagnet and a non-magnetic insulator in contact.

In two such subsystems, designated α and β, the energy differentials may be written as

$$dE_\alpha = T_\alpha dS_\alpha, \quad dE_\beta = T_\beta dS_\beta, \tag{5.3}$$

where T is the temperature and S is the entropy. By overall energy conservation $dE_\alpha = -dE_\beta$, so

$$dS_\alpha = \frac{dE_\alpha}{T_\alpha}, \quad dS_\beta = -\frac{dE_\alpha}{T_\beta}. \tag{5.4}$$

Since the total change in entropy must be non-negative, we must have

$$0 \leq \dot{S}_\alpha + \dot{S}_\beta = \left(\frac{1}{T_\alpha} - \frac{1}{T_\beta}\right)\dot{E}_\alpha = \left(\frac{T_\beta - T_\alpha}{T_\alpha T_\beta}\right)\dot{E}_\alpha. \tag{5.5}$$

For $\dot{S}_\alpha + \dot{S}_\beta \geq 0$ to hold we must have

$$\dot{E}_\alpha = \zeta \left(T_\beta - T_\alpha \right), \tag{5.6}$$

where $\zeta > 0$. By now it should be unsurprising that the energy flux between two subsystems is driven by a difference in intensive thermodynamic quantities. The proportionality coefficient ζ has units of a specific heat divided by time, and as noted below depends either on a boundary conductance (for systems that share a common surface) or a relaxation time (for systems that share the same volume).

Specific heats per unit volume (C) are defined via

$$\dot{\varepsilon}_\alpha = C_\alpha \dot{T}_\alpha, \quad \dot{\varepsilon}_\beta = C_\beta \dot{T}_\beta, \tag{5.7}$$

where $\varepsilon = E/V$ and V is the volume of the system. Use of $\dot{E}_\beta = -\dot{E}_\alpha$ and Eqs. (5.6) and (5.7) yields

$$\dot{T}_\alpha = \frac{T_\beta - T_\alpha}{\tau_\alpha}, \quad \dot{T}_\beta = \frac{T_\alpha - T_\beta}{\tau_\beta}, \tag{5.8}$$

where $\tau_\alpha \equiv C_\alpha V_\alpha / \zeta$ and $\tau_\beta \equiv C_\beta V_\beta / \zeta$ have units of time. Then

$$\Delta \dot{T}_{\alpha\beta} \equiv \dot{T}_\beta - \dot{T}_\alpha = -\frac{T_\beta - T_\alpha}{\tau_{\alpha\beta}}, \tag{5.9}$$

where we define

$$\tau_{\alpha\beta} \equiv \frac{\tau_\alpha \tau_\beta}{\tau_\alpha + \tau_\beta}. \tag{5.10}$$

Equation (5.9) justifies Eq. (1) of Ref. 73.

2. Two Systems Occupying the Same Volume

Energy conservation in two systems that occupy the same volume V (e.g., the phonon and magnon systems within a ferromagnet) gives $\dot{\varepsilon}_\alpha = -\dot{\varepsilon}_\beta$, so that substi-

tution of Eqs. (5.8) and (5.6) into Eq. (5.7) yields

$$\frac{C_\alpha}{\tau_\alpha} = \frac{C_\beta}{\tau_\beta} = \frac{\zeta}{V}. \tag{5.11}$$

Then, with $\tau_\beta = (C_\beta/C_\alpha)\tau_\alpha$, equation (5.10) gives

$$\frac{C_\alpha}{\tau_\alpha} = \frac{C_\beta}{\tau_\beta} = \left(\frac{C_\alpha C_\beta}{C_\alpha + C_\beta}\right)\tau_{\alpha\beta}^{-1}. \tag{5.12}$$

This is the case studied by Ref. 73.

3. Two Systems with a Contact Surface

For two systems in thermal contact over a surface of area A (e.g., the ferromagnet and substrate's respective phonon systems in Fig. 10a), we write $\zeta = h_K A$,[15,19] so that

$$\dot{E}_\alpha = -\dot{E}_\beta = h_K A\left(T_\beta - T_\alpha\right). \tag{5.13}$$

Here h_K is the thermal boundary conductance. Substitution of Eqs. (5.13) and (5.8) into Eq. (5.7) gives

$$\tau_\alpha = \frac{d_\alpha C_\alpha}{h_K}, \quad \tau_\beta = \frac{d_\beta C_\beta}{h_K}, \tag{5.14}$$

where d is the thickness of the material in the direction normal to the contact surface. Equation (5.10) then gives

$$\tau_{\alpha\beta} = \frac{1}{h_K}\left(\frac{d_\alpha C_\alpha d_\beta C_\beta}{d_\alpha C_\alpha + d_\beta C_\beta}\right). \tag{5.15}$$

B. Heat Flow in 1D in the Spin-Seebeck System

We now consider the system of Fig. 11, a ferromagnet/substrate system where a thermal gradient is applied by a heater at $x = -L/2$ and a heat sink at $x = L/2$. For

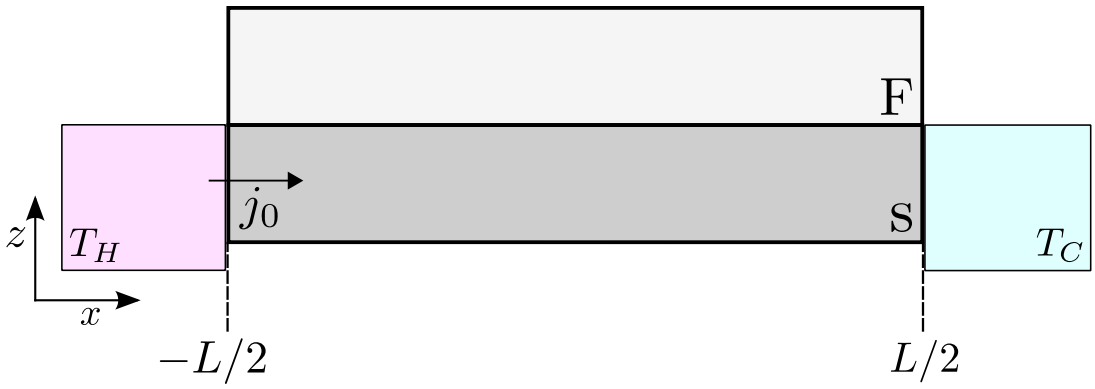

Fig. 11. An xz-plane cross section of the spin-Seebeck system (see Fig. 10a), depicting the placement of the heater and heat sink. The heater and heat sink, represented by squares at $x < -L/2$ and $x > L/2$, maintain temperatures T_H and T_C, where $T_H > T_C$. For sample isolation, they are in contact only with the substrate (s, dark gray), and not with the ferromagnetic sample (F, light gray); this affects the relative amplitudes of the modes, but not the mode lengths. The total heat flux input by the heater at $x = -L/2$ is j_0, and a similar heat flux must exit the substrate at $x = L/2$.

sample isolation, we take them to be in contact only with the substrate. This affects the relative amplitudes of temperature and thermal flux in each mode, but does not change the mode lengths.

This section takes heat to flow only along the length of the materials (the x-direction in Figs. 10 and 11), i.e., heat flow in each system is uniform in the yz-plane (further below, both flow along x *and* z are considered). Conservation of energy, with an energy source (which has not been considered thus far by this dissertation), is given by

$$\dot{\varepsilon} + \partial_x j_x^{\varepsilon} = \mathcal{S}^{\varepsilon}, \tag{5.16}$$

where $\mathcal{S}^{\varepsilon}$ represents the rate of heat transfer per unit volume from one subsystem to another. We consider steady state solutions, so that $\dot{\varepsilon} = 0$. This section further

takes the magnon subsystem (m) in the ferromagnet to only transfer energy to/from the phonon subsystem (p) in the ferromagnet. Similarly it takes the substrate (s) to only transfer energy to/from the phonon subsystem (p) in the ferromagnet, thereby neglecting the magnon-substrate coupling.

The rate of energy transfer per volume ($V = Ad$) between substrate phonons and sample phonons (an energy source $\mathcal{S}$) is found from Eq. (5.13) as

$$\mathcal{S}^{\varepsilon}_{s\to p} = \frac{h_K}{d_F}\left(T_s - T_p\right), \quad \mathcal{S}^{\varepsilon}_{p\to s} = \frac{h_K}{d_s}\left(T_p - T_s\right). \tag{5.17}$$

Here $\mathcal{S}^{\varepsilon}_{\alpha\to\beta}$ is the volume rate of energy transfer from system α to system β. (This is an approximation, as it treats the surface energy transfer between sample and substrate as a volume energy transfer; this energy transfer is properly treated as a z-directional heat flow further below.) The volume rate of energy transfer between the magnons and phonons in the sample is found by substitution of Eqs. (5.8) and (5.11) into Eq. (5.7), which gives

$$\mathcal{S}^{\varepsilon}_{m\to p} = -\mathcal{S}^{\varepsilon}_{p\to m} = \frac{C_m}{\tau_m}\left(T_m - T_p\right). \tag{5.18}$$

Here we have used Eq. (5.11) to replace C_p/τ_p with C_m/τ_m. Applied in turn to the substrate, magnons, and phonons, Eq. (5.16) gives

$$\partial_x j_x^{\varepsilon_s} = \frac{h_K}{d_s}\left(T_p - T_s\right), \tag{5.19}$$

$$\partial_x j_x^{\varepsilon_m} = -\frac{C_m}{\tau_m}\left(T_m - T_p\right), \tag{5.20}$$

$$\partial_x j_x^{\varepsilon_p} = \frac{h_K}{d_F}\left(T_s - T_p\right) + \frac{C_m}{\tau_m}\left(T_m - T_p\right). \tag{5.21}$$

From Eqs. (2.8) and (2.10), with no particle flow,

$$j_i^{\varepsilon} = -\kappa\partial_i T, \tag{5.22}$$

where $\kappa > 0$, i.e., heat flows from hot to cold. Substitution of Eqs. (5.19), (5.20), and (5.21) into the linearized gradient of Eq. (5.22) in turn gives

$$-\left(\frac{d_s\kappa_s}{h_K}\right)\partial_x^2 T_s = T_p - T_s, \tag{5.23}$$

$$-\left(\frac{\kappa_m\tau_m}{C_m}\right)\partial_x^2 T_m = T_p - T_m, \tag{5.24}$$

$$-\kappa_p\partial_x^2 T_p = -\frac{h_K}{d_F}\left(T_p - T_s\right) - \frac{C_m}{\tau_m}\left(T_p - T_m\right). \tag{5.25}$$

1. Characteristic Lengths

We denote the inhomogeneous parts of T_s, T_p, and T_m with primes. They all vary as $e^{\pm qx}$, so the characteristic length is $\lambda = q^{-1}$. Then, solving Eqs. (5.23) and (5.24) for T_s' and T_m' yields

$$T_s' = \frac{T_p'}{1 - \left(\frac{d_s\kappa_s}{h_K}\right)q^2}, \quad T_m' = \frac{T_p'}{1 - \left(\frac{\kappa_m\tau_m}{C_m}\right)q^2}. \tag{5.26}$$

Substitution of Eq. (5.26) into Eq. (5.25) gives

$$-\kappa_p q^2 = \frac{h_K}{d_F}\left(\frac{\frac{d_s\kappa_s}{h_K}q^2}{1 - \frac{d_s\kappa_s}{h_K}q^2}\right) + \frac{C_m}{\tau_m}\left(\frac{\frac{\kappa_m\tau_m}{C_m}q^2}{1 - \frac{\kappa_m\tau_m}{C_m}q^2}\right). \tag{5.27}$$

This is cubic in q^2. One solution is $q_\infty^2 = \lambda_\infty^{-2} = 0$, corresponding to the usual linear temperature profile, which is equivalent for T_s, T_p, and T_m.

It is convenient to define the inverse lengths $q_{mp} = \lambda_{mp}^{-1}$ and $q_{ps} = \lambda_{ps}^{-1}$, the former associated with magnon-phonon equilibration within the ferromagnet and the latter associated with sample-substrate phonon equilibration. They satisfy

$$q_{mp}^2 \equiv \frac{C_m}{\tau_m}\left(\frac{\kappa_m + \kappa_p}{\kappa_m\kappa_p}\right), \quad q_{ps}^2 \equiv h_K\left(\frac{d_F\kappa_p + d_s\kappa_s}{d_F\kappa_p d_s\kappa_s}\right). \tag{5.28}$$

These can be thought of as representing pure modes of the magnon-phonon system and the sample-substrate phonon system. Then for $q^2 \neq 0$, equation (5.27) can be

written as

$$0 = q^4 - q^2\left(q_{mp}^2 + q_{ps}^2\right) + \left(q_{mp}^2 q_{ps}^2 - q_{mp}^2 q_{ps}^2 R_{mp} R_{ps}\right), \tag{5.29}$$

where the dimensionless ratios R_{mp} and R_{ps} are given by Eq. (5.2). The solutions are

$$q_{\pm}^2 = \frac{q_{mp}^2 + q_{ps}^2}{2} \pm \sqrt{\left(\frac{q_{mp}^2 - q_{ps}^2}{2}\right)^2 + q_{mp}^2 q_{ps}^2 R_{mp} R_{ps}}. \tag{5.30}$$

We now consider two extreme cases. If there is no substrate (or if $h_K \to 0$), then

$$|q| \to q_{mp} = \sqrt{\frac{C_m}{\tau_m}\left(\frac{\kappa_p + \kappa_m}{\kappa_p \kappa_m}\right)}, \tag{5.31}$$

which on use of Eq. (5.12) reproduces the result of Ref. 73 (which employs A for q). If there is a substrate but no magnons (or $\tau_m \to \infty$), then

$$|q| \to q_{ps} = \sqrt{h_K\left(\frac{d_s\kappa_s + d_F\kappa_p}{d_s\kappa_s d_F\kappa_p}\right)}, \tag{5.32}$$

as in Eq. (5.1).

The coupling factor ($R_{mp}R_{ps} \leq 1$) between these modes further splits the two solutions; for $R_{mp}R_{ps} \neq 0$, the (shorter) characteristic length $\lambda_+ = 1/q_+$ decreases and the (longer) length $\lambda_- = 1/q_-$ increases. For three values of $q_{mp}/q_{ps} \geq 1$, Fig. 12 shows the characteristic lengths λ_- and λ_+, normalized by the pure mode phonon-magnon relaxation length ($\lambda_{mp} = 1/q_{mp}$), versus the coupling factor $R_{mp}R_{ps}$. For $q_{ps} \geq q_{mp}$ the plots are the same when λ_+ and λ_- are normalized by q_{ps} rather than q_{mp}.

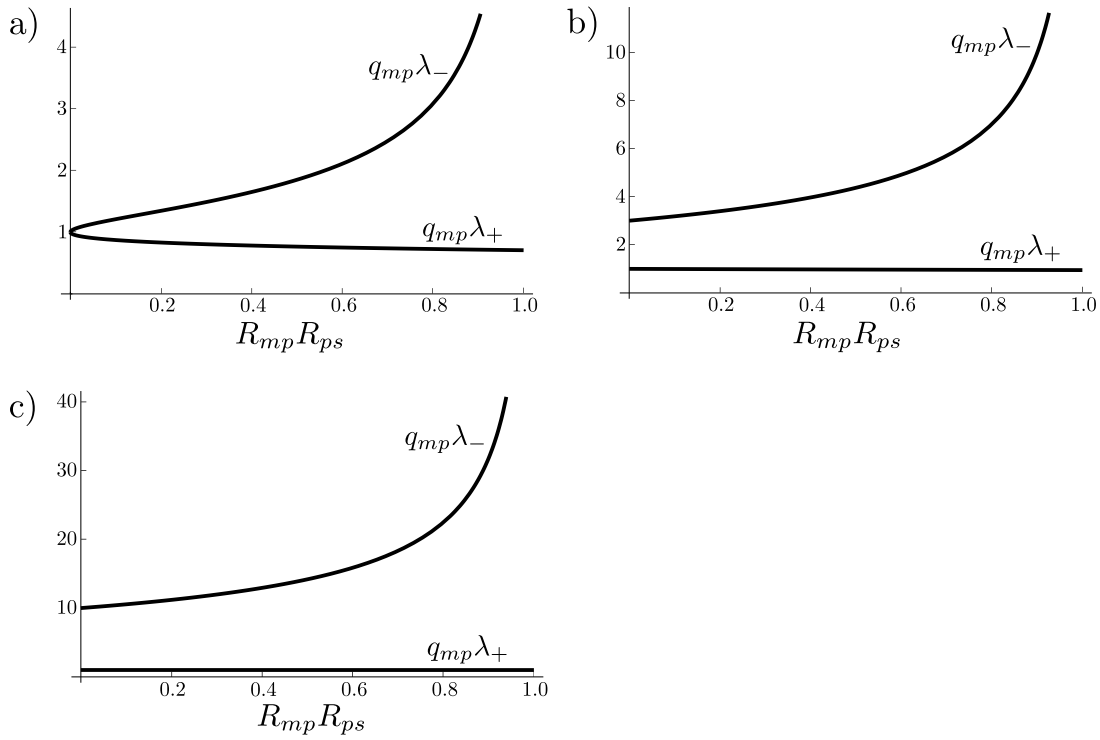

Fig. 12. The effect of mode coupling on the characteristic lengths associated with thermal equilibration in the spin-Seebeck system. The two characteristic lengths λ_+ and λ_-, normalized here by $\lambda_{mp} = q_{mp}^{-1}$, are shown as functions of the coupling factor $R_{mp}R_{ps} \leq 1$, for: (a) $q_{mp} = q_{ps}$, which corresponds to equivalent pure mode lengths $\lambda_{mp} = \lambda_{ps}$; (b) $q_{mp} = 3q_{ps}$, which corresponds to $\lambda_{ps} = 3\lambda_{mp}$; and (c) $q_{mp} = 10q_{ps}$, which corresponds to $\lambda_{ps} = 10\lambda_{mp}$. For $q_{ps} \geq q_{mp}$, the plots are the same when λ_+ and λ_- are normalized by λ_{ps} rather than λ_{mp}. By definition, $R_{mp}R_{ps} \leq 1$.

2. Thermal Profile and Fluxes along x

We write the phonon temperature in the ferromagnet as

$$T_p = T_0 + \alpha x + \sum_{\gamma=+,-} \left[T_\gamma^a \sinh(q_\gamma x) + T_\gamma^b \cosh(q_\gamma x) \right], \tag{5.33}$$

where T_0, T_+^a, T_-^a, T_+^b, and T_-^b are temperatures, and α is a temperature gradient. The temperatures $T_\pm^a$ and $T_\pm^b$ are found by application of the boundary conditions on

the heat currents, which are proportional to $\partial_x T_{(p,m,s)}$, with $T^b_\pm = 0$ if the heat fluxes have symmetric boundary conditions.

Recall that for a solitary isolated system under an applied temperature gradient, as considered by the example in Chapter I, we have $T = T_0 + \alpha x$.

Using Eq. (5.28), substitution of the inhomogeneous part of Eq. (5.33) into Eq. (5.26) gives, with no new parameters,

$$T_s = T_0 + \alpha x + \sum_{\gamma=+,-} \left[\frac{q_{ps}^2}{q_{ps}^2 - \left(\frac{d_s\kappa_s + d_F\kappa_p}{d_F\kappa_p} \right) q_\gamma^2} \right] \left[T^a_\gamma \sinh(q_\gamma x) + T^b_\gamma \cosh(q_\gamma x) \right], \tag{5.34}$$

$$T_m = T_0 + \alpha x + \sum_{\gamma=+,-} \left[\frac{q_{mp}^2}{q_{mp}^2 - \left(\frac{\kappa_m + \kappa_p}{\kappa_p} \right) q_\gamma^2} \right] \left[T^a_\gamma \sinh(q_\gamma x) + T^b_\gamma \cosh(q_\gamma x) \right]. \tag{5.35}$$

Substituting Eqs. (5.33), (5.34) and (5.35) into Eq. (5.22) in turn gives the heat current in each subsystem:

$$j_x^{\varepsilon_p} = -\kappa_p \alpha - \kappa_p \sum_{\gamma=+,-} q_\gamma \left[T^a_\gamma \cosh(q_\gamma x) + T^b_\gamma \sinh(q_\gamma x) \right], \tag{5.36}$$

$$j_x^{\varepsilon_s} = -\kappa_s \alpha - \kappa_s \sum_{\gamma=+,-} q_\gamma \left[\frac{q_{ps}^2}{q_{ps}^2 - \left(\frac{d_s\kappa_s + d_F\kappa_p}{d_F\kappa_p} \right) q_\gamma^2} \right] \left[T^a_\gamma \cosh(q_\gamma x) + T^b_\gamma \sinh(q_\gamma x) \right], \tag{5.37}$$

$$j_x^{\varepsilon_m} = -\kappa_m \alpha - \kappa_m \sum_{\gamma=+,-} q_\gamma \left[\frac{q_{mp}^2}{q_{mp}^2 - \left(\frac{\kappa_m + \kappa_p}{\kappa_p} \right) q_\gamma^2} \right] \left[T^a_\gamma \cosh(q_\gamma x) + T^b_\gamma \sinh(q_\gamma x) \right]. \tag{5.38}$$

The total heat flux in the ferromagnet $j_x^{\varepsilon_F} \equiv j_x^{\varepsilon_p} + j_x^{\varepsilon_m}$ is

$$j_x^{\varepsilon_F} = -\left(\kappa_p + \kappa_m\right)\alpha - \sum_{\gamma=+,-} q_\gamma \left[\frac{\left(\kappa_m + \kappa_p\right)\left(q_{mp}^2 - q_\gamma^2\right)}{q_{mp}^2 - \left(\frac{\kappa_m+\kappa_p}{\kappa_p}\right) q_\gamma^2}\right] \left[T_\gamma^a \cosh\left(q_\gamma x\right) + T_\gamma^b \sinh\left(q_\gamma x\right)\right]. \quad (5.39)$$

The boundary conditions on $j_x^{\varepsilon_{(s,p,m)}}$ at $x = -L/2$ and $x = L/2$ give α, T_γ^a and T_γ^b.

Because heat flux is continuous, the total heat flux (integrated over all subsystems) due to *each* surface mode must be zero. This condition is satisfied by Eqs. (5.36), (5.37), and (5.38) on substitution from Eqs. (5.28) and (5.30).

There are five unknowns in Eqs. (5.36), (5.37), and (5.38) (α, T_+^a, T_-^a, T_+^b, and T_-^b), and seemingly six boundary conditions (for each of the three fluxes, one at $x = -L/2$ and one at $x = L/2$). However, because the total energy flux is conserved (i.e., no heat losses at the top of the ferromagnet d_F or at the bottom of the substrate $-d_s$ in Fig. 10), there are only five independent conditions.

For comparison to the theory of Ref. 73, we now consider the bulk system if the heaters contact the sample and there is no substrate (so that $q_+^2 = q_{mp}^2$ and $q_-^2 = 0 = q_s^2$). Then $j_x^{\varepsilon_F} \to -(\kappa_p + \kappa_m)\alpha$, which reproduces the homogeneous result of Ref. 73 (where $Q \equiv j_x^{\varepsilon_F}$), and satisfies the condition of zero total heat flux due to the surface mode. If the heaters directly transfer energy only to and from phonons (so that heat flow in the magnon system vanishes at $x = L/2$ and $x = -L/2$), then $T_+^a \to \kappa_m\alpha/[q_m\kappa_p \cosh\left(q_m L/2\right)]$ and $T_+^b \to 0$, which reproduces the inhomogeneous result of Ref. 73. As noted above, because $T_\pm^b$ is associated with a term proportional to $\sinh\left(q_\pm x\right)$ in the heat flux, $T_\pm^b = 0$ for symmetric boundary conditions on the heat fluxes (i.e., the same heat current is injected into each system at the "hot" side as is withdrawn from each system at the "cold" side).

C. Heat Flow in 2D in the Spin-Seebeck System

We have so far omitted any consideration of how heat flows across the sample-substrate interface, which is now addressed. We now consider heat flux along z, to explicitly permit heat transfer between the substrate and the sample. We first detail the analytic theory, then present its numerical solution.

1. Analytic Theory

To completely describe the z-dependence of the temperatures and heat fluxes in the system, the z-dependence of the heat flux input by the heater at $x = -L/2$ must be considered. In principle, it may have any functional form, and therefore properly requires a Fourier series in $\sin(kz)$ and $\cos(kz)$ that includes an infinite number of lengths k^{-1} associated with the z-direction. However, if the thickness (along z) of the substrate is much smaller than its length (along x), then k^{-1} should be very small compared to $\lambda_\pm = q_\pm^{-1}$ of Eq. (5.30). The contributions from this z-dependence should decay along x over a distance on the order of the non-uniformity along z, and therefore we do not explicitly include them in the analytic theory. The cost of neglecting these high k values is that we cannot specify a heat input with a complicated variation along the thickness.

We thus generalize equations (5.33)-(5.35) to take the form

$$\begin{aligned} T_{(s,p,m)}(x,z) =& T_{0_{(s,p,m)}} + \alpha_{(s,p,m)}x \\ &+ \sum_{\gamma=+,-} \left[T^a_{(s,p,m)\gamma}(z)\sinh(q_\gamma x) + T^b_{(s,p,m)\gamma}(z)\cosh(q_\gamma x) \right]. \end{aligned} \tag{5.40}$$

The forms of $T^a_{(s,p,m)\gamma}(z)$ and $T^b_{(s,p,m)\gamma}(z)$ are determined by the conditions on the heat flux. We take symmetric boundary conditions on heat flux along x, which give $T^b_{(s,p,m)\gamma}(z) = 0$. Then, substitution of Eq. (5.40) into Eq. (5.22) gives the heat fluxes

along x and z to be

$$j_x^{\varepsilon_{(s,p,m)}} = -\kappa_{(s,p,m)}\alpha_{(s,p,m)} - \kappa_{(s,p,m)} \sum_{\gamma=+,-} q_\gamma T^a_{(s,p,m)\gamma}(z) \cosh(q_\gamma x), \tag{5.41}$$

$$j_z^{\varepsilon_{(s,p,m)}} = -\kappa_{(s,p,m)} \sum_{\gamma=+,-} \partial_z T^a_{(s,p,m)\gamma}(z) \sinh(q_\gamma x). \tag{5.42}$$

This section finds the functional forms of $T^a_{(s,p,m)}(z)$ and shows their amplitudes for example material parameters. The details of determining the amplitudes from bulk and boundary conditions are given below.

On properly treating the heat transfer between sample phonons and substrate phonons as z-directional currents, and heat transfer between sample magnons and sample phonons as a source/sink as for the 1D case, employing Eqs. (5.22) and (5.16) gives

$$\partial_i^2 T_s = 0, \tag{5.43}$$

$$-\kappa_p \partial_i^2 T_p = \frac{C_m}{\tau_m}(T_m - T_p), \tag{5.44}$$

$$-\kappa_m \partial_i^2 T_m = -\frac{C_m}{\tau_m}(T_m - T_p). \tag{5.45}$$

Equations (5.43)-(5.45) are identical to Eqs. (5.23)-(5.25), but with phonon-substrate heat transfer in the form of fluxes rather than sources. These equations give

$$T_{0_m} = T_{0_p} \equiv T_0, \qquad \alpha_m = \alpha_p \equiv \alpha, \tag{5.46}$$

but they do not explicitly impose any conditions on T_{0_s} or α_s. For steady-state flow, however, we must take

$$T_{0_s} = T_0, \qquad \alpha_s = \alpha. \tag{5.47}$$

This relation guarantees that for any two of $\kappa_{(s,p,m)}$ to continuously go to zero, we recover the expected $j_x^\varepsilon = -\kappa\alpha$. We now find $T^a_{(s,p,m)}(z)$ by substituting Eq. (5.40)

into Eq. (5.43) and the decoupled forms of Eqs. (5.44) and (5.45).

Substitution of Eq. (5.40) into Eq. (5.43) gives

$$\partial_z^2 T^a_{s\gamma}(z) = -q_\gamma^2 T^a_{s\gamma}(z), \tag{5.48}$$

so that $T^a_{s\gamma}(z)$ is sinusoidal:

$$T^a_{s\gamma}(z) = A^{(1)}_{s\gamma} \cos(q_\gamma z) + A^{(2)}_{s\gamma} \sin(q_\gamma z). \tag{5.49}$$

Here, $A^{(1)}_{s\gamma}$ and $A^{(2)}_{s\gamma}$ are constants determined by conditions on heat flux (see Appendix E).

Decoupled equations for T_p and T_m (and therefore $T^a_{p\gamma}(z)$ and $T^a_{m\gamma}(z)$) are found by combination of Eqs. (5.44) and (5.45). Addition and subtraction gives

$$-\kappa_p \partial_i^2 T_p - \kappa_m \partial_i^2 T_m = 0, \tag{5.50}$$

$$-\kappa_p \partial_i^2 T_p + \kappa_m \partial_i^2 T_m = 2\frac{C_m}{\tau_m}(T_m - T_p). \tag{5.51}$$

Combination of Eqs. (5.50) and (5.51) gives

$$\partial_i^2 \partial_j^2 T_p - q_{mp}^2 \partial_i^2 T_p = 0, \tag{5.52}$$

$$\partial_i^2 \partial_j^2 T_m - q_{mp}^2 \partial_i^2 T_m = 0. \tag{5.53}$$

where we have employed Eq. (5.28). Use of Eq. (5.40) in Eqs. (5.52) and (5.53) gives, for $\gamma = \pm$,

$$\partial_z^4 T^a_{(p,m)\gamma}(z) + q_\gamma^4 T^a_{(p,m)\gamma}(z) + 2q_\gamma^2 \partial_z^2 T^a_{(p,m)\gamma}(z) - q_{mp}^2 \partial_z^2 T^a_{(p,m)\gamma}(z) - q_{mp}^2 q_\gamma^2 T^a_{(p,m)\gamma}(z) = 0. \tag{5.54}$$

The solution of Eq. (5.54) is

$$T^{a}_{(p,m)\gamma}(z) = A^{(1)}_{(p,m)\gamma} e^{\sqrt{q^2_{mp}-q^2_\gamma}\,z} + A^{(2)}_{(p,m)\gamma} e^{-\sqrt{q^2_{mp}-q^2_\gamma}\,z} + A^{(3)}_{(p,m)\gamma} \cos(q_\gamma z) + A^{(4)}_{(p,m)\gamma} \sin(q_\gamma z). \quad (5.55)$$

Here, $A^{(1,2,3,4)}_{(p,m)\gamma}$ are constants determined by conditions on heat flux (see below).

Due to the mode splitting discussed above for 1D heat flow, $q_+ \geq q_m$ and $q_- \leq q_m$. Therefore, for coupling $R_{mp}R_{ps} \neq 0$, the exponential terms in Eq. (5.55) are, in fact, oscillating terms for $q_\gamma = q_+$.

Although T_0, α, $A^{(1,2)}_{s\pm}$, and $A^{(1,2,3,4)}_{(p,m)\pm}$ are twenty-two unknowns associated with the temperatures and heat fluxes, they are not free parameters. Energy conservation in the bulk gives eight conditions, energy conservation at the boundaries $z = -d_s$ and $z = d_F$ (i.e., no heat loss to the vacuum at the surfaces) gives six boundary conditions, and there are four boundary conditions associated with interfacial energy transfer, given by Refs. 19 and 15. Only four conditions can be varied: the average temperature T_0, the temperature gradient α, and two conditions associated with the relative amounts of heat carried by each subsystem at a given short distance from the heater. All four of these conditions are set experimentally, but the last two are not obvious; they are approximated in Appendix E.

If the 2D mode lengths are similar to those for 1D, the theory demonstrates that, in the system shown in Fig. 10, there are two dominant surface modes (and thus two largest characteristic lengths) associated with thermal equilibration: one largely associated with energy equilibration between magnons and phonons within the ferromagnet, and the other largely associated with energy equilibration between phonons in the ferromagnet and the substrate. The coupling between the two surface modes increases the larger and decreases the smaller of the characteristic lengths.

This theory provides testable predictions for the change in the 1D characteristic lengths. Equations (5.30) and (5.28) show that quadrupling the thickness of both the sample and substrate should approximately double the observed characteristic length. The theory also suggests that polishing (roughening) the substrate before depositing the sample, which increases (decreases) h_K, should decrease (increase) the observed length; to test this behavior, measurements could be taken on a series of samples with increasingly rough sample/substrate interfaces. Finally, regardless of which mode causes the measured effect, changing the coupling factor between the modes (by changing κ_m/κ_p or $d_s\kappa_s/d_F\kappa_p$) modifies the lengths.

2. Numerical Solution

We find, however, that it is an oversimplification to use the $q_\pm$ from Eq. (5.30) as the inverse lengths associated with 2D flow. Indeed, numerical solution with either of these values for q can be shown to be inconsistent with energy conservation. Unfortunately, since the 2D heat flow equations are nonlinear, analytic solution is not possible in general. However, an iterative approach (given for Mathematica in pseudocode below) can be used to find consistent values for q: solve the appropriate boundary conditions for the coefficients using $q_{\text{init}} = q_+$ or $q_{\text{init}} = q_-$; using these values for the coefficients, find the q_{new} that guarantees energy conservation; begin the loop again using an appropriately chosen q'_{init} in between q_{init} and q_{new}. One must iterate until q_{new} and q_{init} converge. The algorithm is given explicitly by Appendix F.

We now present the results of this method, calculated using Mathematica, for material parameters given in Table III.

Following Table III, the 1D solution from Eq. (5.30) gives

$$q_- = 3257 \text{ m}^{-1}, \quad q_+ = 3.651 \times 10^6 \text{ m}^{-1}. \tag{5.56}$$

Table III. Parameters used for numerical calculations of normal mode contributions to the heat fluxes in the spin-Seebeck system. [(a)]Estimate for a Ni film on a Si-N substrate at 100K from Fig. 5b of Ref. 77. [(b)]Value unknown; κ_m/κ_p is likely to be lower at high temperature. [(c)]Estimate from Ref. 38 for the maximum phonon-magnon equilibration length in Permalloy. [(d)]Estimate for Rh:Fe on Al_2O_3 from Fig. 34 of Ref. 19. [(e)]Calculated using the above parameters and Eq. (5.32). [(f)]Calculated using the above parameters and Eqs. (5.30) and (5.2).

Parameter	Value	Units	Ref.
κ_s	3	W/m-K	77[(a)]
κ_p	30	W/m-K	77[(a)]
κ_m/κ_p	1/10		[(b)]
d_F	50	nm	77
d_s	500	nm	77
q_{mp}	3.33×10^4	m^{-1}	38[(c)]
h_K	1×10^7	W/m^2-K	19[(d)]
q_{ps}	5×10^2	m^{-1}	[(e)]
q_+	5.00×10^4	m^{-1}	[(f)]
q_-	4.88×10^2	m^{-1}	[(f)]

Using these as trial values for the numerical solution of 2D heat flow boundary conditions, we find 2D inverse lengths consistent with energy conservation to be

$$q_-^{(2D)} = 3257 \text{ m}^{-1}, \quad q_+^{(2D)} = 2.839 \times 10^6 \text{ m}^{-1}. \tag{5.57}$$

The subsystem contributions to heat flow along z and along x for the two modes associated with $q_-^{(2D)}$ and $q_+^{(2D)}$ are respectively shown in Figs. 13 and 14. Fig. 14 explains the significant difference between q_+ and $q_+^{(2D)}$; the 1D solutions q_+ and q_- should apply for heat flux along x uniform in z. This holds for the $q_-^{(2D)}$ mode in Fig. 14a, whereas the $q_-^{(2D)}$ displays significant curvature in Fig. 14b.

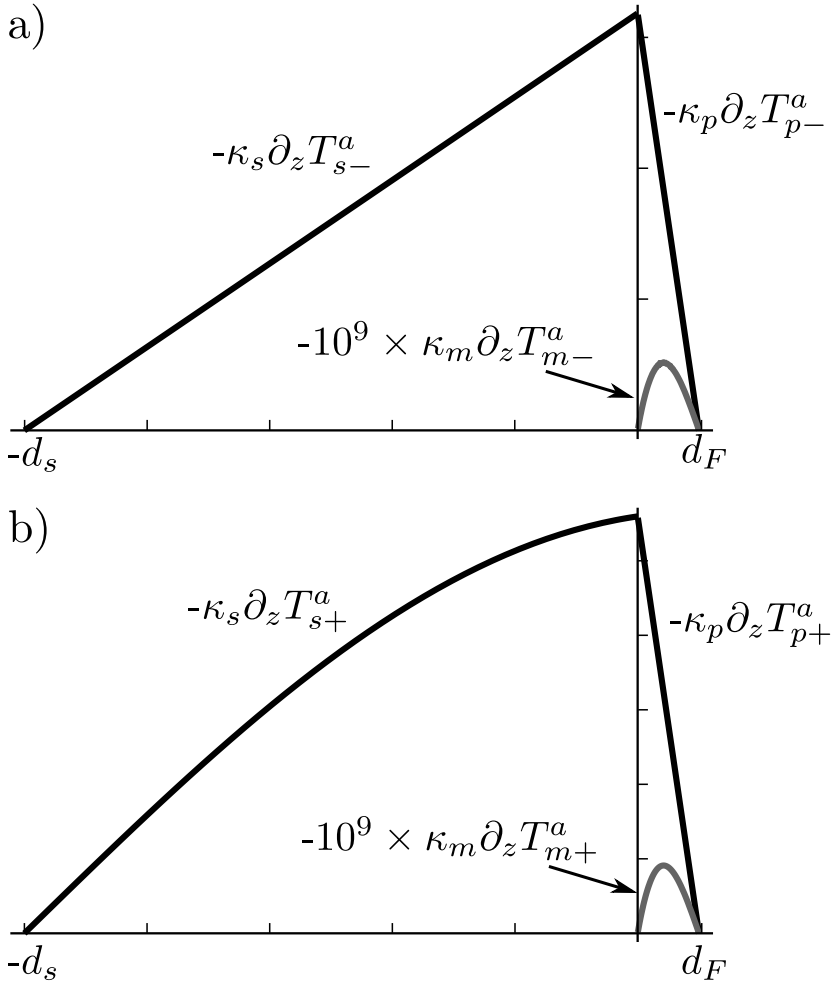

Fig. 13. The relative magnitudes of phonon and magnon heat flux along z at a given x as a function of z (i.e., $-\kappa_{(s,p,m)} \partial_z T^a_{(s,p,m)\pm}(z)$), in the thermal equilibration modes with the largest lengths, (a) $\lambda_-^{(2D)} = 1/q_-^{(2D)}$ and (b) $\lambda_+^{(2D)} = 1/q_+^{(2D)}$, in arbitrary units. The substrate is at $z < 0$ and the sample is at $z > 0$, and the sample magnon heat flux is dark grey to distinguish it from phonon heat flux. For the parameter values of Table III, in both modes the sample is too thin for magnons to build up much heat flux along z. No heat loss at the top of the sample d_F or the bottom of the substrate requires that each heat flux is zero at these points.

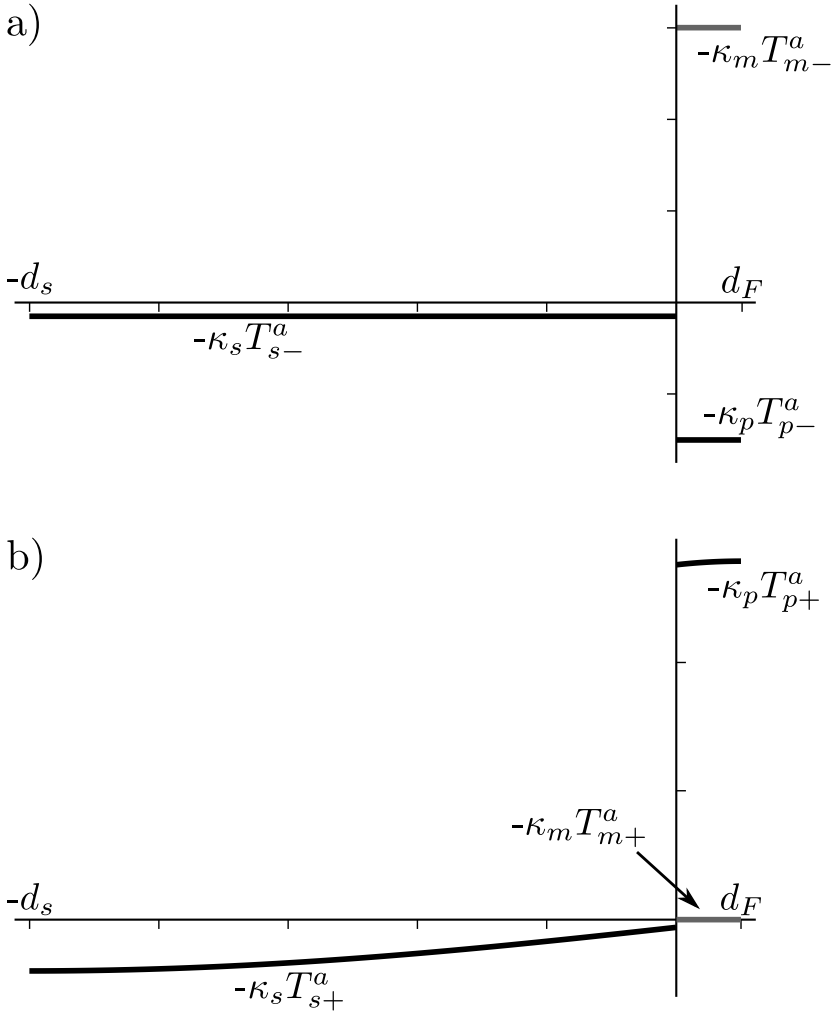

Fig. 14. The relative magnitudes of phonon and magnon heat flux along x at a given x as a function of z (i.e., $-\kappa_{(s,p,m)}T^a_{(s,p,m)\pm}(z)$), in the thermal equilibration modes with the largest lengths, (a) $\lambda_-^{(2D)} = 1/q_-^{(2D)}$ and (b) $\lambda_+^{(2D)} = 1/q_+^{(2D)}$, in arbitrary units. The substrate is at $z < 0$ and the sample is at $z > 0$, and the sample magnon heat flux is dark grey to distinguish it from phonon heat flux. For the parameter values of Table III, (a) shows that along x the heat in the $q_-^{(2D)}$ surface mode is carried by all three subsystems, with magnon heat flow opposing sample and substrate phonon heat flow, and (b) shows that along x the heat in the $q_+^{(2D)}$ surface mode is carried mostly by the phonon subsystems, with sample phonon heat flow opposing substrate phonon heat flow. Integration over z from $-d_s$ to d_F of the total heat flux along x for each surface mode gives zero by continuity of the heat flux.

It is noteworthy that other consistent solutions $q_n^{(2D)} > q_+^{(2D)} > q_-^{(2D)}$ can be found numerically. These may in fact represent the Fourier-series with infinite wavevectors necessary to fully treat any arbitrary heat input, as mentioned above, but this is not obvious. Although further investigation into the nature of these solutions is warranted, since we are here searching for the largest possible lengths associated with heat flow, the larger q (and therefore smaller λ) solutions are irrelevant to the current discussion.

D. On the Anomalous Spin-Seebeck Length

It is unlikely that the present theory can account for the anomalously large length (~ 1 mm) observed in the spin-Seebeck experiments.

On one hand, for the sample-substrate length λ_{ps} to be on the order of 1 mm, with $\kappa_s \approx \kappa_p \sim 10^2$ W/m-K, $d_s \sim 100$ nm, and $d_F \sim 10$ nm, Eq. (5.28) gives an abnormally small thermal boundary conductance $h_K \sim 1$ W/m^2-K. Although h_K is not known for the particular combinations of materials used in Refs. 31, 32, or 33, Fig. 34 of Ref. 19 gives $h_K \approx 10^7$ W/m^2-K (for Rh:Fe on Al_2O_3 at $T = 50$ K). We do not expect that thermal matching between substrate and sample in the spin-Seebeck experiments to be considerably worse.

On the other hand, for the magnon-phonon length λ_{mp} to be on the order of 1 mm, the mode coupling (given by $R_{mp}R_{ps}$ in Eq. (5.30)) would have to account for a large increase of λ_{mp} (at least three-fold in the case of Permalloy.[38]) Because spin-Seebeck experiments are carried out near room temperature[31,32] or at $T \geq 40$ K,[33] it is unlikely that the magnons carry a significant amount of the heat flux in the ferromagnet, i.e., it is likely that $\kappa_m \ll \kappa_p$. Since the mode coupling term R_{mp} is proportional to κ_m/κ_p, mode coupling is likely a weak effect.

However, the only applied gradient in the spin-Seebeck experiments is of temperature. If, as has been suggested, the effect is due to a spin flux along z in the ferromagnet, then the fluxes are likely driven in large part by internal thermal gradients along z; this thermal gradient is shown by the present theory to have a $\sinh(x)$ dependence, as does the spin flux measured by Ref. 33. The present theory is thus an important piece of the puzzle for describing such a spin flux.

CHAPTER VI

SUMMARY

We have developed the irreversible thermodynamics of transport in both bulk and interfacial systems. We have treated transport of both conserved and nonconserved properties. To describe transport using irreversible thermodynamics, we first make general calculations of entropy production and heating.

In general, entropy production calculations are relatively straightforward for single carrier systems. We find the regime where interfacial heating and entropy production dominate that due to bulk currents; it depends on the bulk conductivity and interfacial conductance, as well the distance over which the interface adjusts.

Nontrivial complications occur for similar calculations for two-carrier systems when scattering (e.g., of spins) or recombination (e.g., of holes and electrons in semiconductors) due to an interface is considered. On taking the generally nonconserved current to be continuous at the interface, however, we make the comparison between the interfacial entropy production (and the rate of heating) due to the electric potential and that due to the magnetization potential. For typical interfacial properties, we find that a rather strong difference ~ 20 T in internal magnetization potentials across an interface is necessary to produce the same heating as a 10^{-3} V voltage difference.

We apply these general irreversible thermodynamics methods and results to transport in three systems with a variety of carriers and interfacial properties.

Metal oxide growth is considered here as a bulk system driven by surface chemical reactions at the metal/oxide and the oxide/atmosphere interfaces. Previous theory by Mott is shown to be inconsistent, with a decreasing bulk electric field but no discharge current. We show that Mott's theory is instead the first order of a consistent asymptotic series expansion in $t^{-k/2}$ of field, fluxes, and concentrations. At second

order (t^{-1}), we find nonuniform concentrations in the bulk, and unequal charge on the surfaces. At third order ($t^{-3/2}$) we find unequal, nonuniform fluxes of ions and electrons. The method used here can be employed to find the transport variables at any order, provided all previous orders are calculated. Using these results, we show the first correction to the parabolic growth rate law to be logarithmic in time.

We next consider magnetic and electric transport at isolated interfaces and in multilayers of ferromagnetic and nonmagnetic materials. We calculate the normal eigenmodes and associated characteristic lengths for spin and charge transport, and consider the behavior of a such a system through which a constant electric current is driven. We discuss and find all of the applicable boundary conditions, and show numerical results for the field, potential, charge, and spin accumulation in copper and cobalt. The present results differ from previous theory because of both the inclusion of charge-screening (which allows continuity of electric field and potential, and affects spin accumulation in a ferromagnet) as well as the inclusion of both the chemical potential and the internal magnetic field. Results, particularly for a nonmagnetic material, depend on the consideration of both of these properties.

Finally, we consider themal transport in the spin-Seebeck system, which consists of a thin-film ferromagnet on an insulating nonmagnetic substrate. Transport within and between both of the materials is considered, with phonons in the substrate and magnons and phonons in the sample responsible for heat flow. We calculate the normal modes and their associated lengths for the simplified case of 1D heat flow, and provide the analytic theory for heat flow in 2D, which requires the consideration of at least twenty boundary conditions. Numerical results show that the analytically calculated 1D lengths can be very close to the two largest 2D lengths. However, using particular results of Ref. 38, the theory does not appear to explain the abnormally large lengths associated with spin current that are observed in spin-Seebeck

experiments by Refs. 31–33.

On the other hand, the present theory does find that heat flux along z displays the same $\sinh(x)$ dependence as the spin current measured in one of the spin-Seebeck experiments.[33] The thermal gradient along z predicted by the present theory precisely tracks the measured spin current if a particular length predicted by Ref. 38 is underestimated. Further study of this thermal equilibration length is thus warranted.

REFERENCES

[1]L. Onsager, Phys. Rev. **37**, 405 (1931).

[2]I. Prigogine, *Introduction to the Thermodynamics of Irreversible Processes*, 3rd ed. (Interscience, New York, 1987).

[3]S. R. de Groot, *Thermodynamics of Irreversible Processes* (North-Holland Publishing Company, Amsterdam, The Netherlands, 1951).

[4]S. R. de Groot and P. Mazur, *Non-Equilibrium Thermodynamics* (Dover, New York, 1984).

[5]B. I. Halperin and P. C. Hohenberg, Phys. Rev. **188**, 898 (1969).

[6]D. Forster, T. Lubensky, P. Martin, J. Swift, and P. Pershan, Phys. Rev. Lett. **26**, 1016 (1971).

[7]P. Martin, O. Parodi, and P. Pershan, Phys. Rev. A **6**, 2401 (1972).

[8]R. Graham, Phys. Rev. Lett. **33**, 1431 (1975).

[9]C.-R. Hu and W. M. Saslow, Phys. Rev. Lett. **38**, 605 (1977).

[10]M. Liu, Phys. Rev. Lett. **43**, 1740 (1979).

[11]D. Forster, *Hydrodynamic Fluctuations, Broken Symmetry, and Correlation Functions* (Benjamin, Reading, MA, 1975).

[12]L. Reichl, *A Modern Course in Statistical Physics*, 2nd ed. (Wiley-VCH, Berlin, 1998).

[13]M. R. Sears and W. M. Saslow, Phys. Rev. B **82**, 134304 (2010).

[14]M. R. Sears and W. M. Saslow, Phys. Rev. B **82**, 134523 (2010).

[15]G. L. Pollack, Rev. Mod. Phys. **41**, 48 (1969).

[16]M. Johnson and R. H. Silsbee, Phys. Rev. B **35**, 4959 (1987).

[17]I. M. Khalatnikov, *Introduction to the Theory of Superfluidity* (W. A. Benjamin, Inc., New York, 1965).

[18]L. J. Challis, J. Phys. C **7**, 481 (1974).

[19]E. T. Swartz and R. O. Pohl, Rev. Mod. Phys. **61**, 605 (1989).

[20]J. Bass and W. P. Pratt, J. Phys. Cond. Mat. **19**, 183210 (2007).

[21]P. C. van Son, H. van Kempen, and P. Wyder, Phys. Rev. Lett. **58**, 2271 (1987).

[22]T. Valet and A. Fert, Phys. Rev. B **48**, 7099 (1993).

[23]D. G. Cahill, J. Appl. Phys. **93**, 793 (2003).

[24]M. E. Lumpkin, W. M. Saslow, and W. M. Visscher, Phys. Rev. B **17**, 4295 (1978).

[25]A. Maiti, G. Mahan, and S. Pantelides, Solid State Comm. **102**, 517 (1997).

[26]W. M. Saslow, Phys. Rev. B **11**, 2544 (1975).

[27]D. R. Penn and M. D. Stiles, Phys. Rev. B **59**, 13338 (1999).

[28]M. Hatami, G. E. W. Bauer, Q. Zhang, and P. J. Kelly, Phys. Rev. Lett. **99**, 066603 (2007).

[30]H. Yu, S. Granville, D. P. Yu, and J.-P. Ansermet, Phys. Rev. Lett. **104**, 146601 (2010).

[31]K. Uchida, Nature **455**, 778 (2008).

[32]K. Uchida, Nature Materials **9**, 894 (2010).

[33]C. M. Jaworski, Nature Materials **9**, 898 (2010).

[34]S. Kjelstrup and D. Bedeaux, *Non-Equilibrium Thermodynamics of Heterogeneous Systems* (World Scientific, Singapore, 2008).

[35]G. D. Mahan, *Many Particle Physics*, 3rd ed. (Kluwer Academic/Plenum Publishers, New York, 2000).

[36]H. B. Callen, *Thermodynamics* (Wiley, New York, 1960).

[37]L. D. Landau and E. M. Lifshitz, *Fluid Dynamics*, 2nd ed. (Pergamon, Cambridge, UK, 1987).

[38]J. Xiao, G. E. W. Bauer, K. Uchida, E. Saitoh, and S. Maekawa, Phys. Rev. B **81**, 214418 (2010).

[39]J. A. Katine, F. J. Albert, R. A. Buhrman, E. B. Myers, and D. C. Ralph, Phys. Rev. Lett. **84**, 3149 (2000).

[40]W. M. Saslow, Phys. Rev. B **76**, 184434 (2007).

[41]M. Krčmar and W. M. Saslow, Phys. Rev. B **65**, 233313 (2002).

[42]W. M. Saslow, Phys. Rev. E **59**, 1343 (1999).

[43]M. D. Stiles and D. R. Penn, Phys. Rev. B **61**, 3200 (2000).

[44]N. F. Mott, Trans. Faraday Soc. **35**, 1175 (1939).

[45]R. L. Hoffmann, B. J. Norris, and J. F. Wager, Appl. Phys. Lett. **82**, 733 (2003).

[46]N. F. Mott, Trans. Faraday Soc. **35**, 472 (1940).

[47]N. F. Mott, Trans. Faraday Soc. **43**, 429 (1947).

[48]N. Cabrera and N. F. Mott, Rep. Prog. Phys. **12**, 163 (1949).

[49]G. Z. Tammann, Z. Anorg. Allg. Chem. **111**, 78 (1920).

[50]R. Baca, IOP Conf. Series: Mat. Sci. and Eng. **8**, 012043 (2010).

[51]C. Wagner, *Atom Movements*, 3rd ed., pp. 153-173 (Am. Soc. for Metals, Cleveland, OH, 1951).

[52]W. M. Saslow, Phys. Rev. Lett. **76**, 4849 (1996).

[53]Y. Yang and W. M. Saslow, J. Chem. Phys. **109**, 10331 (1998).

[54]M. R. Sears and W. M. Saslow, Solid State Ionics **181**, 1074 (2010).

[55]D. R. Crow, *Principles and Applications of Electrochemistry*, 4th ed. (Blackie Academic & Professional, London, 1994).

[56]J. M. Rubi and S. Kjelstrup, J. Phys. Chem. B **107**, 13471 (2003).

[57]J. Fleig, Phys. Chem. Chem. Phys. **7**, 2027 (2005).

[58]J. M. Rubi and S. Kjelstrup, J. Phys. Chem. **55**, 540 (1951).

[59]M. Martin, W. Mader, and E. Fromm, Thin Solid Films **250**, 61 (1994).

[60]S. K. Lahiri, N. K. W. Singh, K. W. Heng, L. Ang, and L. C. Goh, Microelectronics Journal **29**, 335 (1998).

[61]L. P. H. Jeurgens, W. G. Sloof, F. D. Tichelaar, and E. J. Mittemeijer, J. Appl. Phys. **92**, 1649 (2002).

[62]C. Zhong, Appl. Phys. A **90**, 263 (2008).

[63]M. N. Baibich, J. M. Broto, A. Fert, F. N. V. Dau, and F. Petroff, Phys. Rev. Lett. **61**, 2472 (1988).

[64]G. Binasch, P. Grünberg, F. Saurenbach, and W. Zinn, Phys. Rev. B **39**, 4828 (1989).

[65]S. Hershfield and H. L. Zhao, Phys. Rev. B **56**, 3296 (1997).

[66]J. Kerr, Philos. Mag. **3**, 321 (1877).

[67]K. Postava, J. Magn. Magn. Mater. **163**, 8 (1996).

[68]A. A. Bakun, B. P. Zakharchenya, A. A. Rogachev, M. N. Tkachuk, and V. G. Fleĭsher, JETP Lett. **40**, 464 (1984).

[69]J. Bass, J. Appl. Phys. **75**, 6699 (1995).

[70]S. Celozzi, R. Araneo, and G. Lovat, *Electromagnetic Shielding* (John Wiley & Sons, Inc., Hoboken, NJ, 2008).

[71]M. D. Stiles, J. Xiao, and A. Zangwill, Phys. Rev. B **69**, 054408 (2004).

[72]R. Bowers, Phys. Rev. **102**, 1486 (1956).

[73]D. J. Sanders and D. Walton, Phys. Rev. B **15**, 1489 (1977).

[74]H. Adachi, Appl. Phys. Lett. **97**, 252506 (2010).

[75]C. M. Jaworski, e-print arXiv:cond-mat/1102.1024v1 (2011).

[76]J. M. Ziman, *Electrons & Phonons* (Oxford University Press, London, 1960).

[77]B. L. Zink, A. D. Avery, R. Sultan, D. Bassett, and M. R. Pufall, Solid State Comm. **150**, 514 (2010).

APPENDIX A

TRANSPORT IN METAL OXIDE AT ORDER t^{-1}

By the continuity Eqs. (3.29) J_{a2} and J_{b2} must be uniform, and by Eq. (3.37) they are related by

$$J_{a2} = ZJ_{b2}. \tag{A.1}$$

For $k = 2$, the Nernst-Planck equations from Eqs. (3.45) and (3.46) are

$$J_{a2} + \frac{D_a}{V_T} n_0 E_2 + D_a \partial_x N_{a2} = -\frac{D_a}{V_T} N_{a1} E_1, \tag{A.2}$$

$$J_{b2} - \frac{D_b}{V_T} n_0 E_2 + D_b \partial_x N_{b2} = \frac{ZD_b}{V_T} N_{b1} E_1. \tag{A.3}$$

Taking spatial derivatives of Eqs. (A.2) and (A.3), and using Gauss's Law, Eq. (3.42), and the uniformity of J_{a2} and J_{b2}, yields

$$\frac{D_a n_0}{V_T \epsilon} \rho_2 + D_a \partial_x^2 N_{a2} = -\frac{D_a}{V_T} \partial_x (N_{a1} E_1), \tag{A.4}$$

$$-\frac{D_b n_0}{V_T \epsilon} \rho_2 + D_b \partial_x^2 N_{b2} = \frac{ZD_b}{V_T} \partial_x (N_{b1} E_1). \tag{A.5}$$

The right hand sides are found from Eq. (3.55);

$$\frac{D_a n_0}{V_T \epsilon} \rho_2 + D_a \partial_x^2 N_{a2} = -D_a \frac{R_D n_0 E_1^2}{V_T^2}, \tag{A.6}$$

$$-\frac{D_b n_0}{V_T \epsilon} \rho_2 + D_b \partial_x^2 N_{b2} = D_b \frac{R_D n_0 E_1^2}{V_T^2}, \tag{A.7}$$

where the dimensionless ratio R_D is defined in Eq. (3.56).

Subtracting Eq. (A.6) multiplied by $1/D_a$ from Eq. (A.7) multiplied by Z/D_b yields

$$\partial_x^2 \rho_2 - (1 + Z) \frac{n_0 e}{V_T \epsilon} \rho_2 = (1 + Z) \frac{R_D n_0 e E_1^2}{V_T^2}. \tag{A.8}$$

The solution to this equation, with

$$l_s \equiv \sqrt{\frac{V_T \epsilon}{(1+Z) n_0 e}} = \sqrt{\frac{k_B T \epsilon}{(1+Z) n_0 e^2}}, \tag{A.9}$$

and with new integration constants $P_2^{(+)}$ and $P_2^{(-)}$, is

$$\rho_2 = P_2^{(+)} e^{x/l_s} + P_2^{(-)} e^{-x/l_s} - \frac{R_D \epsilon E_1^2}{V_T}. \tag{A.10}$$

From Eq. (A.10) we infer that N_{a2} and ZN_{b2} are polynomials whose terms that are linear or higher are equal, and they may have different exponential terms.

Substituting ρ_2 from Eq. (A.10) into Gauss's Law, Eq. (3.42), and integrating $\partial_x E_2$ yields

$$E_2 = \frac{l_s}{\epsilon} \left(P_2^{(+)} e^{x/l_s} - P_2^{(-)} e^{-x/l_s} \right) - \frac{R_D E_1^2}{V_T} x + F_2, \tag{A.11}$$

where F_2 is a new integration constant with units V-s/m.

By Eq. (3.55), (N_{a1}, N_{b1}) are linear in x, so that the right-hand-side of the Nernst-Planck Eq. (A.2) is linear in x. Moreover, the continuity Eq. (3.29) implies that J_{a2} is constant. Therefore by Eq. (A.11) for E_2, the Nernst-Planck equation allows $\partial_x N_{a2}$ to be linear, so N_{a2} can be quadratic in x. Moreover, the exponential terms in $(D_a/V_T) n_0 E_2 + D_a \partial_x N_{a2}$ must cancel. Finally, from Eq. (A.10) any linear or quadratic terms in N_{a2} and ZN_{b2} must be equal. With $(M_{20}, M_{21}, M_{22}, P_{a2}^{(\pm)})$ being new integration constants, we therefore conclude that the following form must hold:

$$N_{a2} = M_{20} + M_{21} x + M_{22} x^2 + P_{a2}^{(+)} e^{x/l_s} + P_{a2}^{(-)} e^{-x/l_s}. \tag{A.12}$$

Use of Eq. (3.31) for $k = 2$ ($\rho_2 = e(ZN_{b2} - N_{a2})$), and ρ_2 given Eq. (A.10), yields

$$N_{b2} = \frac{M_{20}}{Z} - \frac{1}{Z}\frac{R_D \epsilon E_1^2}{V_T e} + \frac{M_{21}}{Z}x + \frac{M_{22}}{Z}x^2 + \left(\frac{P_2^{(+)} + eP_{a2}^{(+)}}{Ze}\right)e^{x/l_s} + \left(\frac{P_2^{(-)} + eP_{a2}^{(-)}}{Ze}\right)e^{-x/l_s}. \tag{A.13}$$

Addition of Eq. (A.2) divided by D_a and Eq. (A.3) divided by D_b gives, with Eqs. (A.1) and (3.55),

$$J_{a2}\left(\frac{1}{D_a} + \frac{1}{ZD_b}\right) + \partial_x\left(N_{a2} + N_{b2}\right) = 0. \tag{A.14}$$

Substitution for N_{a2} and N_{b2} from Eqs. (A.12) and (A.13) gives an equation that can be used to solve for some of the constants:

$$M_{21}\left(1 + \frac{1}{Z}\right) + 2M_{22}\left(1 + \frac{1}{Z}\right)x + \frac{1}{l_s}\left(P_{a2}^{(+)}\left(1 + \frac{1}{Z}\right) + \frac{P_2^{(+)}}{Ze}\right)e^{x/l_s} - \frac{1}{l_s}\left(P_{a2}^{(-)}\left(1 + \frac{1}{Z}\right) + \frac{P_2^{(-)}}{Ze}\right)e^{-x/l_s} = -J_{a2}\left(\frac{1}{D_a} + \frac{1}{Z^2 D_b}\right). \tag{A.15}$$

Since J_{a2} is uniform, comparison of powers of x yields the conditions

$$P_2^{(+)} = -(1+Z)eP_{a2}^{(+)}, \quad P_2^{(-)} = -(1+Z)eP_{a2}^{(-)}, \tag{A.16}$$

$$J_{a2} = ZJ_{b2} = -(1+Z)\left(\frac{D_a D_b}{ZD_b + D_a}\right)M_{21}, \tag{A.17}$$

$$M_{22} = 0. \tag{A.18}$$

We may thus rewrite Eqs. (A.12) and (A.13) as

$$N_{a2} = M_{20} + M_{21}x + P_{a2}^{(+)}e^{x/l_s} + P_{a2}^{(-)}e^{-x/l_s}, \tag{A.19}$$

$$N_{b2} = \frac{M_{20}}{Z} - \frac{1}{Z}\frac{R_D \epsilon E_1^2}{V_T e} + \frac{M_{21}}{Z}x - P_{a2}^{(+)}e^{x/l_s} - P_{a2}^{(-)}e^{-x/l_s}. \tag{A.20}$$

Note that in Eq. (A.2) the exponential and linear coefficients already match, by

construction. A new constraint, however, is found by comparing the constant terms,

$$-(1+Z)\left(\frac{D_a D_b}{Z^2 D_b + D_a}\right) M_{21} + \frac{D_a n_0}{V_T} F_2 + D_a M_{21} = -\frac{D_a M_1 E_1}{V_T}, \tag{A.21}$$

yielding the condition that

$$F_2 = \frac{V_T M_{21}}{n_0 R_D} - \frac{M_1 E_1}{n_0}. \tag{A.22}$$

We are thus left with four independent constants of integration, which we take to be M_{20}, M_{21}, $P_2^{(+)}$, and $P_2^{(-)}$. The reaction rates for electrons and ions at each interface, needed to produce the correct ion fluxes, provide the 4 conditions necessary to solve for these constants.

For completeness we note that, from Gauss's Law at each surface (3.43),

$$E_2(0) = \frac{\Sigma_2^{(0)}}{\epsilon}, \quad E_2(L) = -\frac{\Sigma_2^{(L)}}{\epsilon}. \tag{A.23}$$

Then Eqs. (A.11) and (A.22) yield

$$\Sigma_2^{(0)} = l_s\left(P_2^{(+)} - P_2^{(-)}\right) + \frac{\epsilon V_T M_{21}}{n_0 R_D} - \frac{\epsilon M_1 E_1}{n_0}, \tag{A.24}$$

$$\Sigma_2^{(L)} = -l_s\left(P_2^{(+)} e^{L/l_s} - P_2^{(-)} e^{-L/l_s}\right) + \frac{\epsilon R_D E_1^2}{V_T} L - \frac{\epsilon V_T M_{21}}{n_0 R_D} + \frac{\epsilon M_1 E_1}{n_0}. \tag{A.25}$$

APPENDIX B

TRANSPORT IN METAL OXIDE AT ORDER $t^{-3/2}$

Recall that in order $k = 3$, all coefficients must be multiplied by $t^{3/2}$ to find the physical variables (j, n, E).

Using the $k = 1$ coefficients for electron and metal ion number densities from Eq. (3.55) and the continuity equations from Eq. (3.30) for $k = 3$,

$$\partial_x J_{a3} = \frac{R_D n_0 E_1}{2V_T} x + \frac{M_1}{2}, \quad \partial_x J_{b3} = \frac{R_D n_0 E_1}{2V_T Z} x + \frac{M_1}{2Z} x. \tag{B.1}$$

Integration of these two equations gives two integration constants. However, these two constants are constrained by charge conservation across the interface at $x = 0$, Eq. (3.38),

$$Z J_{b3}|_{x=0} = J_{a3}|_{x=0} + \frac{\Sigma_1^{(0)}}{2e}, \tag{B.2}$$

where $\Sigma_1^{(0)}$ is given by Eq. (3.58). Integration of the continuity relations in Eq. (B.1) then yields only a single new integration constant, denoted K_3:

$$J_{a3} = \frac{R_D n_0 E_1}{4V_T} x^2 + \frac{M_1}{2} x + K_3, \tag{B.3}$$

$$J_{b3} = \frac{R_D n_0 E_1}{4V_T Z} x^2 + \frac{M_1}{2Z} x + \frac{K_3}{Z} + \frac{\epsilon E_1}{2Ze}. \tag{B.4}$$

There is a uniform net electric charge flux (i.e., current density) at order $k = 3$,

$$J_3 = e\left(Z J_{b3} - J_{a3}\right) = \frac{\epsilon E_1}{2}, \tag{B.5}$$

due to the discharge of the surfaces in order $k = 1$.

For $k = 3$, the Nernst-Planck equations from Eqs. (3.45) and (3.46) are

$$J_{a3} + \frac{D_a}{V_T} n_0 E_3 + D_a \partial_x N_{a3} = -\frac{D_a}{V_T} \left(N_{a2} E_1 + N_{a1} E_2 \right), \tag{B.6}$$

$$J_{b3} - \frac{D_b}{V_T} n_0 E_3 + D_b \partial_x N_{b3} = \frac{Z D_b}{V_T} \left(N_{b2} E_1 + N_{b1} E_2 \right). \tag{B.7}$$

Taking spatial derivatives of Eqs. (B.6) and (B.7), and using Gauss's Law, Eq. (3.42),

$$\partial_x J_{a3} + \frac{D_a n_0}{V_T \epsilon} \rho_3 + D_a \partial_x^2 N_{a3} = -\frac{D_a}{V_T} \partial_x \left(N_{a2} E_1 + N_{a1} E_2 \right), \tag{B.8}$$

$$\partial_x J_{b3} - \frac{D_b n_0}{V_T \epsilon} \rho_3 + D_b \partial_x^2 N_{b3} = \frac{Z D_b}{V_T} \partial_x \left(N_{b2} E_1 + N_{b1} E_2 \right). \tag{B.9}$$

Subtracting Eq. (B.8) multiplied by $1/D_a$ from Eq. (B.9) multiplied by Z/D_b yields an equation for ρ_3,

$$\begin{aligned} e \left(\frac{1}{D_b} - \frac{1}{D_a} \right) \partial_x J_{a3} - (1 + Z) \frac{n_0 e}{V_T \epsilon} \rho_3 + \partial_x^2 \rho_3 = \\ \frac{e E_1}{V_T} (\partial_x N_{a2} + Z^2 \partial_x N_{b2}) + \frac{e}{V_T} (\partial_x N_{a1} + Z^2 \partial_x N_{b1}) E_2 + \frac{e}{V_T} (N_{a1} + Z^2 N_{b1}) \partial_x E_2. \end{aligned} \tag{B.10}$$

Substitution for (N_{a1}, N_{b1}) from Eq. (3.55), (N_{a2}, N_{b2}) from Eqs. (A.19) and (A.20),

E_2 from Eq. (A.11), and J_{a3} from Eq. (B.3) yields

$$\begin{aligned}\partial_x^2\rho_3 - \frac{1}{l_s^2}\Delta\rho_3 = \\ e\left(\frac{D_b - D_a}{D_a D_b}\right)\left(\frac{R_D n_0 E_1}{2V_T}x + \frac{M_1}{2}\right) \\ + \frac{E_1}{V_T}\left((1+Z)eM_{21} - \left(\frac{1-Z^2}{1+Z}\right)\frac{P_2^{(+)}}{el_s}e^{x/l_s} + \left(\frac{1-Z^2}{1+Z}\right)\frac{P_2^{(-)}}{el_s}e^{-x/l_s}\right) \\ + (1+Z)\frac{R_D n_0 e E_1}{V_T^2}\left(F_2 - \frac{R_D E_1^2}{V_T}x + \frac{l_s P_2^{(+)}}{\epsilon}e^{x/l_s} - \frac{l_s P_2^{(-)}}{\epsilon}e^{-x/l_s}\right) \\ + (1+Z)\frac{e}{V_T}\left(\frac{R_D n_0 E_1}{V_T}x + M_1\right)\left(-\frac{R_D E_1^2}{V_T} + \frac{P_2^{(+)}}{\epsilon}e^{x/l_s} + \frac{P_2^{(-)}}{\epsilon}e^{-x/l_s}\right).\end{aligned} \tag{B.11}$$

The solution to this second order differential equation, with two new integration constants $\beta_1^{(+)}$ and $\beta_1^{(-)}$, is

$$\begin{aligned}\rho_3 =& \alpha_1 + \alpha_2 x + \beta_1^{(+)}e^{x/l_s} + \beta_1^{(-)}e^{-x/l_s} + \beta_2^{(+)}xe^{x/l_s} \\ &+ \beta_2^{(-)}xe^{-x/l_s} + \beta_3^{(+)}x^2e^{x/l_s} + e\beta_3^{(-)}x^2e^{-x/l_s},\end{aligned} \tag{B.12}$$

where, with substitution of F_2 from Eq. (A.22),

$$\alpha_1 = -\left(\frac{D_b - D_a}{D_a D_b}\right)\frac{M_1 e l_s^2}{2} - 2\frac{\epsilon E_1 M_{21}}{n_0} + 2\frac{\epsilon R_D M_1 E_1^2}{n_0 V_T}, \tag{B.13}$$

$$\alpha_2 = -\left(\frac{D_b - D_a}{D_a D_b}\right)\frac{\epsilon R_D E_1}{2(1+Z)} + 2\frac{\epsilon R_D^2 E_1^3}{V_T^2}, \tag{B.14}$$

$$\beta_2^{(+)} = \left(-\left(\frac{1-Z^2}{1+Z}\right)\frac{E_1}{2V_T} + \frac{R_D E_1}{4V_T} + \frac{M_1}{2n_0 l_s}\right)P_2^{(+)} \tag{B.15}$$

$$\beta_2^{(-)} = \left(-\left(\frac{1-Z^2}{1+Z}\right)\frac{E_1}{2V_T} + \frac{R_D E_1}{4V_T} - \frac{M_1}{2n_0 l_s}\right)P_2^{(-)} \tag{B.16}$$

$$\beta_3^{(+)} = \frac{R_D E_1}{4V_T l_s}P_2^{(+)}, \qquad \beta_3^{(-)} = -\frac{R_D E_1}{4V_T l_s}P_2^{(-)}. \tag{B.17}$$

From Eq. (B.12) we infer that N_{a3} and ZN_{b3} may include polynomials whose terms that are quadratic and higher are equal, and may include exponential terms that

differ.

Substituting ρ_3 from Eq. (B.12) into Gauss's Law, Eq. (3.42), and integrating $\partial_x E_3$ gives

$$\begin{aligned}
E_3 =& F_3 + \frac{\alpha_1}{\epsilon}x + \frac{\alpha_2}{2\epsilon}x^2 \\
&+ \frac{l_s}{\epsilon}\left(\beta_1^{(+)} - l_s\beta_2^{(+)} + 2l_s^2\beta_3^{(+)}\right)e^{x/l_s} - \frac{l_s}{\epsilon}\left(\beta_1^{(-)} + l_s\beta_2^{(-)} + 2l_s^2\beta_3^{(-)}\right)e^{-x/l_s} \\
&+ \frac{l_s}{\epsilon}\left(\beta_2^{(+)} - 2l_s\beta_3^{(+)}\right)xe^{x/l_s} - \frac{l_s}{\epsilon}\left(\beta_2^{(-)} + 2l_s\beta_3^{(-)}\right)xe^{-x/l_s} \\
&+ \frac{l_s}{\epsilon}\beta_3^{(+)}x^2e^{x/l_s} - \frac{l_s}{\epsilon}\beta_3^{(-)}x^2e^{-x/l_s},
\end{aligned} \tag{B.18}$$

where F_3 is a new integration constant, with units V-s$^{3/2}$/m.

Substitution of the coefficients N_{a1} from Eq. (3.55), N_{a2} from Eq. (A.12), E_2 from Eq. (A.11), J_{a3} from Eq. (B.3), and E_3 from Eq. (B.18) into the $k = 3$ Nernst-Planck equation for electrons, Eq. (B.6), yields

$$\begin{aligned}
\partial_x N_{a3} =& -\left(\frac{M_{20}E_1}{V_T} + \frac{M_1F_2}{V_T} + \frac{n_0F_3}{V_T} + \frac{K_3}{D_a}\right) \\
&+ \left(\frac{R_DM_1E_1^2}{V_T^2} - \frac{M_{21}E_1}{V_T} - \frac{R_Dn_0F_2E_1}{V_T^2} - \frac{n_0\alpha_1}{\epsilon V_T} - \frac{M_1}{2D_a}\right)x \\
&+ \left(\frac{R_D^2n_0E_1^3}{V_T^3} - \frac{n_0\alpha_2}{2\epsilon V_T} - \frac{R_Dn_0E_1}{4D_aV_T}\right)x^2 \\
&+ \left(\frac{E_1P_2^{(+)}}{(1+Z)eV_T} - \frac{l_sM_1P_2^{(+)}}{\epsilon V_T} - \frac{n_0l_s}{\epsilon V_T}\left(\beta_1^{(+)} - l_s\beta_2^{(+)} + 2l_s^2\beta_3^{(+)}\right)\right)e^{x/l_s} \\
&+ \left(\frac{E_1P_2^{(-)}}{(1+Z)eV_T} + \frac{l_sM_1P_2^{(-)}}{\epsilon V_T} + \frac{n_0l_s}{\epsilon V_T}\left(\beta_1^{(-)} + l_s\beta_2^{(-)} + 2l_s^2\beta_3^{(-)}\right)\right)e^{-x/l_s} \\
&+ \left(-\frac{n_0l_sR_DE_1P_2^{(+)}}{\epsilon V_T^2} - \frac{n_0l_s}{\epsilon V_T}\left(\beta_2^{(+)} - 2l_s\beta_3^{(+)}\right)\right)xe^{x/l_s} \\
&+ \left(\frac{n_0l_sR_DE_1P_2^{(-)}}{\epsilon V_T^2} + \frac{n_0l_s}{\epsilon V_T}\left(\beta_2^{(-)} + 2l_s\beta_3^{(-)}\right)\right)xe^{-x/l_s} \\
&- \frac{n_0l_s}{\epsilon V_T}\beta_3^{(+)}x^2e^{x/l_s} + \frac{n_0l_s}{\epsilon V_T}\beta_3^{(-)}x^2e^{-x/l_s}.
\end{aligned} \tag{B.19}$$

The solution to this first order differential equation, with one new integration constant M_{30}, is

$$\begin{aligned} N_{a3} =& M_{30} + M_{31}x + M_{32}x^2 + M_{33}x^3 + \gamma_1^{(+)}e^{x/l_s} + \gamma_1^{(-)}e^{-x/l_s} \\ &+ \gamma_2^{(+)}xe^{x/l_s} + \gamma_2^{(-)}xe^{-x/l_s} + \gamma_3^{(+)}x^2e^{x/l_s} + \gamma_3^{(-)}x^2e^{-x/l_s}, \end{aligned} \tag{B.20}$$

where

$$M_{31} = -\left(\frac{M_{20}E_1}{V_T} + \frac{M_1F_2}{V_T} + \frac{n_0F_3}{V_T} + \frac{K_3}{D_a}\right), \tag{B.21}$$

$$M_{32} = \frac{1}{2}\left(\frac{R_DM_1E_1^2}{V_T^2} - \frac{M_{21}E_1}{V_T} - \frac{R_Dn_0F_2E_1}{V_T^2} - \frac{n_0\alpha_1}{\epsilon V_T} - \frac{M_1}{2D_a}\right), \tag{B.22}$$

$$M_{33} = \frac{1}{3}\left(\frac{R_D^2n_0E_1^3}{V_T^3} - \frac{n_0\alpha_2}{2\epsilon V_T} - \frac{R_Dn_0E_1}{4D_aV_T}\right), \tag{B.23}$$

$$\begin{aligned} \gamma_1^{(+)} =& \left(\frac{(R_D+1)l_sE_1}{V_T} - \frac{M_1}{n_0}\right)\frac{P_2^{(+)}}{(1+Z)e} \\ &- \frac{1}{(1+Z)e}\left(\beta_1^{(+)} - 2l_s\beta_2^{(+)} + 6l_s^2\beta_3^{(+)}\right), \end{aligned} \tag{B.24}$$

$$\begin{aligned} \gamma_1^{(-)} =& -\left(\frac{M_1}{n_0} + \frac{(R_D+1)l_sE_1}{V_T}\right)\frac{P_2^{(-)}}{(1+Z)e} \\ &- \frac{1}{(1+Z)e}\left(\beta_1^{(-)} + 2l_s\beta_2^{(-)} + 6l_s^2\beta_3^{(-)}\right), \end{aligned} \tag{B.25}$$

$$\gamma_2^{(+)} = -\frac{R_DE_1P_2^{(+)}}{(1+Z)eV_T} - \frac{1}{(1+Z)e}\left(\beta_2^{(+)} - 4l_s\beta_3^{(+)}\right), \tag{B.26}$$

$$\gamma_2^{(-)} = -\frac{R_DE_1P_2^{(-)}}{(1+Z)eV_T} - \frac{1}{(1+Z)e}\left(\beta_2^{(-)} + 4l_s\beta_3^{(-)}\right), \tag{B.27}$$

$$\gamma_3^{(+)} = -\frac{\beta_3^{(+)}}{(1+Z)e}, \qquad \gamma_3^{(-)} = -\frac{\beta_3^{(-)}}{(1+Z)e}. \tag{B.28}$$

Use of Eq. (3.31) for $k = 3$, that is, $\rho_3 = e(ZN_{b3} - N_{a3})$, as well as ρ_3 from Eq. (B.12)

and N_{a3} from (B.20), gives

$$\begin{aligned} N_{b3} = &\left(\frac{\alpha_1 + eM_{30}}{Ze}\right) + \left(\frac{\alpha_2 + eM_{31}}{Ze}\right) x + \left(\frac{M_{32}}{Z}\right) x^2 + \left(\frac{M_{33}}{Z}\right) x^3 \\ &+ \left(\frac{\beta_1^{(+)} + e\gamma_1^{(+)}}{Ze}\right) e^{x/l_s} + \left(\frac{\beta_1^{(-)} + e\gamma_1^{(-)}}{Ze}\right) e^{-x/l_s} \\ &+ \left(\frac{\beta_2^{(+)} + e\gamma_2^{(+)}}{Ze}\right) x e^{x/l_s} + \left(\frac{\beta_2^{(-)} + e\gamma_2^{(-)}}{Ze}\right) x e^{-x/l_s} \\ &+ \left(\frac{\beta_3^{(+)} + e\gamma_3^{(+)}}{Ze}\right) x^2 e^{x/l_s} + \left(\frac{\beta_3^{(-)} + e\gamma_3^{(-)}}{Ze}\right) x^2 e^{-x/l_s}. \end{aligned} \tag{B.29}$$

We now have J_{a3}, J_{b3}, E_3, N_{a3} and N_{b3} with five constants of integration, K_3, $\beta_1^{(+)}$, $\beta_1^{(-)}$, F_3, and M_{30}. To reduce this from five to four, we add Eq. (B.6) divided by D_a and Eq. (B.7) divided by D_b,

$$\frac{J_{a3}}{D_a} + \frac{J_{b3}}{D_b} + \partial_x(N_{a3} + N_{b3}) = \frac{1}{V_T}\left(\frac{\rho_2 E_1}{e} + \frac{\rho_1 E_2}{e}\right). \tag{B.30}$$

As for $k = 2$, in Eq. (B.30) the exponential, quadratic, and linear terms match, by construction. A new constraint, however, is found by comparing the constant terms,

$$\frac{K_3}{D_a} + \frac{K_3}{ZD_b} + \frac{\epsilon E_1}{2ZeD_b} + M_{31} + \frac{\alpha_2 + eM_{31}}{Ze} = -\frac{R_D \epsilon E_1^3}{V_T^2 e}. \tag{B.31}$$

Substituting M_{31} from Eq. (B.21) yields

$$\begin{aligned} F_3 = &\left[\frac{D_b - D_a}{(1+Z)D_a D_b}\right] K_3 - \frac{M_{20}E_1}{n_0} - \frac{M_1 F_2}{n_0} \\ &- \left[\frac{1}{(1+Z)e}\right]\left(\frac{ZR_D\epsilon E_1^3}{V_T^2} + \frac{\epsilon E_1}{2D_b} + \alpha_2\right), \end{aligned} \tag{B.32}$$

a relation between integration constants F_3 and K_3.

We are thus left with four independent constants of integration, which we take to be K_3, M_{30}, $\beta_1^{(+)}$, and $\beta_1^{(-)}$. The reaction rates for electrons and ions at each interface, needed to produce the correct ion fluxes, provide the four conditions necessary to solve

for these constants.

For completeness, we note that from Gauss's Law at each surface, Eq. (3.43),

$$E_3(0) = \frac{\Sigma_3^{(0)}}{\epsilon}, \quad E_3(L) = -\frac{\Sigma_3^{(L)}}{\epsilon}. \tag{B.33}$$

Then, Eq. (B.18) yields

$$\Sigma_3^{(0)} = \epsilon F_3 + l_s\left(\beta_1^{(+)} - l_s\beta_2^{(+)} + 2l_s^2\beta_3^{(+)}\right) - l_s\left(\beta_1^{(-)} + l_s\beta_2^{(-)} + 2l_s^2\beta_3^{(-)}\right), \tag{B.34}$$

$$\begin{aligned}\Sigma_3^{(L)} = &-\epsilon F_3 - \alpha_1 L - \frac{\alpha_2}{2}L^2 - l_s\left(\beta_1^{(+)} - l_s\beta_2^{(+)} + 2l_s^2\beta_3^{(+)}\right)e^{L/l_s} \\ &+ l_s\left(\beta_1^{(-)} + l_s\beta_2^{(-)} + 2l_s^2\beta_3^{(-)}\right)e^{-L/l_s} - l_s\left(\beta_2^{(+)} - 2l_s\beta_3^{(+)}\right)Le^{L/l_s} \\ &+ l_s\left(\beta_2^{(-)} + 2l_s\beta_3^{(-)}\right)Le^{-L/l_s} - l_s\beta_3^{(+)}L^2e^{L/l_s} + l_s\beta_3^{(-)}L^2e^{-L/l_s}.\end{aligned} \tag{B.35}$$

We have verified that

$$\Sigma_3^{(0)} + \Sigma_3^{(L)} + \int_0^L \rho_3 dx = 0, \tag{B.36}$$

so there is no net charge in the system.

APPENDIX C

BOUNDARY CONDITIONS FOR PERPENDICULAR CURRENT CROSSING AN ISOLATED INTERFACE

Boundary conditions (i-viii) for an isolated interface (that is, one that is effectively an infinite distance from any other interface) through which an electric current is passed are discussed in Chapter IV. They are here found explicitly, in numerical order.

(i-ii): From Eqs. (4.64) and (4.65), continuity of $\delta\phi$ and δE across the interface at $x_{\rm int} = 0$ gives

$$\xi^{(\rm I)}V_S^{(\rm I)} + \phi_{0_Q}^{(\rm I)} + B^{(\rm I)} = \xi^{(\rm II)}V_S^{(\rm II)} + \phi_{0_Q}^{(\rm II)} + B^{(\rm II)}, \tag{C.1}$$

$$-\frac{\xi^{(\rm I)}V_S^{(\rm I)}}{\ell_{\rm sf}^{(\rm I)}} - \frac{\phi_{0_Q}^{(\rm I)}}{\ell_Q^{(\rm I)}} + A^{(\rm I)} = \frac{\xi^{(\rm II)}V_S^{(\rm II)}}{\ell_S^{(\rm II)}} + \frac{\phi_{0_Q}^{(\rm II)}}{\ell_Q^{(\rm II)}} + A^{(\rm II)}. \tag{C.2}$$

Recall that $\xi = 0$ for a non-magnetic material.

(iii-iv): Separately setting the current in each material $(j_\uparrow + j_\downarrow)$ to a known (measurable) constant J gives

$$J = j_\uparrow^{(\rm I)} + j_\downarrow^{(\rm I)} = j_{\uparrow_Q}^{(\rm I)} + j_{\downarrow_Q}^{(\rm I)} + j_{\uparrow_S}^{(\rm I)} + j_{\downarrow_S}^{(\rm I)} + j_{\uparrow_{dc}}^{(\rm I)} + j_{\downarrow_{dc}}^{(\rm I)}, \tag{C.3}$$

$$J = j_\uparrow^{(\rm II)} + j_\downarrow^{(\rm II)} = j_{\uparrow_Q}^{(\rm II)} + j_{\downarrow_Q}^{(\rm II)} + j_{\uparrow_S}^{(\rm II)} + j_{\downarrow_S}^{(\rm II)} + j_{\uparrow_{dc}}^{(\rm II)} + j_{\downarrow_{dc}}^{(\rm II)}. \tag{C.4}$$

As discussed above, since the charge mode is associated with zero deviation of magnetoelectrochemical potential, it does not lead to any overall electric current (i.e., $j_{\uparrow_Q} = 0 = j_{\downarrow_Q}$). Also, as discussed above, the spin-diffusion mode has equal and opposite up- and down-spin currents, so that it too does not lead to any overall electric current (i.e., $j_{\uparrow_S} + j_{\downarrow_S} = 0$). Substitution from Eq. (4.63) into Eqs. (C.3)-(C.4) then

gives

$$J = -\left(\sigma_{\uparrow}^{(\mathrm{I})} + \sigma_{\downarrow}^{(\mathrm{I})}\right)\frac{A^{(\mathrm{I})}}{e}, \tag{C.5}$$

$$J = -\left(\sigma_{\uparrow}^{(\mathrm{II})} + \sigma_{\downarrow}^{(\mathrm{II})}\right)\frac{A^{(\mathrm{II})}}{e}. \tag{C.6}$$

(v): Although the electric current is continuous everywhere, in principle at the interface there may be spin-flips, so that spin current is not continuous across the interface. However, we neglect interfacial spin flips (as is typical in this type of theory). We thus take

$$j_{\uparrow}^{(\mathrm{I})}(0) \equiv j_{\uparrow}^{(\mathrm{II})}(0), \qquad j_{\downarrow}^{(\mathrm{I})}(0) \equiv j_{\downarrow}^{(\mathrm{II})}(0). \tag{C.7}$$

We now find the up- and down-spin currents in each mode, then substitute them into Eq. (C.7). Recall that there is no up- or down-spin current associated with the charge mode. For the spin mode, substitution of Eqs. (4.19)-(4.20) into Eq. (4.1) gives

$$j_{\uparrow S}^{(\mathrm{I,II})} = (\mp)\frac{1}{e\ell_{\mathrm{sf}}}\left(\frac{\sigma_{\uparrow}\sigma_{\downarrow}}{\sigma_{\uparrow}+\sigma_{\downarrow}}\right)V_S e^{(\pm)x/\ell_{\mathrm{sf}}}, \tag{C.8}$$

$$j_{\downarrow S}^{(\mathrm{I,II})} = (\pm)\frac{1}{e\ell_{\mathrm{sf}}}\left(\frac{\sigma_{\uparrow}\sigma_{\downarrow}}{\sigma_{\uparrow}+\sigma_{\downarrow}}\right)V_S e^{(\pm)x/\ell_{\mathrm{sf}}}. \tag{C.9}$$

Equation (4.63) gives the spin current for the dc mode.

At the interface ($x = 0$), substitution of Eqs. (C.8) and (4.63) into the first relation given in Eq. (C.7) gives

$$-\frac{1}{e\ell_{\mathrm{sf}}^{(\mathrm{I})}}\left(\frac{\sigma_{\uparrow}^{(\mathrm{I})}\sigma_{\downarrow}^{(\mathrm{I})}}{\sigma_{\uparrow}^{(\mathrm{I})}+\sigma_{\downarrow}^{(\mathrm{I})}}\right)V_S^{(\mathrm{I})} - \frac{\sigma_{\uparrow}^{(\mathrm{I})}}{e}A^{(\mathrm{I})} = \frac{1}{e\ell_{\mathrm{sf}}^{(\mathrm{II})}}\left(\frac{\sigma_{\uparrow}^{(\mathrm{II})}\sigma_{\downarrow}^{(\mathrm{II})}}{\sigma_{\uparrow}^{(\mathrm{II})}+\sigma_{\downarrow}^{(\mathrm{II})}}\right)V_S^{(\mathrm{II})} - \frac{\sigma_{\uparrow}^{(\mathrm{II})}}{e}A^{(\mathrm{II})}. \tag{C.10}$$

As discussed above, the second relation given in Eq. (C.7) is then automatically satisfied by Eqs. (C.5)-(C.6), which constrain the sums of the up- and down-spin currents.

(vi-vii): Neglecting cross-terms in Eqs. (2.51)-(2.52), the spin currents across the interface are given by

$$j_{\uparrow_{\rm int}} = -\frac{g_\uparrow}{e^2}(\Delta\bar{\mu}_\uparrow)_{\rm int}, \tag{C.11}$$

$$j_{\downarrow_{\rm int}} = -\frac{g_\downarrow}{e^2}(\Delta\bar{\mu}_\downarrow)_{\rm int}, \tag{C.12}$$

Since without the electric field associated with the *dc* mode there is no steady-state current, the currents are proportional to the differences in $\delta\bar{\mu}$ rather than $\bar{\mu}$. We now find $(\Delta\delta\bar{\mu})_{\rm int}$ for each mode and then substitute them into Eqs. (C.11)-(C.12).

The charge mode has $\delta\bar{\mu}_{\uparrow_Q} = 0 = \delta\bar{\mu}_{\downarrow_Q}$, so by Eqs. (C.11)-(C.12) it does not affect the current crossing the boundary. At the $x = x_{\rm int} = 0$ interface, Eqs. (4.19) and (4.20) give

$$(\Delta\delta\bar{\mu}_{\uparrow_S})_{\rm int} = \left(\frac{\sigma_\downarrow^{(\rm II)}}{\sigma_\uparrow^{(\rm II)}+\sigma_\downarrow^{(\rm II)}}\right) eV_S^{(\rm II)} - \left(\frac{\sigma_\downarrow^{(\rm I)}}{\sigma_\uparrow^{(\rm I)}+\sigma_\downarrow^{(\rm I)}}\right) eV_S^{(\rm I)}, \tag{C.13}$$

$$(\Delta\delta\bar{\mu}_S^{\downarrow})_{\rm int} = -\left(\frac{\sigma_\uparrow^{(\rm II)}}{\sigma_\uparrow^{(\rm II)}+\sigma_\downarrow^{(\rm II)}}\right) eV_S^{(\rm II)} + \left(\frac{\sigma_\uparrow^{(\rm I)}}{\sigma_\uparrow^{(\rm I)}+\sigma_\downarrow^{(\rm I)}}\right) eV_S^{(\rm I)}. \tag{C.14}$$

At the $x = x_{\rm int} = 0$ interface, equation (4.61) gives

$$(\Delta\delta\bar{\mu}_{\uparrow_{dc}})_{\rm int} = (\Delta\delta\bar{\mu}_{\downarrow_{dc}})_{\rm int} = -\,e\left(B^{(\rm II)} - B^{(\rm I)}\right). \tag{C.15}$$

Substitution of Eqs. (C.13)-(C.15) into Eqs. (C.11)-(C.12) yields

$$j_{\uparrow_{\rm int}} = -\frac{g_\uparrow}{e}\left[\frac{\sigma_\downarrow^{(\rm II)}V_S^{(\rm II)}}{\sigma_\uparrow^{(\rm II)}+\sigma_\downarrow^{(\rm II)}} - \frac{\sigma_\downarrow^{(\rm I)}V_S^{(\rm I)}}{\sigma_\uparrow^{(\rm I)}+\sigma_\downarrow^{(\rm I)}} - \left(B^{(\rm II)} - B^{(\rm I)}\right)\right], \tag{C.16}$$

$$j_{\downarrow_{\rm int}} = -\frac{g_\downarrow}{e}\left[-\frac{\sigma_\uparrow^{(\rm II)}V_S^{(\rm II)}}{\sigma_\uparrow^{(\rm II)}+\sigma_\downarrow^{(\rm II)}} + \frac{\sigma_\uparrow^{(\rm I)}V_S^{(\rm I)}}{\sigma_\uparrow^{(\rm I)}+\sigma_\downarrow^{(\rm I)}} - \left(B^{(\rm II)} - B^{(\rm I)}\right)\right]. \tag{C.17}$$

Then, for spin currents continuous across the interface, we set

$$j_{\uparrow_{\rm int}} \equiv j_\uparrow^{(\rm II)}(0), \qquad j_{\downarrow_{\rm int}} \equiv j_\downarrow^{(\rm II)}(0). \tag{C.18}$$

By Eq. (C.7) one may equivalently use $j_{\uparrow_{\rm int}} \equiv j_{\uparrow}^{(\rm I)}(0)$ and $j_{\uparrow_{\rm int}} \equiv j_{\downarrow}^{(\rm I)}(0)$. Substitution of Eqs. (4.63) and (C.8)-(C.9) (at $x = x_{\rm int} = 0$) into Eq. (C.17) then gives

$$\begin{aligned} j_{\uparrow}^{(\rm II)}(0) =& \frac{1}{e\ell_{\rm sf}^{(\rm II)}} \left(\frac{\sigma_{\uparrow}^{(\rm II)}\sigma_{\downarrow}^{(\rm II)}}{\sigma_{\uparrow}^{(\rm II)} + \sigma_{\downarrow}^{(\rm II)}} \right) V_S^{(\rm II)} - \frac{\sigma_{\uparrow}^{(\rm II)}}{e} A^{(\rm II)} \\ =& -\frac{g_{\uparrow}}{e} \left[\frac{\sigma_{\downarrow}^{(\rm II)} V_S^{(\rm II)}}{\sigma_{\uparrow}^{(\rm II)} + \sigma_{\downarrow}^{(\rm II)}} - \frac{\sigma_{\downarrow}^{(\rm I)} V_S^{(\rm I)}}{\sigma_{\uparrow}^{(\rm I)} + \sigma_{\downarrow}^{(\rm I)}} - \left(B^{(\rm II)} - B^{(\rm I)} \right) \right], \end{aligned} \tag{C.19}$$

$$\begin{aligned} j_{\downarrow}^{(\rm II)}(0) =& -\frac{1}{e\ell_{\rm sf}^{(\rm II)}} \left(\frac{\sigma_{\uparrow}^{(\rm II)}\sigma_{\downarrow}^{(\rm II)}}{\sigma_{\uparrow}^{(\rm II)} + \sigma_{\downarrow}^{(\rm II)}} \right) V_S^{(\rm II)} - \frac{\sigma_{\downarrow}^{(\rm II)}}{e} A^{(\rm II)} \\ =& -\frac{g_{\downarrow}}{e} \left[-\frac{\sigma_{\uparrow}^{(\rm II)} V_S^{(\rm II)}}{\sigma_{\uparrow}^{(\rm II)} + \sigma_{\downarrow}^{(\rm II)}} + \frac{\sigma_{\uparrow}^{(\rm I)} V_S^{(\rm I)}}{\sigma_{\uparrow}^{(\rm I)} + \sigma_{\downarrow}^{(\rm I)}} - \left(B^{(\rm II)} - B^{(\rm I)} \right) \right]. \end{aligned} \tag{C.20}$$

(viii): There is an arbitrary constant potential. We set

$$B^{(\rm II)} \equiv 0. \tag{C.21}$$

Equations (C.1)-(C.2), (C.5)-(C.6), (C.10), (C.19)-(C.20), and (C.21) are general for an isolated interface between any two materials.

We now write the boundary conditions Eqs. (C.1)-(C.2), (C.5)-(C.6), (C.10), (C.19)-(C.20), and (C.21) in terms of dimensionless variables.

We now consider the specific case of a FM-NM interface as in Fig. 6. Since $\sigma_{\uparrow}^{(\rm II)} = \sigma_{\downarrow}^{(\rm II)}$, we define

$$\sigma^{(\rm II)} \equiv \sigma_{\uparrow}^{(\rm II)} + \sigma_{\downarrow}^{(\rm II)} = 2\sigma_{\uparrow}^{(\rm II)}. \tag{C.22}$$

Further, we take $\ell_{S\uparrow}^{(\rm II)} = \ell_{S\downarrow}^{(\rm II)}$ and $N_{\uparrow}^{(\rm II)} = N_{\downarrow}^{(\rm II)}$, so that, as discussed above, we have $\xi^{(\rm II)} = 0$.

We take the electric current $-eJ$ to be known, and use J as a "reference" flux, $-eJ/\sigma^{(\rm II)}$ as a reference field, and $-e\ell J/\sigma^{(\rm II)}$ as a reference voltage, where ℓ is a length

(which we set to be $\ell_{\rm sf}^{\rm Cu}$ below). We therefore define the following variables:

$$\bar{\gamma}_S^{(\rm I)} \equiv \frac{\sigma^{(\rm II)} V_S^{(\rm I)}}{e\ell J}, \quad \bar{\gamma}_S^{(\rm II)} \equiv \frac{\sigma^{(\rm II)} V_S^{(\rm II)}}{e\ell J}, \quad \gamma_Q^{(\rm I)} \equiv \frac{\sigma^{(\rm II)} \phi_{0_Q}^{(\rm I)}}{e\ell J}, \quad \gamma_Q^{(\rm II)} \equiv \frac{\sigma^{(\rm II)} \phi_{0_Q}^{(\rm II)}}{e\ell J},$$
$$\gamma_{dc}^{(\rm I)} \equiv \frac{\sigma^{(\rm II)} B^{(\rm I)}}{e\ell J}, \quad \gamma_{dc}^{(\rm II)} \equiv \frac{\sigma^{(\rm II)} B^{(\rm II)}}{e\ell J}, \quad \Upsilon^{(\rm I)} \equiv \frac{\sigma^{(\rm II)} A_{(\rm I)}}{eJ}, \quad \Upsilon^{(\rm II)} \equiv \frac{\sigma^{(\rm II)} A_{(\rm II)}}{eJ}. \tag{C.23}$$

The terms γ_Q and γ_{dc} are the respective dimensionless potentials of the charge and bulk modes. The bar on $\bar{\gamma}_S$ is to distinguish it from the dimensionless potential in the spin mode, which is given by $\xi\bar{\gamma}_S$.

The eight boundary condition equations are now written in terms of these dimensionless variables. Multiplication of Eq. (C.1) by $\sigma^{(\rm II)}/(e\ell J)$, and multiplication of Eq. (C.2) by $\sigma^{(\rm II)}/(eJ)$ gives

$$\xi^{(\rm I)}\bar{\gamma}_S^{(\rm I)} + \gamma_Q^{(\rm I)} + \gamma_{dc}^{(\rm I)} = \gamma_Q^{(\rm II)} + \gamma_{dc}^{(\rm II)}, \tag{C.24}$$

$$-\left(\frac{\ell}{\ell_{\rm sf}^{(\rm I)}}\right)\xi^{(\rm I)}\bar{\gamma}_S^{(\rm I)} - \left(\frac{\ell}{\ell_Q^{(\rm I)}}\right)\gamma_Q^{(\rm I)} + \Upsilon^{(\rm I)} = \left(\frac{\ell}{\ell_Q^{(\rm II)}}\right)\gamma_Q^{(\rm II)} + \Upsilon^{(\rm II)}. \tag{C.25}$$

Multiplication of Eqs. (C.5)-(C.6) by $1/J$ gives

$$1 = -\left(\frac{\sigma_\uparrow^{(\rm I)} + \sigma_\downarrow^{(\rm I)}}{\sigma^{(\rm II)}}\right)\Upsilon^{(\rm I)}, \tag{C.26}$$

$$1 = -\Upsilon^{(\rm II)}. \tag{C.27}$$

Multiplication of Eqs. (C.10) and (C.19)-(C.20) by $1/J$ gives

$$-\frac{\ell}{\ell_{\rm sf}^{(\rm I)}\sigma^{(\rm II)}}\left(\frac{\sigma_\uparrow^{(\rm I)}\sigma_\downarrow^{(\rm I)}}{\sigma_\uparrow^{(\rm I)} + \sigma_\downarrow^{(\rm I)}}\right)\bar{\gamma}_S^{(\rm I)} - \frac{\sigma_\uparrow^{(\rm I)}}{\sigma^{(\rm II)}}\Upsilon^{(\rm I)} = \frac{\ell}{4\ell_{\rm sf}^{(\rm II)}}\bar{\gamma}_S^{(\rm II)} - \frac{1}{2}\Upsilon^{(\rm II)}, \tag{C.28}$$

$$\frac{\ell}{4\ell_{\rm sf}^{(\rm II)}}\bar{\gamma}_S^{(\rm II)} - \frac{1}{2}\Upsilon^{(\rm II)} = -\frac{g_\uparrow\ell}{\sigma^{(\rm II)}}\left[\frac{\bar{\gamma}_S^{(\rm II)}}{2} - \frac{\sigma_\downarrow^{(\rm I)}\bar{\gamma}_S^{(\rm I)}}{\sigma_\uparrow^{(\rm I)} + \sigma_\downarrow^{(\rm I)}} - \left(\gamma_{dc}^{(\rm II)} - \gamma_{dc}^{(\rm I)}\right)\right], \tag{C.29}$$

$$-\frac{\ell}{4\ell_{\rm sf}^{(\rm II)}}\bar{\gamma}_S^{(\rm II)} - \frac{1}{2}\Upsilon^{(\rm II)} = -\frac{g_\downarrow\ell}{\sigma^{(\rm II)}}\left[-\frac{\bar{\gamma}_S^{(\rm II)}}{2} + \frac{\sigma_\uparrow^{(\rm I)}\bar{\gamma}_S^{(\rm I)}}{\sigma_\uparrow^{(\rm I)} + \sigma_\downarrow^{(\rm I)}} - \left(\gamma_{dc}^{(\rm II)} - \gamma_{dc}^{(\rm I)}\right)\right]. \tag{C.30}$$

Here we have used $\sigma_{\uparrow}^{(\mathrm{II})} = \sigma_{\downarrow}^{(\mathrm{II})} = (1/2)\sigma^{(\mathrm{II})}$ from the definition given in Eq. (C.22). Finally, Eq. (C.21) gives

$$\gamma_{dc}^{(\mathrm{II})} = 0. \tag{C.31}$$

For the eight dimensionless unknowns in Eq. (C.23), there are eight conditions, given in Eqs. (C.24)-(C.31). The numerical results for a Co/Cu interface are given in Chapter IV.

APPENDIX D

BOUNDARY CONDITIONS FOR PERPENDICULAR CURRENT CROSSING A TWO-INTERFACE MULTILAYER

Boundary conditions (i-xiv) for a two-interface multilayer through which an electric current is passed are discussed in Chapter IV. They are here found explicitly for interfaces at $x = -d/2$ and $x = d/2$, as in Fig. 5.

(i-iv): Equations (4.64) and (4.65) give

$$\xi^{(\mathrm{I})}V_S^{(\mathrm{I})} + \phi_{0_Q}^{(\mathrm{I})} + B^{(\mathrm{I})} + \left(\frac{d}{2}\right)A^{(\mathrm{I})}$$
$$= \xi^{(\mathrm{II})}V_S^{(\mathrm{IIa})} + \xi^{(\mathrm{II})}V_S^{(\mathrm{IIb})}e^{-d/\ell_{\mathrm{sf}}^{(\mathrm{II})}} + \phi_{0_Q}^{(\mathrm{IIa})} + \phi_{0_Q}^{(\mathrm{IIb})}e^{-d/\ell_Q^{(\mathrm{II})}} + B^{(\mathrm{II})} + \left(\frac{d}{2}\right)A^{(\mathrm{II})}, \quad \text{(D.1)}$$

$$\xi^{(\mathrm{III})}V_S^{(\mathrm{III})} + \phi_{0_Q}^{(\mathrm{III})} + B^{(\mathrm{III})} - \left(\frac{d}{2}\right)A^{(\mathrm{III})}$$
$$= \xi^{(\mathrm{II})}V_S^{(\mathrm{IIa})}e^{-d/\ell_{\mathrm{sf}}^{(\mathrm{II})}} + \xi^{(\mathrm{II})}V_S^{(\mathrm{IIb})} + \phi_{0_Q}^{(\mathrm{IIa})}e^{-d/\ell_Q^{(\mathrm{II})}} + \phi_{0_Q}^{(\mathrm{IIb})} + B^{(\mathrm{II})} - \left(\frac{d}{2}\right)A^{(\mathrm{II})}, \quad \text{(D.2)}$$

$$-\frac{\xi^{(\mathrm{I})}}{\ell_{\mathrm{sf}}^{(\mathrm{I})}}V_S^{(\mathrm{I})} - \frac{1}{\ell_Q^{(\mathrm{I})}}\phi_{0_Q}^{(\mathrm{I})} + A^{(\mathrm{I})}$$
$$= \frac{\xi^{(\mathrm{II})}}{\ell_{\mathrm{sf}}^{(\mathrm{II})}}V_S^{(\mathrm{IIa})} - \frac{\xi^{(\mathrm{II})}}{\ell_{\mathrm{sf}}^{(\mathrm{II})}}V_S^{(\mathrm{IIb})}e^{-d/\ell_{\mathrm{sf}}^{(\mathrm{II})}} + \frac{1}{\ell_Q^{(\mathrm{II})}}\phi_{0_Q}^{(\mathrm{IIa})} - \frac{1}{\ell_Q^{(\mathrm{II})}}\phi_{0_Q}^{(\mathrm{IIb})}e^{-d/\ell_Q^{(\mathrm{II})}} + A^{(\mathrm{II})}, \quad \text{(D.3)}$$

$$\frac{\xi^{(\mathrm{III})}}{\ell_{\mathrm{sf}}^{(\mathrm{III})}}V_S^{(\mathrm{III})} + \frac{1}{\ell_Q^{(\mathrm{III})}}\phi_{0_Q}^{(\mathrm{III})} + A^{(\mathrm{III})}$$
$$= \frac{\xi^{(\mathrm{II})}}{\ell_{\mathrm{sf}}^{(\mathrm{II})}}V_S^{(\mathrm{IIa})}e^{-d/\ell_{\mathrm{sf}}^{(\mathrm{II})}} - \frac{\xi^{(\mathrm{II})}}{\ell_{\mathrm{sf}}^{(\mathrm{II})}}V_S^{(\mathrm{IIb})} + \frac{1}{\ell_Q^{(\mathrm{II})}}\phi_{0_Q}^{(\mathrm{IIa})}e^{-d/\ell_Q^{(\mathrm{II})}} - \frac{1}{\ell_Q^{(\mathrm{II})}}\phi_{0_Q}^{(\mathrm{IIb})} + A^{(\mathrm{II})}. \quad \text{(D.4)}$$

Recall that $\xi = 0$ for a non-magnetic material (e.g., $\xi^{(\mathrm{II})} = 0$ for the configuration in Fig. 5).

(v-vii): We take the electric current $-eJ$ to be a known, measurable quantity. Because the total electric current in each surface mode is zero, the dc mode is respon-

sible for the entire electric current. Equation (4.63) gives

$$J = j_\uparrow + j_\downarrow = -\frac{(\sigma_\uparrow + \sigma_\downarrow)\, A}{e}, \tag{D.5}$$

so that application to each material yields

$$J = -\frac{\left(\sigma_\uparrow^{(\mathrm{I})} + \sigma_\downarrow^{(\mathrm{I})}\right) A^{(\mathrm{I})}}{e}, \tag{D.6}$$

$$J = -\frac{\left(\sigma_\uparrow^{(\mathrm{II})} + \sigma_\downarrow^{(\mathrm{II})}\right) A^{(\mathrm{II})}}{e}, \tag{D.7}$$

$$J = -\frac{\left(\sigma_\uparrow^{(\mathrm{III})} + \sigma_\downarrow^{(\mathrm{III})}\right) A^{(\mathrm{III})}}{e}. \tag{D.8}$$

(viii-ix): We take the spin current to be continuous at each interface. Since conditions [5-7] already constrain the sum of the up- and down-spin currents, we only have to enforce the up-spin current to be continuous, as the down-spin current is then guaranteed to be so. In the context of the system shown in Fig. 5, we have

$$j_\uparrow^{(\mathrm{I})}\left(-\frac{d}{2}\right) = j_\uparrow^{(\mathrm{II})}\left(-\frac{d}{2}\right), \tag{D.9}$$

$$j_\uparrow^{(\mathrm{II})}\left(\frac{d}{2}\right) = j_\uparrow^{(\mathrm{III})}\left(\frac{d}{2}\right). \tag{D.10}$$

The charge mode is characterized by $\delta\bar{\mu}^\uparrow = 0 = \delta\bar{\mu}^\downarrow$, so that it has zero up- and down-spin currents. By Eqs. (4.63), (C.8), and (C.9), the total up- and down-spin currents are given by

$$j_\uparrow = \pm\frac{\sigma_\uparrow V_S}{2e\ell_{\mathrm{sf}}} e^{\mp(x-x_{\mathrm{int}})/\ell_{\mathrm{sf}}} - \frac{\sigma_\uparrow A}{e}, \tag{D.11}$$

$$j_\downarrow = \mp\frac{\sigma_\downarrow V_S}{2e\ell_{\mathrm{sf}}} e^{\mp(x-x_{\mathrm{int}})/\ell_{\mathrm{sf}}} - \frac{\sigma_\downarrow A}{e}. \tag{D.12}$$

Note that there is an exponential term from the spin mode current for each interface

bordering a given material. Equations (D.9) and (D.10) may be written as

$$-\frac{\sigma_{\uparrow}^{(\mathrm{I})}V_S^{(\mathrm{I})}}{2e\ell_{\mathrm{sf}}^{(\mathrm{I})}}-\frac{\sigma_{\uparrow}^{(\mathrm{I})}A^{(\mathrm{I})}}{e}=\frac{\sigma_{\uparrow}^{(\mathrm{II})}}{2e\ell_{\mathrm{sf}}^{(\mathrm{II})}}\left(V_S^{(\mathrm{IIa})}-V_S^{(\mathrm{IIb})}e^{-d/\ell_{\mathrm{sf}}^{(\mathrm{II})}}\right)-\frac{\sigma_{\uparrow}^{(\mathrm{II})}A^{(\mathrm{II})}}{e}, \tag{D.13}$$

$$\frac{\sigma_{\uparrow}^{(\mathrm{II})}}{2e\ell_{\mathrm{sf}}^{(\mathrm{II})}}\left(V_S^{(\mathrm{IIa})}e^{-d/\ell_{\mathrm{sf}}^{(\mathrm{II})}}-V_S^{(\mathrm{IIb})}\right)-\frac{\sigma_{\uparrow}^{(\mathrm{II})}A^{(\mathrm{II})}}{e}=\frac{\sigma_{\uparrow}^{(\mathrm{III})}V_S^{(\mathrm{III})}}{2e\ell_{\mathrm{sf}}^{(\mathrm{III})}}-\frac{\sigma_{\uparrow}^{(\mathrm{III})}A^{(\mathrm{III})}}{e}. \tag{D.14}$$

(x-xiii): At each interface, the up- and down-spin currents are proportional to the discontinuity in the respective deviations of up- and down-spin magnetoelectrochemical potentials:

$$j_{\uparrow_{\mathrm{int}}}\left(-\frac{d}{2}\right)=-\frac{g_{\uparrow}^{(a)}}{e^2}\left[\delta\bar{\mu}_{\uparrow}^{(\mathrm{II})}\left(-\frac{d}{2}\right)-\delta\bar{\mu}_{\uparrow}^{(\mathrm{I})}\left(-\frac{d}{2}\right)\right], \tag{D.15}$$

$$j_{\downarrow_{\mathrm{int}}}\left(-\frac{d}{2}\right)=-\frac{g_{\downarrow}^{(a)}}{e^2}\left[\delta\bar{\mu}_{\downarrow}^{(\mathrm{II})}\left(-\frac{d}{2}\right)-\delta\bar{\mu}_{\downarrow}^{(\mathrm{I})}\left(-\frac{d}{2}\right)\right], \tag{D.16}$$

$$j_{\uparrow_{\mathrm{int}}}\left(\frac{d}{2}\right)=-\frac{g_{\uparrow}^{(b)}}{e^2}\left[\delta\bar{\mu}_{\uparrow}^{(\mathrm{III})}\left(\frac{d}{2}\right)-\delta\bar{\mu}_{\uparrow}^{(\mathrm{II})}\left(\frac{d}{2}\right)\right], \tag{D.17}$$

$$j_{\downarrow_{\mathrm{int}}}\left(\frac{d}{2}\right)=-\frac{g_{\downarrow}^{(b)}}{e^2}\left[\delta\bar{\mu}_{\downarrow}^{(\mathrm{III})}\left(\frac{d}{2}\right)-\delta\bar{\mu}_{\downarrow}^{(\mathrm{II})}\left(\frac{d}{2}\right)\right]. \tag{D.18}$$

Presumably, if material (I) is the same as material (III), then $g_{(\uparrow,\downarrow)}^{(a)}=g_{(\uparrow,\downarrow)}^{(b)}$.

We find the magnetoelectrochemical deviations from Eq. (4.19), which gives

$\delta\bar{\mu}_{\uparrow_S} = -(\ell^2_{\uparrow_S}/\ell^2_{\downarrow_S})\delta\bar{\mu}_{\downarrow_S}$, and from Eq. (4.61), which gives $\delta\bar{\mu}_{\uparrow_{dc}} = \delta\bar{\mu}_{\downarrow_{dc}} = -e\delta\phi_{dc}$:

$$\delta\bar{\mu}^{(\mathrm{I})}_{\uparrow}\left(-\frac{d}{2}\right) = \frac{{\ell^{(\mathrm{I})}_{\mathrm{sf}}}^2}{{\ell^{(\mathrm{I})}_{\uparrow_S}}^2} eV_S^{(\mathrm{I})} - e\left[\frac{A^{(\mathrm{I})}d}{2} + B^{(\mathrm{I})}\right], \tag{D.19}$$

$$\delta\bar{\mu}^{(\mathrm{I})}_{\downarrow}\left(-\frac{d}{2}\right) = -\frac{{\ell^{(\mathrm{I})}_{\mathrm{sf}}}^2}{{\ell^{(\mathrm{I})}_{\downarrow_S}}^2} eV_S^{(\mathrm{I})} - e\left[\frac{A^{(\mathrm{I})}d}{2} + B^{(\mathrm{I})}\right], \tag{D.20}$$

$$\delta\bar{\mu}^{(\mathrm{II})}_{\uparrow}\left(-\frac{d}{2}\right) = \frac{{\ell^{(\mathrm{II})}_{\mathrm{sf}}}^2}{{\ell^{(\mathrm{II})}_{\uparrow_S}}^2} e\left(V_S^{(\mathrm{IIa})} + V_S^{(\mathrm{IIb})} e^{-d/\ell^{(\mathrm{II})}_{\mathrm{sf}}}\right) - e\left[\frac{A^{(\mathrm{II})}d}{2} + B^{(\mathrm{II})}\right], \tag{D.21}$$

$$\delta\bar{\mu}^{(\mathrm{II})}_{\downarrow}\left(-\frac{d}{2}\right) = -\frac{{\ell^{(\mathrm{II})}_{\mathrm{sf}}}^2}{{\ell^{(\mathrm{II})}_{\downarrow_S}}^2} e\left(V_S^{(\mathrm{IIa})} + V_S^{(\mathrm{IIb})} e^{-d/\ell^{(\mathrm{II})}_{\mathrm{sf}}}\right) - e\left[\frac{A^{(\mathrm{II})}d}{2} + B^{(\mathrm{II})}\right], \tag{D.22}$$

$$\delta\bar{\mu}^{(\mathrm{II})}_{\uparrow}\left(\frac{d}{2}\right) = \frac{{\ell^{(\mathrm{II})}_{\mathrm{sf}}}^2}{{\ell^{(\mathrm{II})}_{\uparrow_S}}^2} e\left(V_S^{(\mathrm{IIa})} e^{-d/\ell^{(\mathrm{II})}_{\mathrm{sf}}} + V_S^{(\mathrm{IIb})}\right) - e\left[-\frac{A^{(\mathrm{II})}d}{2} + B^{(\mathrm{II})}\right], \tag{D.23}$$

$$\delta\bar{\mu}^{(\mathrm{II})}_{\downarrow}\left(\frac{d}{2}\right) = -\frac{{\ell^{(\mathrm{II})}_{\mathrm{sf}}}^2}{{\ell^{(\mathrm{II})}_{\downarrow_S}}^2} e\left(V_S^{(\mathrm{IIa})} e^{-d/\ell^{(\mathrm{II})}_{\mathrm{sf}}} + V_S^{(\mathrm{IIb})}\right) - e\left[-\frac{A^{(\mathrm{II})}d}{2} + B^{(\mathrm{II})}\right], \tag{D.24}$$

$$\delta\bar{\mu}^{(\mathrm{III})}_{\uparrow}\left(\frac{d}{2}\right) = \frac{{\ell^{(\mathrm{III})}_{\mathrm{sf}}}^2}{{\ell^{(\mathrm{III})}_{\uparrow_S}}^2} eV_S^{(\mathrm{III})} - e\left[-\frac{A^{(\mathrm{III})}d}{2} + B^{(\mathrm{III})}\right], \tag{D.25}$$

$$\delta\bar{\mu}^{(\mathrm{III})}_{\downarrow}\left(\frac{d}{2}\right) = -\frac{{\ell^{(\mathrm{III})}_{\mathrm{sf}}}^2}{{\ell^{(\mathrm{III})}_{\downarrow_S}}^2} eV_S^{(\mathrm{III})} - e\left[-\frac{A^{(\mathrm{III})}d}{2} + B^{(\mathrm{III})}\right]. \tag{D.26}$$

Substitution of Eqs. (D.11)-(D.12) and (D.19)-(D.26) into Eqs. (D.15)-(D.18)

gives

$$-\frac{\sigma_{\uparrow}^{(\mathrm{I})}V_S^{(\mathrm{I})}}{2e\ell_{\mathrm{sf}}^{(\mathrm{I})}}-\frac{\sigma_{\uparrow}^{(\mathrm{I})}A^{(\mathrm{I})}}{e}=-\frac{g_{\uparrow}^{(a)}}{e}\left[\frac{{\ell_{\mathrm{sf}}^{(\mathrm{II})}}^2}{{\ell_{\uparrow_S}^{(\mathrm{II})}}^2}\left(V_S^{(\mathrm{IIa})}+V_S^{(\mathrm{IIb})}e^{-d/\ell_{\mathrm{sf}}^{(\mathrm{II})}}\right)\right.$$
$$\left.-\frac{A^{(\mathrm{II})}d}{2}-B^{(\mathrm{II})}-\frac{{\ell_{\mathrm{sf}}^{(\mathrm{I})}}^2}{{\ell_{\uparrow_S}^{(\mathrm{I})}}^2}V_S^{(\mathrm{I})}+\frac{A^{(\mathrm{I})}d}{2}+B^{(\mathrm{I})}\right], \quad \text{(D.27)}$$

$$\frac{\sigma_{\downarrow}^{(\mathrm{I})}V_S^{(\mathrm{I})}}{2e\ell_{\mathrm{sf}}^{(\mathrm{I})}}-\frac{\sigma_{\downarrow}^{(\mathrm{I})}A^{(\mathrm{I})}}{e}=-\frac{g_{\downarrow}^{(a)}}{e}\left[-\frac{{\ell_{\mathrm{sf}}^{(\mathrm{II})}}^2}{{\ell_{\downarrow_S}^{(\mathrm{II})}}^2}\left(V_S^{(\mathrm{IIa})}+V_S^{(\mathrm{IIb})}e^{-d/\ell_{\mathrm{sf}}^{(\mathrm{II})}}\right)\right.$$
$$\left.-\frac{A^{(\mathrm{II})}d}{2}-B^{(\mathrm{II})}+\frac{{\ell_{\mathrm{sf}}^{(\mathrm{I})}}^2}{{\ell_{\downarrow_S}^{(\mathrm{I})}}^2}V_S^{(\mathrm{I})}+\frac{A^{(\mathrm{I})}d}{2}+B^{(\mathrm{I})}\right], \quad \text{(D.28)}$$

$$\frac{\sigma_{\uparrow}^{(\mathrm{III})}V_S^{(\mathrm{III})}}{2e\ell_{\mathrm{sf}}^{(\mathrm{III})}}-\frac{\sigma_{\uparrow}^{(\mathrm{III})}A^{(\mathrm{III})}}{e}=-\frac{g_{\uparrow}^{(b)}}{e}\left[\frac{{\ell_{\mathrm{sf}}^{(\mathrm{III})}}^2}{{\ell_{\uparrow_S}^{(\mathrm{III})}}^2}V_S^{(\mathrm{III})}+\frac{A^{(\mathrm{III})}d}{2}-B^{(\mathrm{III})}\right.$$
$$\left.-\frac{{\ell_{\mathrm{sf}}^{(\mathrm{II})}}^2}{{\ell_{\uparrow_S}^{(\mathrm{II})}}^2}\left(V_S^{(\mathrm{IIa})}e^{-d/\ell_{\mathrm{sf}}^{(\mathrm{II})}}+V_S^{(\mathrm{IIb})}\right)-\frac{A^{(\mathrm{II})}d}{2}+B^{(\mathrm{II})}\right], \quad \text{(D.29)}$$

$$-\frac{\sigma_{\downarrow}^{(\mathrm{III})}V_S^{(\mathrm{III})}}{2e\ell_{\mathrm{sf}}^{(\mathrm{III})}}-\frac{\sigma_{\downarrow}^{(\mathrm{III})}A^{(\mathrm{III})}}{e}=-\frac{g_{\downarrow}^{(b)}}{e}\left[-\frac{{\ell_{\mathrm{sf}}^{(\mathrm{III})}}^2}{{\ell_{\downarrow_S}^{(\mathrm{III})}}^2}V_S^{(\mathrm{III})}+\frac{A^{(\mathrm{III})}d}{2}-B^{(\mathrm{III})}\right.$$
$$\left.+\frac{{\ell_{\mathrm{sf}}^{(\mathrm{II})}}^2}{{\ell_{\downarrow_S}^{(\mathrm{II})}}^2}\left(V_S^{(\mathrm{IIa})}e^{-d/\ell_{\mathrm{sf}}^{(\mathrm{II})}}+V_S^{(\mathrm{IIb})}\right)-\frac{A^{(\mathrm{II})}d}{2}+B^{(\mathrm{II})}\right]. \quad \text{(D.30)}$$

(xiv): We are free to choose a "zero" of electric potential, so we set

$$B^{(\mathrm{II})}=0. \quad \text{(D.31)}$$

The fourteen boundary conditions in Eqs. (D.1)-(D.4), (D.6)-(D.8), (D.13)-(D.14), (D.27)-(D.30), and (D.31) allow us to solve for the 14 unknowns. We now rewrite the equations in terms of dimensionless variables.

We define the voltage

$$\widetilde{V} \equiv \frac{e\ell_{\rm sf}^{\rm Cu} J}{\sigma^{\rm Cu}}, \tag{D.32}$$

where $\ell_{\rm sf}^{\rm Cu}$ is the spin-diffusion length in Cu and $\sigma^{\rm Cu} = \sigma_{\uparrow}^{\rm Cu} + \sigma_{\downarrow}^{\rm Cu}$ is the total conductivity of copper. For the 14 variables, we define 14 corresponding dimensionless quantities:

$$\begin{gathered}
\gamma_S^{(\rm I)} \equiv \frac{V_S^{(\rm I)}}{\widetilde{V}}, \quad \gamma_S^{(\rm IIa)} \equiv \frac{V_S^{(\rm IIa)}}{\widetilde{V}}, \quad \gamma_S^{(\rm IIb)} \equiv \frac{V_S^{(\rm IIb)}}{\widetilde{V}}, \\
\gamma_S^{(\rm III)} \equiv \frac{V_S^{(\rm III)}}{\widetilde{V}}, \quad \gamma_Q^{(\rm I)} \equiv \frac{\phi_{0_Q}^{(\rm I)}}{\widetilde{V}}, \quad \gamma_Q^{(\rm IIa)} \equiv \frac{\phi_{0_Q}^{(\rm IIa)}}{\widetilde{V}}, \\
\gamma_Q^{(\rm IIb)} \equiv \frac{\phi_{0_Q}^{(\rm IIb)}}{\widetilde{V}}, \quad \gamma_Q^{(\rm III)} \equiv \frac{\phi_{0_Q}^{(\rm III)}}{\widetilde{V}}, \quad \gamma_{dc}^{(\rm I)} \equiv \frac{B^{(\rm I)}}{\widetilde{V}}, \\
\gamma_{dc}^{(\rm II)} \equiv \frac{B^{(\rm II)}}{\widetilde{V}}, \quad \gamma_{dc}^{(\rm III)} \equiv \frac{B^{(\rm III)}}{\widetilde{V}}, \quad \Upsilon^{(\rm I)} \equiv \frac{A^{(\rm I)}\ell_{\rm sf}^{\rm Cu}}{\widetilde{V}}, \\
\Upsilon^{(\rm II)} \equiv \frac{A^{(\rm III)}\ell_{\rm sf}^{\rm Cu}}{\widetilde{V}}, \quad \Upsilon^{(\rm III)} \equiv \frac{A^{(\rm III)}\ell_{\rm sf}^{\rm Cu}}{\widetilde{V}}.
\end{gathered} \tag{D.33}$$

Below we rewrite Eqs. (D.1)-(D.4), (D.6)-(D.8), (D.13)-(D.14), (D.27)-(D.30), and (D.31) in terms of these variables.

Division of Eqs. (D.1)-(D.2) by $\widetilde{V}$ and multiplication of Eqs. (D.3)-(D.4) by

$\ell_{\rm sf}^{\rm Cu}/\widetilde{V}$ gives

$$\xi^{(\rm I)}\gamma_S^{(\rm I)}+\gamma_Q^{(\rm I)}+\gamma_{dc}^{(\rm I)}-\left(-\frac{d}{2}\right)\Upsilon^{(\rm I)} = \xi^{(\rm II)}\left(\gamma_S^{(\rm IIa)}+\gamma_S^{(\rm IIb)}e^{-d/\ell_{\rm sf}^{(\rm II)}}\right)+\gamma_Q^{(\rm IIa)}+\gamma_Q^{(\rm IIb)}e^{-d/\ell_Q^{(\rm II)}}+\gamma_{dc}^{(\rm II)}-\left(-\frac{d}{2}\right)\Upsilon^{(\rm II)}, \tag{D.34}$$

$$\xi^{(\rm III)}\gamma_S^{(\rm III)}+\gamma_Q^{(\rm III)}+\gamma_{dc}^{(\rm III)}-\left(\frac{d}{2}\right)\Upsilon^{(\rm III)} = \xi^{(\rm II)}\left(\gamma_S^{(\rm IIa)}e^{-d/\ell_{\rm sf}^{(\rm II)}}+\gamma_S^{(\rm IIb)}\right)+\gamma_Q^{(\rm IIa)}e^{-d/\ell_Q^{(\rm II)}}+\gamma_Q^{(\rm IIb)}+\gamma_{dc}^{(\rm II)}-\left(\frac{d}{2}\right)\Upsilon^{(\rm II)}, \tag{D.35}$$

$$-\frac{\ell_{\rm sf}^{\rm Cu}}{\ell_{\rm sf}^{(\rm I)}}\xi^{(\rm I)}\gamma_S^{(\rm I)}-\frac{\ell_{\rm sf}^{\rm Cu}}{\ell_Q^{(\rm I)}}\gamma_Q^{(\rm I)}+\Upsilon^{(\rm I)} = \frac{\ell_{\rm sf}^{\rm Cu}}{\ell_{\rm sf}^{(\rm II)}}\xi^{(\rm II)}\left(\gamma_S^{(\rm IIa)}-\gamma_S^{(\rm IIb)}e^{-d/\ell_{\rm sf}^{(\rm II)}}\right)+\frac{\ell_{\rm sf}^{\rm Cu}}{\ell_Q^{(\rm II)}}\left(\gamma_Q^{(\rm IIa)}-\gamma_Q^{(\rm IIb)}e^{-d/\ell_Q^{(\rm II)}}\right)+\Upsilon^{(\rm II)}, \tag{D.36}$$

$$\frac{\ell_{\rm sf}^{\rm Cu}}{\ell_{\rm sf}^{(\rm III)}}\xi^{(\rm III)}\gamma_S^{(\rm III)}+\frac{\ell_{\rm sf}^{\rm Cu}}{\ell_Q^{(\rm III)}}\gamma_Q^{(\rm III)}+\Upsilon^{(\rm III)} = \frac{\ell_{\rm sf}^{\rm Cu}}{\ell_{\rm sf}^{(\rm II)}}\xi^{(\rm II)}\left(\gamma_S^{(\rm IIa)}e^{-d/\ell_{\rm sf}^{(\rm II)}}-\gamma_S^{(\rm IIb)}\right)+\frac{\ell_{\rm sf}^{\rm Cu}}{\ell_Q^{(\rm II)}}\left(\gamma_Q^{(\rm IIa)}e^{-d/\ell_Q^{(\rm II)}}-\gamma_Q^{(\rm IIb)}\right)+\Upsilon^{(\rm II)}. \tag{D.37}$$

Division of Eqs. (D.6)-(D.8) by J gives

$$\Upsilon^{(\rm I)}=-\frac{\sigma^{\rm Cu}}{\sigma_\uparrow^{(\rm I)}+\sigma_\downarrow^{(\rm I)}}, \tag{D.38}$$

$$\Upsilon^{(\rm II)}=-\frac{\sigma^{\rm Cu}}{\sigma_\uparrow^{(\rm II)}+\sigma_\downarrow^{(\rm II)}}, \tag{D.39}$$

$$\Upsilon^{(\rm III)}=-\frac{\sigma^{\rm Cu}}{\sigma_\uparrow^{(\rm III)}+\sigma_\downarrow^{(\rm III)}}. \tag{D.40}$$

Division of Eqs. (D.13)-(D.14) by J gives

$$-\frac{\sigma_{\uparrow}^{(\mathrm{I})}\ell_{\mathrm{sf}}^{\mathrm{Cu}}}{2\sigma^{\mathrm{Cu}}\ell_{\mathrm{sf}}^{(\mathrm{I})}}\gamma_S^{(\mathrm{I})}-\frac{\sigma_{\uparrow}^{(\mathrm{I})}}{\sigma^{\mathrm{Cu}}}\Upsilon^{(\mathrm{I})}=\frac{\sigma_{\uparrow}^{(\mathrm{II})}\ell_{\mathrm{sf}}^{\mathrm{Cu}}}{2\sigma^{\mathrm{Cu}}\ell_{\mathrm{sf}}^{(\mathrm{II})}}\left(\gamma_S^{(\mathrm{IIa})}-\gamma_S^{(\mathrm{IIb})}e^{-d/\ell_{\mathrm{sf}}^{(\mathrm{II})}}\right)-\frac{\sigma_{\uparrow}^{(\mathrm{II})}}{\sigma^{\mathrm{Cu}}}\Upsilon^{(\mathrm{II})}, \tag{D.41}$$

$$\frac{\sigma_{\uparrow}^{(\mathrm{II})}\ell_{\mathrm{sf}}^{\mathrm{Cu}}}{2\sigma^{\mathrm{Cu}}\ell_{\mathrm{sf}}^{(\mathrm{II})}}\left(\gamma_S^{(\mathrm{IIa})}e^{-d/\ell_{\mathrm{sf}}^{(\mathrm{II})}}-\gamma_S^{(\mathrm{IIb})}\right)-\frac{\sigma_{\uparrow}^{(\mathrm{II})}}{\sigma^{\mathrm{Cu}}}\Upsilon^{(\mathrm{II})}=\frac{\sigma_{\uparrow}^{(\mathrm{III})}\ell_{\mathrm{sf}}^{\mathrm{Cu}}}{2\sigma^{\mathrm{Cu}}\ell_{\mathrm{sf}}^{(\mathrm{III})}}\gamma_S^{(\mathrm{III})}-\frac{\sigma_{\uparrow}^{(\mathrm{III})}}{\sigma^{\mathrm{Cu}}}\Upsilon^{(\mathrm{III})}. \tag{D.42}$$

Division of Eqs. (D.27)-(D.30) by J gives

$$-\frac{\sigma_{\uparrow}^{(\mathrm{I})}\ell_{\mathrm{sf}}^{\mathrm{Cu}}}{2\sigma^{\mathrm{Cu}}\ell_{\mathrm{sf}}^{(\mathrm{I})}}\gamma_S^{(\mathrm{I})}-\frac{\sigma_{\uparrow}^{(\mathrm{I})}}{\sigma^{\mathrm{Cu}}}\Upsilon^{(\mathrm{I})}=-\frac{G_{\uparrow}^{(a)}\ell_{\mathrm{sf}}^{\mathrm{Cu}}}{\sigma^{\mathrm{Cu}}}\left[\frac{{\ell_{\mathrm{sf}}^{(\mathrm{II})}}^2}{{\ell_{S\uparrow}^{(\mathrm{II})}}^2}\left(\gamma_S^{(\mathrm{IIa})}+\gamma_S^{(\mathrm{IIb})}e^{-d/\ell_{\mathrm{sf}}^{(\mathrm{II})}}\right)\right.$$
$$\left.-\frac{d}{2\ell_{\mathrm{sf}}^{\mathrm{Cu}}}\Upsilon^{(\mathrm{II})}-\gamma_{dc}^{(\mathrm{II})}-\frac{{\ell_{\mathrm{sf}}^{(\mathrm{I})}}^2}{{\ell_{S\uparrow}^{(\mathrm{I})}}^2}\gamma_S^{(\mathrm{I})}+\frac{d}{2\ell_{\mathrm{sf}}^{\mathrm{Cu}}}\Upsilon^{(\mathrm{I})}+\gamma_{dc}^{(\mathrm{I})}\right], \tag{D.43}$$

$$\frac{\sigma_{\downarrow}^{(\mathrm{I})}\ell_{\mathrm{sf}}^{\mathrm{Cu}}}{2\sigma^{\mathrm{Cu}}\ell_{\mathrm{sf}}^{(\mathrm{I})}}\gamma_S^{(\mathrm{I})}-\frac{\sigma_{\downarrow}^{(\mathrm{I})}}{\sigma^{\mathrm{Cu}}}\Upsilon^{(\mathrm{I})}=-\frac{G_{\downarrow}^{(a)}\ell_{\mathrm{sf}}^{\mathrm{Cu}}}{\sigma^{\mathrm{Cu}}}\left[-\frac{{\ell_{\mathrm{sf}}^{(\mathrm{II})}}^2}{{\ell_{S\downarrow}^{(\mathrm{II})}}^2}\left(\gamma_S^{(\mathrm{IIa})}+\gamma_S^{(\mathrm{IIb})}e^{-d/\ell_{\mathrm{sf}}^{(\mathrm{II})}}\right)\right.$$
$$\left.-\frac{d}{2\ell_{\mathrm{sf}}^{\mathrm{Cu}}}\Upsilon^{(\mathrm{II})}-\gamma_{dc}^{(\mathrm{II})}+\frac{{\ell_{\mathrm{sf}}^{(\mathrm{I})}}^2}{{\ell_{S\downarrow}^{(\mathrm{I})}}^2}\gamma_S^{(\mathrm{I})}+\frac{d}{2\ell_{\mathrm{sf}}^{\mathrm{Cu}}}\Upsilon^{(\mathrm{I})}+\gamma_{dc}^{(\mathrm{I})}\right], \tag{D.44}$$

$$\frac{\sigma_{\uparrow}^{(\mathrm{III})}\ell_{\mathrm{sf}}^{\mathrm{Cu}}}{2\sigma^{\mathrm{Cu}}\ell_{\mathrm{sf}}^{(\mathrm{III})}}\gamma_S^{(\mathrm{III})}-\frac{\sigma_{\uparrow}^{(\mathrm{III})}}{\sigma^{\mathrm{Cu}}}\Upsilon^{(\mathrm{III})}=-\frac{G_{\uparrow}^{(b)}\ell_{\mathrm{sf}}^{\mathrm{Cu}}}{\sigma^{\mathrm{Cu}}}\left[\frac{{\ell_{\mathrm{sf}}^{(\mathrm{III})}}^2}{{\ell_{S\uparrow}^{(\mathrm{III})}}^2}\gamma_S^{(\mathrm{III})}+\frac{d}{2\ell_{\mathrm{sf}}^{\mathrm{Cu}}}\Upsilon^{(\mathrm{III})}-\gamma_{dc}^{(\mathrm{III})}\right.$$
$$\left.-\frac{{\ell_{\mathrm{sf}}^{(\mathrm{II})}}^2}{{\ell_{S\uparrow}^{(\mathrm{II})}}^2}\left(\gamma_S^{(\mathrm{IIa})}e^{-d/\ell_{\mathrm{sf}}^{(\mathrm{II})}}+\gamma_S^{(\mathrm{IIb})}\right)-\frac{d}{2\ell_{\mathrm{sf}}^{\mathrm{Cu}}}\Upsilon^{(\mathrm{II})}+\gamma_{dc}^{(\mathrm{II})}\right], \tag{D.45}$$

$$-\frac{\sigma_{\downarrow}^{(\mathrm{III})}\ell_{\mathrm{sf}}^{\mathrm{Cu}}}{2\sigma^{\mathrm{Cu}}\ell_{\mathrm{sf}}^{(\mathrm{III})}}\gamma_S^{(\mathrm{III})}-\frac{\sigma_{\downarrow}^{(\mathrm{III})}}{\sigma^{\mathrm{Cu}}}\Upsilon^{(\mathrm{III})}=-\frac{G_{\downarrow}^{(b)}}{\sigma^{\mathrm{Cu}}}\left[-\frac{{\ell_{\mathrm{sf}}^{(\mathrm{III})}}^2}{{\ell_{S\downarrow}^{(\mathrm{III})}}^2}\gamma_S^{(\mathrm{III})}+\frac{d}{2\ell_{\mathrm{sf}}^{\mathrm{Cu}}}\Upsilon^{(\mathrm{III})}-\gamma_{dc}^{(\mathrm{III})}\right.$$
$$\left.+\frac{{\ell_{\mathrm{sf}}^{(\mathrm{II})}}^2}{{\ell_{S\downarrow}^{(\mathrm{II})}}^2}\left(\gamma_S^{(\mathrm{IIa})}e^{-d/\ell_{\mathrm{sf}}^{(\mathrm{II})}}+\gamma_S^{(\mathrm{IIb})}\right)-\frac{d}{2\ell_{\mathrm{sf}}^{\mathrm{Cu}}}\Upsilon^{(\mathrm{II})}+\gamma_{dc}^{(\mathrm{II})}\right]. \tag{D.46}$$

Finally, Equation (D.31) gives

$$\gamma_{dc}^{(\mathrm{II})}=0. \tag{D.47}$$

Thus, for the fourteen dimensionless unknowns in Eq. (D.33), there are fourteen equations Eqs. (D.34)-(D.47). The numerical results are plotted in Chapter IV.

APPENDIX E

DETAILS OF 2D HEAT FLOW IN THE SPIN-SEEBECK SYSTEM

With Eqs. (5.46) and (5.47) relating the linear terms in temperature, there are twenty-one unknowns in Eqs. (5.41), (5.42), (5.49) and (5.55): one α, four $A_{s\pm}^{(1,2)}$, eight $A_{p\pm}^{(1,2,3,4)}$ and eight $A_{m\pm}^{(1,2,3,4)}$. This section finds them using bulk conditions and boundary conditions on heat flux.

Bulk Conditions

By matching coefficients of like terms, substitution of Eqs. (5.40) and (5.55) into Eq. (5.51) gives

$$A_{m\gamma}^{(1)} = -\frac{\kappa_p}{\kappa_m} A_{p\gamma}^{(1)}, \quad A_{m\gamma}^{(2)} = -\frac{\kappa_p}{\kappa_m} A_{p\gamma}^{(2)}, \quad A_{m\gamma}^{(3)} = A_{p\gamma}^{(3)}, \quad A_{m\gamma}^{(4)} = A_{p\gamma}^{(4)}. \tag{E.1}$$

Since each is a single condition *for each* $\gamma = \pm$, Eq. (E.1) gives eight conditions.

With no heat leaks at $z = -d_s$ and $z = d_F$, the total heat flux along x is conserved, and is everywhere equal the input heat flux.

$$j_0 = j_x^{\varepsilon_p} + j_x^{\varepsilon_m} + j_x^{\varepsilon_s}. \tag{E.2}$$

The surface terms contribute zero total heat current; there is no overall exponential term in the input heat current, so the sum of all exponential heat currents in the sample must equal zero. Substitution of Eq. (5.41) into Eq. (E.2) gives

$$j_0 = -(\kappa_s + \kappa_p + \kappa_m)\alpha. \tag{E.3}$$

The total heat flux j_0, and therefore α, is determined by the applied temperature gradient.

With the bulk conditions Eqs. (E.1) and (E.3), there are twelve unknowns remaining in Eqs. (5.41), (5.42), (5.49) and (5.55) for which to solve using boundary conditions on the heat flux: the four coefficients $A^{(1)}_{s\pm}$ and $A^{(2)}_{s\pm}$ in Eq. (5.49); and the eight coefficients $A^{(1,2,3,4)}_{p\pm}$ in Eq. (5.55). Note that the $T_{0_{(s,p,m)}} \equiv T_0$ of Eq. (5.40) are related to the average temperature of the heaters, and do not appear in the heat fluxes.

Boundary Conditions on Heat Flux along z

Ten conditions (five for each γ) are given by the boundary conditions on the heat flux along z in the various subsystems at $x = -d_s$, $x = 0$, and $x = d_F$. Namely, for each of $\gamma = \pm$ there are:

(**i-ii**) two conditions given by assuming that there is no heat loss at the top of the sample ($z = d_F$) by either the magnons or the phonons, i.e.,

$$j_z^{\varepsilon_m}(z = d_F) = 0, \tag{E.4}$$

$$j_z^{\varepsilon_p}(z = d_F) = 0; \tag{E.5}$$

(**iii**) one condition given by assuming that there is also no heat loss at the bottom of the substrate ($z = -d_s$), i.e.,

$$j_z^{\varepsilon_s}(z = -d_s) = 0; \tag{E.6}$$

(**iv-v**) and two conditions given by the proportionality between the heat flux at the interface in both the substrate and the phonons in the sample to the temperature difference between them at the interface,[15,19] i.e.,

$$j_z^{\varepsilon_s}(z = 0) = h_K[T_s(z = 0) - T_p(z = 0)], \tag{E.7}$$

$$j_z^{\varepsilon_p}(z = 0) = h_K[T_s(z = 0) - T_p(z = 0)]. \tag{E.8}$$

We assume that the substrate does not transfer heat directly to magnons in the sample. The details of these conditions now presented sequentially.

(**i-ii**) At $z = d_F$, the sample is in contact only with vacuum (for point contact detection; when Pt bars are used as detectors, one may determine the temperatures and heat currents inside the Pt). Applying in turn the two conditions Eqs. (E.4) and (E.5) to equation (5.42) gives

$$\begin{aligned} 0 = \partial_z T^a_{m\gamma}(z)|_{(z=d_F)} =& \sqrt{q^2_{mp} - q^2_\gamma} A^{(1)}_{m\gamma} e^{\sqrt{q^2_{mp}-q^2_\gamma} d_F} - \sqrt{q^2_{mp} - q^2_\gamma} A^{(2)}_{m\gamma} e^{-\sqrt{q^2_{mp}-q^2_\gamma} d_F} \\ & - q_\gamma A^{(3)}_{m\gamma} \sin(q_\gamma d_F) + q_\gamma A^{(4)}_{m\gamma} \cos(q_\gamma d_F), \qquad \text{(E.9)} \\ 0 = \partial_z T^a_{p\gamma}(z)|_{(z=d_F)} =& \sqrt{q^2_{mp} - q^2_\gamma} A^{(1)}_{p\gamma} e^{\sqrt{q^2_{mp}-q^2_\gamma} d_F} - \sqrt{q^2_{mp} - q^2_\gamma} A^{(2)}_{p\gamma} e^{-\sqrt{q^2_{mp}-q^2_\gamma} d_F} \\ & - q_\gamma A^{(3)}_{p\gamma} \sin(q_\gamma d_F) + q_\gamma A^{(4)}_{p\gamma} \cos(q_\gamma d_F). \qquad \text{(E.10)} \end{aligned}$$

Here, we have used the forms of $T^a_{(p,m)\gamma}(z)$ given in Eq. (5.55). Equations (E.9) and (E.10) give four conditions (two for each $\gamma = \pm$). In conjunction with Eq. (E.1), they can be thought of as relating $A^{(3)}_{p\gamma}$ and $A^{(4)}_{p\gamma}$ to $A^{(1)}_{p\gamma}$ and $A^{(2)}_{p\gamma}$.

(**iii**) Similarly, at $z = -d_s$, the substrate is in contact only with vacuum, so we assume that the heat current along z goes to zero at $z = -d_s$. Applying Eq. (E.6) to Eq. (5.42) gives

$$\partial_z T^a_{s\gamma}|_{(z=-d_s)} = 0. \qquad \text{(E.11)}$$

Substitution of Eq. (5.49) into Eq. (E.11) gives

$$A^{(2)}_{s\gamma} = -A^{(1)}_{s\gamma} \tan(q_\gamma d_s). \qquad \text{(E.12)}$$

Equation (E.12) gives two conditions (one for each $\gamma = \pm$).

(**iv**) Using Eqs. (5.46) and (5.47), substitution of Eqs. (5.40) and (5.42) into

Eq. (E.7) gives

$$-\kappa_s \sum_{\gamma=+,-} [\partial_z T^a_{s\gamma}]_{(z=0)} \sinh(q_\gamma x) = h_K \sum_{\gamma=+,-} [T^a_{s\gamma}(0) \sinh(q_\gamma x) - T^a_{p\gamma}(0) \sinh(q_\gamma x)]. \tag{E.13}$$

Substitution of Eqs. (5.49), (5.55), and (E.12) yields, for each γ,

$$\kappa_s q_\gamma A^{(1)}_{s\gamma} \tan(q_\gamma d_s) = h_K \left[A^{(1)}_{s\gamma} - \left(A^{(1)}_{p\gamma} + A^{(2)}_{p\gamma} + A^{(3)}_{p\gamma}\right)\right]. \tag{E.14}$$

Equation (E.14) gives two conditions (one for each $\gamma = \pm$), and can be thought of as relating $A^{(k)}_{s\gamma}$ to $A^{(n)}_{p\gamma}$.

(**v**) Subtracting Eq. (E.7) from Eq. (E.8) gives

$$j_z^{\varepsilon_p}(z=0) = j_z^{\varepsilon_s}(z=0). \tag{E.15}$$

Substituting Eq. (5.42) into Eq. (E.15) and matching like terms gives

$$-\kappa_p [\partial_z T^a_{p\gamma}]_{(z=0)} = -\kappa_s [\partial_z T^a_{s\gamma}]_{(z=0)}. \tag{E.16}$$

Substitution from Eqs. (5.49), (5.55), and (E.12) into Eq. (E.16) gives

$$-\kappa_p \left(\sqrt{q^2_{mp} - q^2_\gamma} A^{(1)}_{p\gamma} - \sqrt{q^2_{mp} - q^2_\gamma} A^{(2)}_{p\gamma} + q_\gamma A^{(4)}_{p\gamma}\right) = \kappa_s q_\gamma A^{(1)}_{s\gamma} \tan(q_\gamma d_s). \tag{E.17}$$

Equation (E.17) gives two conditions (one for each $\gamma = \pm$), and in conjunction with the above conditions can be thought of as relating $A^{(2)}_{p\gamma}$ to $A^{(1)}_{p\gamma}$.

In summary, boundary conditions on heat flux along z give ten conditions, five for each surface mode $q_\gamma = q_+$ and $q_\gamma = q_-$: Eqs. (E.9), (E.10), (E.12), (E.14) and (E.17). In conjunction with the bulk conditions given in Eq. (E.1), they give the contributions to the heat flux for each surface mode. Although their absolute magnitudes are related to the heat input by the heater, their relative magnitudes

are determined by the above bulk and boundary conditions, which arise from energy conservation. Figs. 13 and 14 show the contributions to heat flux along z and along x at a given x as a function of z by each of the surface modes, using the parameters in Table III.

Two unknowns remain, one A_+ and one A_-, now determined by conditions on heat flux along x.

Boundary Conditions on Heat Flux along x

For heaters/heat sinks in contact only with the substrate, the boundary conditions in the x-direction on each energy flux j_x^ε are symmetric (we employ this above in taking $T^b_{(s,p,m)}(z) = 0$). However, as stated above, we are only treating the region far enough away from the heaters that the details of heat flux entering and leaving at $x = \pm L/2$ are irrelevant – only a full solution with an infinite sum over q's can treat the specifics of the interfacial input. Thus, we can not apply boundary conditions at $x = \pm L/2$.

We make the following approximation: at $x = \pm L/2 \mp \ell_S$, where ℓ_S is just far enough away from the heater/heat sink that the details of the input heat flux are irrelevant, we take $\partial_x T_p = 0$ and $\partial_x T_m = 0$. In other words, we assume that the total heat flux in the sample is negligible at this (short) distance away from the heater. We take the heaters to be in contact only with the substrate, and assume that a significant amount of heat does not seep into the sample over the distance ℓ_S. Explicitly,

$$\partial_x T_m(x = -L/2 + \ell_S) = 0, \tag{E.18}$$

$$\partial_x T_p(x = -L/2 + \ell_S) = 0. \tag{E.19}$$

Recall that we take heat flux (and therefore $\partial_x T$) to be symmetric about $x = 0$, so that the conditions at $x = +L/2 - \ell_S$ are not independent. For asymmetric

heater/heat sink, e.g., the heater contacts the substrate and the heat sink contacts both the sample and substrate, there are two additional conditions.

Complete Solution

For the twenty-two unknowns in the temperatures and heat fluxes (one background temperature T_0, one thermal gradient α, and twenty coefficients $A^{(n)}_{(s,p,m)\pm}$), there are twenty-two conditions: one condition from the average temperature of the heater and heat sink; four conditions for each of $\gamma = \pm$ from Eq. (E.1); one condition from Eq. (E.3); one condition for each of $\gamma = \pm$ from each of Eqs. (E.9), (E.10), (E.12), (E.14), (E.17); and one condition from each of Eqs. (E.18) and (E.19). As expected, the entire solution is driven by the input heat flux j_0 in Eq. (E.3), that is, if $j_0 = 0$ then all unknowns are zero and the solution is trivial.

In the end, there are only four unknowns: T_0, the temperature gradient α, and two conditions that specify how the heater (and symmetric heat sink) puts energy into the substrate and the sample phonons and magnons.

APPENDIX F

NUMERICAL ALGORITHM FOR 2D THERMAL EQUILIBRATION EIGENVALUES IN THE SPIN-SEEBECK SYSTEM

To obtain the characteristic 2D thermal equilibration wavevectors q, we employ an iterative algorithm that, on input of a test q, solves Eq. (E.1), Eqs. (E.9)-(E.11), Eq. (E.13), and the additional condition $[\partial_z T_m]_{(z=0)} = 0$ for the coefficients $A_{s,p,m}^{(1,2,3,4)}$. It then uses that solution to find the q that satisfies Eq. (E.8). The algorithm, solved using Mathematica, follows:

$C := 100;$

$\gamma := 1;$

while $\gamma < 200$ **do**

$solnA =$ NSolve[

$\{A_s^{(1)} == 1, \quad A_m^{(1)} == -(\kappa_p/\kappa_m)A_p^{(1)}, \quad A_m^{(2)} == -(\kappa_p/\kappa_m)A_p^{(2)},$

$A_m^{(3)} == A_p^{(3)}, \quad A_m^{(4)} == A_p^{(4)},$

$\partial_z T_m^a[q_{\text{init}}, d_F] == 0, \quad \partial_z T_p^a[q_{\text{init}}, d_F] == 0, \quad \partial_z T_s^a[q_{\text{init}}, -d_s] == 0,$

$-\kappa_p \partial_z T_p^a[q_{\text{init}}, 0] == h_K(T_s^a[q_{\text{init}}, 0] - T_p^a[q_{\text{init}}, 0]),$

$-\kappa_m \partial_z T_m^a[q_{\text{init}}, 0] == h_m(T_s^a[q_{\text{init}}, 0] - T_m^a[q_{\text{init}}, 0])\ \},$

$\{A_s^{(1)}, A_s^{(2)}, A_p^{(1)}, A_p^{(2)}, A_p^{(3)}, A_p^{(4)}, A_m^{(1)}, A_m^{(2)}, A_m^{(3)}, A_m^{(4)}\},$

WorkingPrecision $\to 8000 - 15(\gamma - 1)$

];

$solnqnew =$NSolve[

$-\kappa_s(\partial_z T_s^a[tmp, 0]/.solnA) == h_K[(T_s^a[tmp, 0]/.solnA) - (T_p^a[tmp, 0]/.solnA)]$

$+h_m[(T_s^a[tmp, 0]/.solnA) - (T_m^a[tmp, 0]/.solnA)],$

tmp, WorkingPrecision $\to 5000 - 14 - 15(\gamma - 1)$

];

$q_{\text{new}} := (tmp/.solnqnew)$;

$q_{\text{init}} = q_{\text{init}} - (1/C)(q_{\text{init}} - q_{\text{new}})$;

γ++;

end while

The factor h_m represents the thermal boundary conductance for direct sample magnon excitation by substrate phonons incident to the interface. It has been set to zero in the calculations presented in Chap. V.

We note that care must be taken in determining a new initial value for the next iteration. For q_{init} far from a consistent value (that is, a value that satisfies energy conservation), then q_{init} and q_{new} will differ significantly. Naively choosing $q'_{\text{init}} = 1/2(q_{\text{init}} - q_{\text{new}})$ may result in a non-converging series. Hence we include the factor $1/C$ in the definition of q'_{init} in the above code; in general, convergence is found for $C \approx 100 - 300$.

VITA

Matthew Ryan Sears received his Bachelor of Science degree in physics from The University of Rochester in 2005. He entered the physics program at Texas A&M University in September 2005, and received his Doctorate of Philosophy degree in August 2011. His research interests include magnetic, chemical, and mixed-ionic transport, oxide film growth, defect flow in solids, and supersolidity. He plans to continue his career as a research scientist.

Mr. Sears can be reached at c/o Wayne Saslow, 4242 TAMU, Texas A&M University, College Station, TX 77843-4242. His email is matthewrsears@gmail.com.